

Studies by the U.S. Geological Survey in Alaska, Volume 15

Regional Patterns of Mesozoic-Cenozoic Magmatism in Western Alaska Revealed by New U-Pb and $^{40}\text{Ar}/^{39}\text{Ar}$ Ages

Professional Paper 1814-D

U.S. Department of the Interior
U.S. Geological Survey

Cover. Photograph of the Tonzona pluton in the Alaska Range dated at 58 million years old in the present study (U.S. Geological Survey photograph by Dwight Bradley).

Studies by the U.S. Geological Survey in Alaska, Volume 15

Regional Patterns of Mesozoic-Cenozoic Magmatism in Western Alaska Revealed by New U-Pb and $^{40}\text{Ar}/^{39}\text{Ar}$ Ages

By Dwight C. Bradley, Marti L. Miller, Richard M. Friedman, Paul W. Layer,
Heather A. Bleick, James V. Jones III, Steven E. Box, Susan M. Karl, Nora B.
Shew, Timothy S. White, Alison B. Till, Julie A. Dumoulin, Thomas K. Bundtzen,
Paul B. O'Sullivan, and Thomas D. Ullrich

Professional Paper 1814–D

**U.S. Department of the Interior
U.S. Geological Survey**

U.S. Department of the Interior
SALLY JEWELL, Secretary

U.S. Geological Survey
Suzette M. Kimball, Director

U.S. Geological Survey, Reston, Virginia: 2017

For more information on the USGS—the Federal source for science about the Earth, its natural and living resources, natural hazards, and the environment—visit <https://www.usgs.gov/> or call 1-888-ASK-USGS (1-888-275-8747).

For an overview of USGS information products, including maps, imagery, and publications, visit <https://www.usgs.gov/pubprod/> or <https://store.usgs.gov>.

Any use of trade, firm, or product names is for descriptive purposes only and does not imply endorsement by the U.S. Government.

Although this information product, for the most part, is in the public domain, it also may contain copyrighted materials as noted in the text. Permission to reproduce copyrighted items must be secured from the copyright owner.

Suggested citation:

Bradley, D.C., Miller, M.L., Friedman, R.M., Layer, P.W., Bleick, H.A., Jones, J.V., III, Box, S.E., Karl, S.M., Shew, N.B., White, T.S., Till, A.B., Dumoulin, J.A., Bundtzen, T.K., O'Sullivan, P.B., and Ullrich, T.D., 2017, Regional patterns of Mesozoic-Cenozoic magmatism in western Alaska revealed by new U-Pb and ⁴⁰Ar/³⁹Ar ages, *in* Dumoulin, J.A., ed., Studies by the U.S. Geological Survey in Alaska, vol. 15: U.S. Geological Survey Professional Paper 1814-D, 48 p., <https://doi.org/10.3133/pp1814D>.

ISSN 2330-7102 (online)

Contents

Abstract.....	1
Introduction	1
Geochronology	21
Candle Quadrangle.....	21
CA1. Granite Mountain Pluton, Candle B5 Quadrangle.....	21
Tanana Quadrangle.....	21
TN1. Gabbro in Rampart Group, Tanana B1 Quadrangle	21
Kantishna River Quadrangle.....	21
KH1. Sischu Igneous Complex, Kantishna River A6 Quadrangle.....	21
Medfra Quadrangle.....	21
MD1. Telida Pluton, Medfra C1 Quadrangle	21
Holy Cross Quadrangle.....	21
HC1. Volcanic Rocks of the Yetna River Area, Holy Cross D1 Quadrangle.....	21
Iditarod Quadrangle	21
ID1. Ruby Terrane Orthogneiss, Unit PzPg, Iditarod D4 Quadrangle.....	21
ID2. Gabbro in Dishna River Mafic-ultramafic Complex, Iditarod D3 Quadrangle	22
McGrath Quadrangle.....	22
MG1. Stock South of Lone Mountain, McGrath B4 Quadrangle.....	22
MG2 and MG3. Tephra in Sheep Creek Volcanic Field, McGrath B2 Quadrangle	22
MG4. Windy Fork Pluton, McGrath A3 Quadrangle.....	22
Talkeetna Quadrangle.....	23
TL1. Intrusion at BM Sheep, Talkeetna D5 Quadrangle.....	23
TL2. Tonzona Pluton, Talkeetna D5 Quadrangle.....	23
Sleetmute Quadrangle.....	23
SM1. Intrusion at Hill 1195, Sleetmute D4 Quadrangle	23
SM2. Aghaluk Stock, Sleetmute C7 Quadrangle.....	23
SM3. Intrusion at Hill 1662, Sleetmute C6 Quadrangle.....	23
SM4. Intrusion at Hill 1908, Sleetmute C6 Quadrangle.....	23
SM5. Intrusion in Oskawalik River Drainage, Sleetmute C5 Quadrangle	23
SM6. Henderson Stock, Sleetmute C5 Quadrangle.....	23
SM7. Tephra in Kuskokwim Group, Sleetmute C4 Quadrangle	24
SM8 and SM9. Barometer Pluton, Sleetmute C4 Quadrangle.....	24
SM10. Intrusion in Vreeland Creek Drainage, Sleetmute C4 Quadrangle (97AM81a).....	24
SM11. Red Mountain Pluton, Sleetmute C4 Quadrangle	24
SM12. Felsite in Victoria Creek Headwaters, Sleetmute B8 Quadrangle	24
SM13 and SM14. Buckstock Pluton, Sleetmute B8 and B7 Quadrangles.....	24
SM15. Kaluvarawluk Igneous Complex, Sleetmute B7 Quadrangle.....	24
SM16. Intrusion Near Holokuk Mountain, Sleetmute B6 Quadrangle.....	25
SM17. Chuilnuk Pluton, Sleetmute B5 Quadrangle.....	25
SM18, TA1 and TA2. Timber Creek Pluton, Sleetmute A8 and Taylor Mountains D8 Quadrangles	25
SM19. Intrusion in Timber Creek Headwaters, Sleetmute A8 Quadrangle	25
SM20. Intrusion Near Hill 2639, Sleetmute A7 Quadrangle	25

SM21. Intrusion at Hill 1764, Sleetmute B7 Quadrangle	25
Lime Hills Quadrangle	25
LH1. Stock Near Windy Fork Pluton, Lime Hills D4 Quadrangle	25
LH2. Sill at Gagaryah Barite Deposit, Lime Hills D4 Quadrangle	26
Bethel Quadrangle	26
BH1. Gemuk Mountain Pluton, Bethel C1 Quadrangle	26
BH2. Unnamed Igneous Rocks in Tikchik Terrane, Bethel A1 Quadrangle	26
BH3. Dike Near Shadow Bay, Bethel A1 Quadrangle	26
Taylor Mountains Quadrangle	26
TA3. Felsite in Gemuk Group, Taylor Mountains D8 Quadrangle	26
TA4. Flat Top Basalt, Taylor Mountains D8 Quadrangle	27
TA5. Dike at Hill 2164, Taylor Mountains D8 Quadrangle	27
TA6. Sill at Hill 1768, Taylor Mountains D8 Quadrangle	27
TA7. Intrusion at Hill 2240, Taylor Mountains D7 Quadrangle	27
TA8 and TA9. Sills in Kuskokwim Group, Taylor Mountains D7 Quadrangle	27
TA10. Little Taylor Pluton, Taylor Mountains D4 Quadrangle	27
TA11. Intrusion in Enatalik Creek drainage, Taylor Mountains C8 Quadrangle	28
TA12. Intrusion Near BM Tippy, Taylor Mountains C8 Quadrangle	28
TA13 and TA14. Sills in Kuskokwim Group, Taylor Mountains C1 Quadrangle	28
TA15 and TA16. Shotgun Hills Pluton, Taylor Mountains C6 and B6 Quadrangles	28
TA17. Intrusion South of Shotgun Airstrip, Taylor Mountains B6 Quadrangle	28
TA18 and TA19. Intrusions in Winchester Claim Area, Taylor Mountains B6 Quadrangle	28
TA20. Intrusion Near BM Reach, Taylor Mountains Quadrangle B5	29
TA21. Intrusion at Hill 1311, Taylor Mountains B4 Quadrangle	29
TA22. Dike at Hill 1272, Taylor Mountains B3 Quadrangle	29
TA23, TA24, and TA25. Dikes in Red Bluff Area, Taylor Mountains B1 Quadrangle	29
TA26. Intrusion Near Keefer Creek, Taylor Mountains B1 Quadrangle	29
TA27. Chaufchivak Pluton, Taylor Mountains A7 Quadrangle	29
TA28. Intrusion at Hill 1623, Taylor Mountains A6 Quadrangle	30
TA29. Intrusion Near Hill 1635, Taylor Mountains A6 Quadrangle	30
TA30 and TA31. Tikchik Mountain Pluton, Taylor Mountains A6 Quadrangle	30
TA32. Arrow Pluton, Taylor Mountains A5 Quadrangle	30
TA33. Dike Near Sleitat Mountain, Taylor Mountains A3 Quadrangle	30
TA34. Sleitat Pluton, Taylor Mountains A3 Quadrangle	30
TA35. Old Man Pluton, Taylor Mountains A3 Quadrangle	31
TA36. Intrusion at Hill 1004, Taylor Mountains A3 Quadrangle	31
TA37. Intrusion at Hill 1422, Taylor Mountains A2 Quadrangle	31
TA38. Rhyolite at Hill 1678, Taylor Mountains A1 Quadrangle	31
TA39. Intrusion at Hill 982, Taylor Mountains A1 Quadrangle	31
Lake Clark Quadrangle	31
LC1. Overlook Pluton, Lake Clark B8 Quadrangle	31
Goodnews Bay Quadrangle	31
GO1. Intrusion Near Jacksmith Creek, Goodnews Bay B8 Quadrangle	31
GO2. Dike at Island Mountain, Goodnews Bay B7 Quadrangle	31
Dillingham Quadrangle	32
D11. Tikchik Narrows Pluton, Dillingham D7 Quadrangle	32

Implications for the Magmatic History of Western Alaska.....	32
Pennsylvanian	32
Triassic.....	32
Jurassic.....	32
Early Cretaceous.....	32
Mid-Cretaceous.....	32
Late Cretaceous.....	33
Paleocene and Early Eocene.....	33
Mid-Eocene to Pliocene	36
Acknowledgments.....	37
References Cited.....	37
Appendix 1.—Analytical Methods	44
U-Pb Zircon TIMS Analytical Methods, University of British Columbia	44
U-Pb Zircon SHRIMP-RG Analytical Methods, USGS-Stanford University	44
⁴⁰ Ar/ ³⁹ Ar Analytical Methods, University of Alaska, Fairbanks.....	45
⁴⁰ Ar/ ³⁹ Ar Analytical Methods, University of British Columbia	45
U-Pb Zircon LA-ICP-MS Analytical Methods, Apatite to Zircon, Inc.....	45
Data Modeling	46
Pb/U Fractionation Factor.....	46
Fractionation Factor Adjustment for Integrated alpha-damage	47
Common Pb Correction	47
Preferred Age	47
Appendix 2.—New Geochronology Data for Igneous-Rock Samples from Western Alaska.....	48

Figures

1. Map of western Alaska showing key physiographic features and sample locations identified by number	3
2. Simplified geologic map showing the context of samples in the Sleetmute, Taylor Mountains, Bethel, Dillingham, Lake Clark, and Goodnews Bay, Alaska.....	5
3. Photograph of the Tonzona pluton in the Alaska Range (Talkeetna quadrangle) dated at 58 million years old in the present study.....	5
4. Simplified geologic maps, derived from Wilson and others (2015), showing the context of sample locations in western Alaska.....	7
5. Concordia diagrams for samples of zircon and monazite dated by uranium-lead (U-Pb) thermal ionization mass-spectrometry (TIMS) at the University of British Columbia	14
6. Plots showing weighted average lead-206/uranium-238 (²⁰⁶ Pb/ ²³⁸ U) ages of zircon samples and individual zircon ages.....	15
7. Plots of age spectra showing the results of incremental step heating of argon-40/argon-39 (⁴⁰ Ar/ ³⁹ Ar) samples	17
8. Maps (A to M) showing the distribution of isotopic ages from igneous rocks in western Alaska in 2-million-year increments from 78 to 50 million years ago (Ma).....	34
9. Map showing Late Cretaceous paleogeographic elements and igneous rock samples with ages of 72–68 million years (Ma) in western Alaska	36

Table

1. Summary of new geochronology data for igneous-rock samples from western Alaska.....	8
--	---

Regional Patterns of Mesozoic-Cenozoic Magmatism in Western Alaska Revealed by New U-Pb and $^{40}\text{Ar}/^{39}\text{Ar}$ Ages

By Dwight C. Bradley,¹ Marti L. Miller,¹ Richard M. Friedman,² Paul W. Layer,³ Heather A. Bleick,⁴ James V. Jones III,¹ Steven E. Box,¹ Susan M. Karl,¹ Nora B. Shew,¹ Timothy S. White,¹ Alison B. Till,¹ Julie A. Dumoulin,¹ Thomas K. Bundtzen,⁵ Paul B. O'Sullivan,⁶ and Thomas D. Ullrich²

Abstract

In support of regional geologic framework studies, we obtained 50 new argon-40/argon-39 ($^{40}\text{Ar}/^{39}\text{Ar}$) ages and 33 new uranium-lead (U-Pb) ages from igneous rocks of southwestern Alaska. Most of the samples are from the Sleetmute and Taylor Mountains quadrangles; smaller collections or individual samples are from the Bethel, Candle, Dillingham, Goodnews Bay, Holy Cross, Iditarod, Kantishna River, Lake Clark, Lime Hills, McGrath, Medfra, Talkeetna, and Tanana quadrangles.

A U-Pb zircon age of 317.7 ± 0.6 million years (Ma) reveals the presence of Pennsylvanian intermediate igneous (probably volcanic) rocks in the Tikchik terrane, Bethel quadrangle. A U-Pb zircon age of 229.5 ± 0.2 Ma from gabbro intruding the Rampart Group of the Angayucham-Tozitna terrane, Tanana quadrangle, confirms and tightens a previously cited Triassic age for this intrusive suite. A fresh mafic dike in Goodnews Bay quadrangle yielded a $^{40}\text{Ar}/^{39}\text{Ar}$ whole rock age of 155.0 ± 1.9 Ma; this establishes a Jurassic or older age for the previously unconstrained (Paleozoic? to Mesozoic?) sandstone unit that it intrudes. A thick felsic tuff in the Gemuk Group in Taylor Mountains quadrangle yielded a U-Pb zircon age of 153.0 ± 2.0 Ma, extending the age of magmatism in this part of the Togiak terrane back into the Late Jurassic. We report three new U-Pb zircon ages between 120 and 110 Ma— 112.0 ± 0.9 Ma from syenite in the Candle quadrangle, 114.9 ± 0.3 Ma from orthogneiss assigned to the Ruby terrane in Iditarod quadrangle, and 116.6 ± 0.1 Ma from a gabbro of the Dishna River mafic-ultramafic complex in Iditarod quadrangle. The latter result requires a substantial age revision, from Triassic to Cretaceous, for at least some rocks that have been mapped as the Dishna River mafic-ultramafic complex. A tuff in the Upper Cretaceous Kuskokwim Group yielded a U-Pb zircon (sensitive

high-resolution ion microprobe, SHRIMP) age of 88.3 ± 1.0 Ma; we speculate that the eruptive source was an arc along the trend of the Pebble porphyry copper deposit along the Gulf of Alaska continental margin. More than half of the new ages fall between 75 and 65 Ma, confirming the existence, based on conventional potassium-argon (K-Ar) ages, of a 70-Ma igneous flare-up across southwestern Alaska. Our new ages hint that during this pulse, the locus of magmatism shifted toward the Gulf of Alaska, that is, toward a more outboard position. This shift is consistent with the hypothesis that magmatism was the product of rollback of a subducted slab, which at that time would have been the Resurrection Plate. Intrusive rocks in the Taylor Mountains and Sleetmute quadrangles in the age range of 63 to 59 Ma were emplaced shortly before the onset of ridge subduction as dated by near-trench plutons in the adjacent part of the Chugach accretionary complex. Southwestern Alaska at this time would have been positioned above a very young subducted slab belonging to the Resurrection Plate; magmas, in this scenario, were generated near the edge of the slab window related to ridge subduction. A 56.3 ± 0.2 Ma granite in Taylor Mountains quadrangle and a 54.7 ± 0.7 Ma ashfall tuff in McGrath quadrangle were likely emplaced above the Resurrection-Kula slab window, which by this time is inferred to have entered the region. Another ashfall tuff in McGrath quadrangle, at 42.8 ± 0.5 Ma, likely belongs to the Meshik Arc, the product of renewed subduction after inferred passage of the slab window. A 49.0 ± 0.3 -Ma rhyolite in Taylor Mountains quadrangle is about the age of the transition from slab window to renewed subduction. Two plutons in the western Alaska Range, at 31.8 ± 0.4 and 30.9 ± 0.6 Ma, belong to a suite of gabbro to peralkaline granite of unknown origin. Finally, a 4.6 ± 0.1 -Ma basalt from a flow in Taylor Mountains quadrangle belongs to the Neogene basaltic province of western Alaska. These rocks were erupted in a distal retroarc setting; the cause of magmatism is unknown.

¹U.S. Geological Survey.

²Department of Earth and Ocean Sciences, University of British Columbia, Vancouver, BC.

³Department of Geology and Geophysics, University of Alaska, Fairbanks, AK.

⁴Deceased; former U.S. Geological Survey.

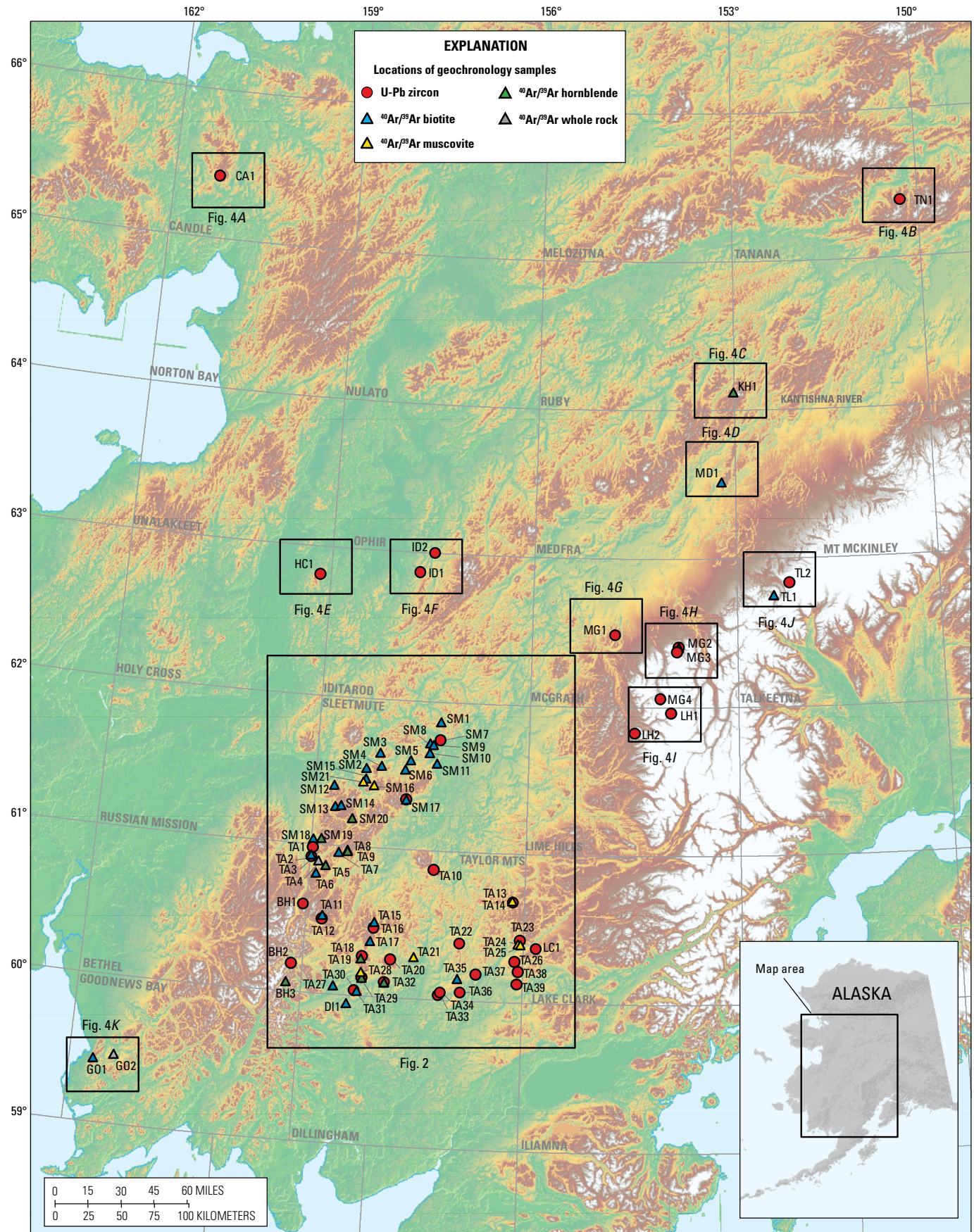
⁵Pacific Rim Geological Consulting, Inc.

⁶Apatite to Zircon, Inc.

Introduction

In this paper we report 50 new argon-40/argon-39 ($^{40}\text{Ar}/^{39}\text{Ar}$) ages and 33 new uranium-lead (U-Pb) ages from Late Paleozoic, Mesozoic, and Cenozoic igneous rocks of western Alaska (fig. 1). Most of the samples were collected

2 Regional Patterns of Mesozoic-Cenozoic Magmatism in Western Alaska Revealed by New U-Pb and ⁴⁰Ar/³⁹Ar Ages



in the course of geologic mapping by the U.S. Geological Survey (USGS) of what had been the largest unmapped swath in the United States—the Sleetmute and Taylor Mountains 1:250,000-scale quadrangles (fig. 2). Samples were collected in the Sleetmute quadrangle in 1993, 1994, 1997, 1998, and 1999 and were dated during that era by $^{40}\text{Ar}/^{39}\text{Ar}$. In the Taylor Mountains quadrangle, samples were collected in 2004, 2005, 2006, and 2008; these were dated by either $^{40}\text{Ar}/^{39}\text{Ar}$ or U-Pb, or in a few cases both. The rest of the samples are from miscellaneous smaller collections from the Bethel, Candle, Dillingham, Goodnews Bay, Holy Cross, Iditarod, Kantishna River, Lake Clark, Lime Hills, McGrath, Medfra, Talkeetna, and Tanana quadrangles (fig. 3 and 4A–K). Samples from the Tanana, Bethel, and Taylor Mountains quadrangles provide new age constraints for magmatism in rocks assigned to the Angayucham-Tozitna, Tikchik, and Togiak terranes, respectively. All of the other samples are from magmatic episodes that postdate the Paleozoic and Mesozoic assembly of these and other Alaskan terranes, including the Farewell, Kilbuck, and Yukon-Tanana.

Table 1 summarizes the geochronological results and identifies the analytical lab for each sample. The data reported here were obtained at four different labs. U-Pb zircon ages were obtained by thermal ionization mass-spectrometry (TIMS) at University of British Columbia (fig. 5; appendix 2, table A1) and by secondary ion mass-spectrometry (SIMS) at

the USGS-Stanford sensitive high-resolution ion microprobe-reverse geometry (SHRIMP-RG) facility at Stanford University (fig. 6; appendix 2, table A2). Almost all of the $^{40}\text{Ar}/^{39}\text{Ar}$ analyses (fig. 7; appendix 2, table A3) were done at the University of Alaska Fairbanks. A single $^{40}\text{Ar}/^{39}\text{Ar}$ analysis (sample MG2: 01ADw7a) was performed at the University of British Columbia (fig. 7; appendix 2, table A4). Analytical methods are detailed in appendix 1.

Each sample is identified using two schemes. The USGS field number uniquely identifies the year, project area, geologist, and station number. Thus, sample 85AM16a was collected in 1985, in Alaska, by Marti Miller, and the station was Miller's 16th. Any trailing letters a, b, c, and so on correspond to different rock types from that location. We also use a simplified scheme organized by quadrangle, wherein samples are identified by a two-letter abbreviation (fig. 1, caption) followed by numbers 1, 2, 3, and so on for each sample in the quadrangle. For example, sample ID2 is the second sample in Iditarod quadrangle.

Petrographic descriptions are based on thin section analysis unless specifically noted. For relating isotopic ages to stratigraphy, we use the time scale of Gradstein and others (2012). Obscure geographic features that are mentioned in the writeups of individual samples (for example hill 1632 or BM Sheep) can be found by referring to the corresponding 1:63,360-scale USGS topographic map, given in table 1.



Figure 1. Map of western Alaska showing key physiographic features and sample locations identified by number. The shaded relief was generated from the U.S. Geological Survey National Elevation Dataset (NED) 2-arc-second Digital Elevation Model (DEM). The black boxes indicate the areas of figures 2 and 4A–I. The gray grid shows the outlines of 1:250,000-scale quadrangles. The samples are identified by a two-letter abbreviation for the 1:250,000-scale quadrangle, followed by a number. Abbreviations for quadrangles are as follows: BH, Bethel; CA, Candle; DI, Dillingham; GO, Goodnews Bay; HC, Holy Cross; ID, Iditarod; KH, Kantishna River; LC, Lake Clark; LH, Lime Hills; MD, Medfra; MG, McGrath; SM, Sleetmute; TA, Taylor Mountains; TL, Talkeetna; TN, Tanana. Within a given 1:250,000-scale quadrangle, sample locations are numbered from west to east in the D-tier of 1:63,360-scale quadrangles (that is, the most northerly tier), then the C-tier, B-tier, and A-tier. $^{40}\text{Ar}/^{39}\text{Ar}$, argon-40/argon-39; U-Pb, uranium-lead.

4 Regional Patterns of Mesozoic-Cenozoic Magmatism in Western Alaska Revealed by New U-Pb and ⁴⁰Ar/³⁹Ar Ages

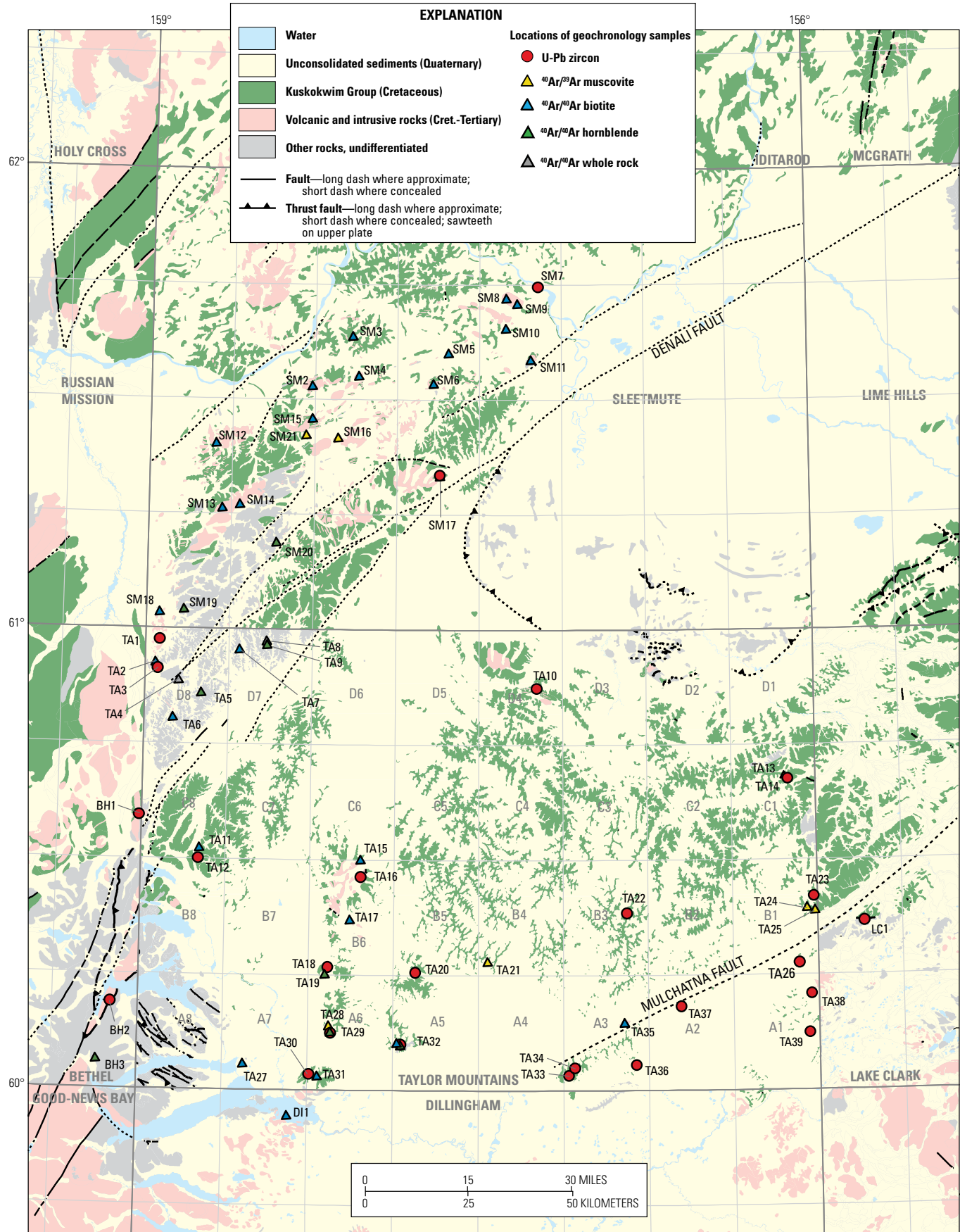


Figure 2. Simplified geologic map showing the context of samples in the Sleetmute, Taylor Mountains, Bethel, Dillingham, Lake Clark, and Goodnews Bay, Alaska, 1:250,000-scale quadrangles, the boundaries of which are bold gray lines. A grid of thin gray lines shows the outlines of 1:63,360-scale quadrangles. These are labeled A1 to D8 for regions south of 62° N latitude (as shown for Taylor Mountains quadrangle), or A1 to D6 north of that line. Geology derived from Wilson and others (2015). Faults are shown by solid or dashed lines. $^{40}\text{Ar}/^{39}\text{Ar}$, argon-40/argon-39; U-Pb, uranium-lead.

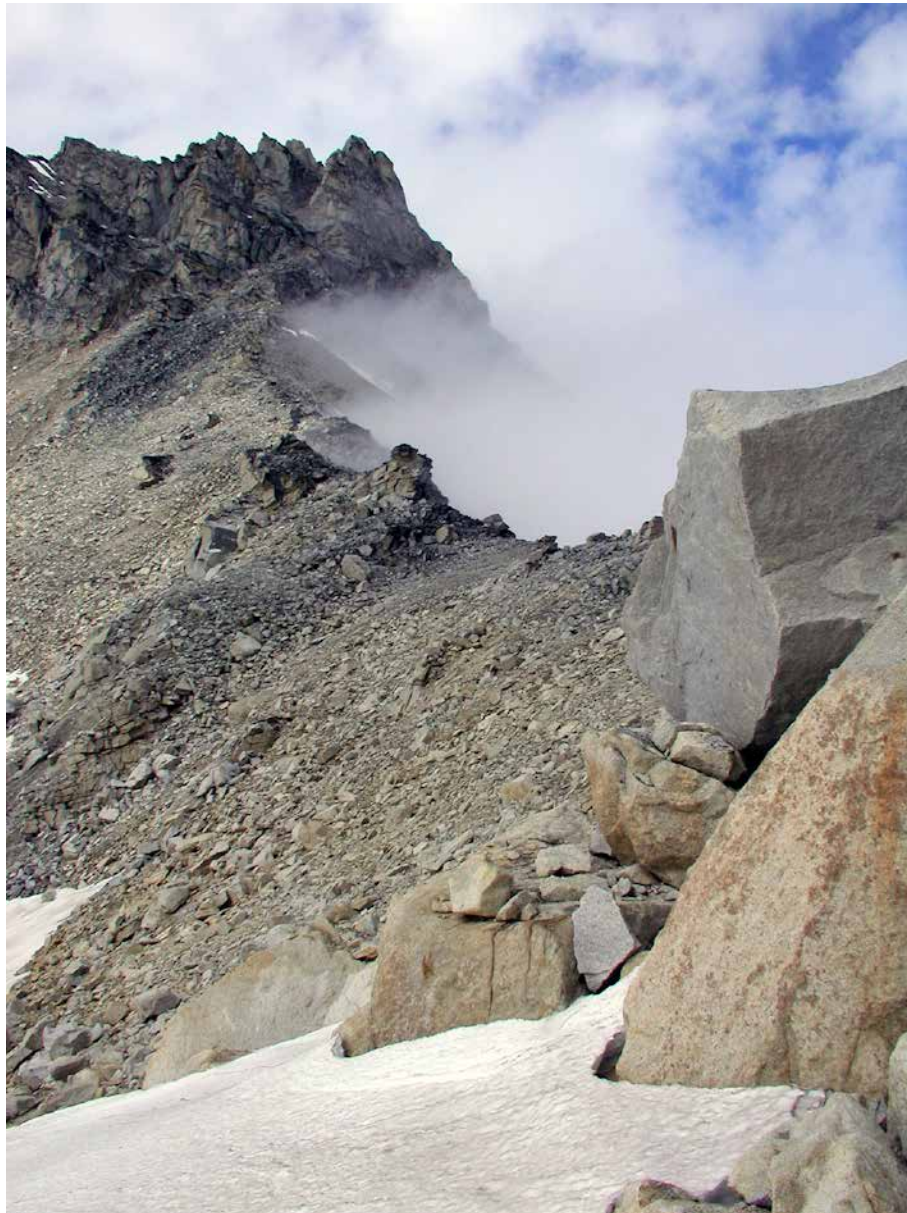
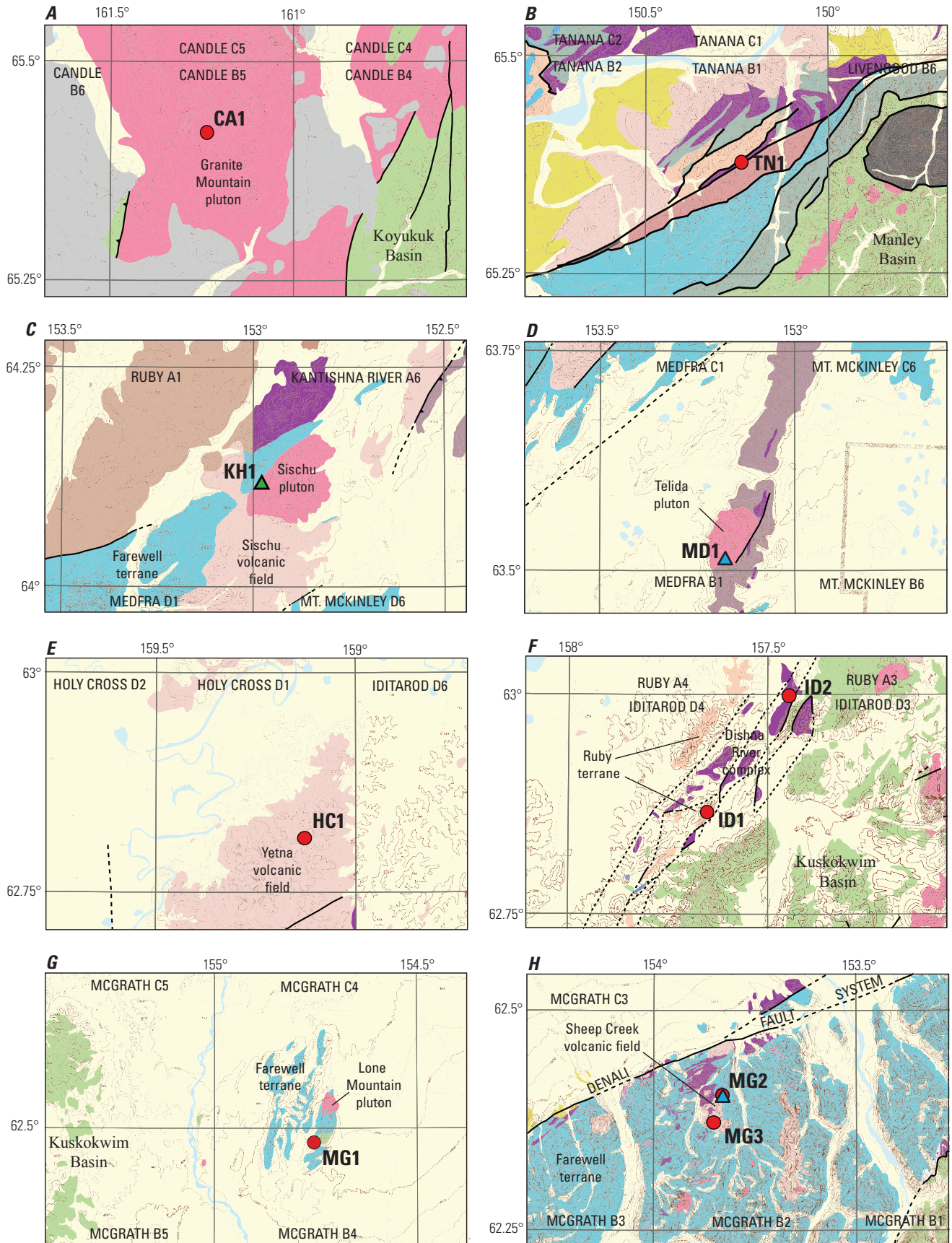


Figure 3. Photograph of the Tonzona pluton in the Alaska Range (Talkeetna quadrangle) dated at 58 million years old in the present study (U.S. Geological Survey photograph by Dwight Bradley).

6 Regional Patterns of Mesozoic-Cenozoic Magmatism in Western Alaska Revealed by New U-Pb and ⁴⁰Ar/³⁹Ar Ages



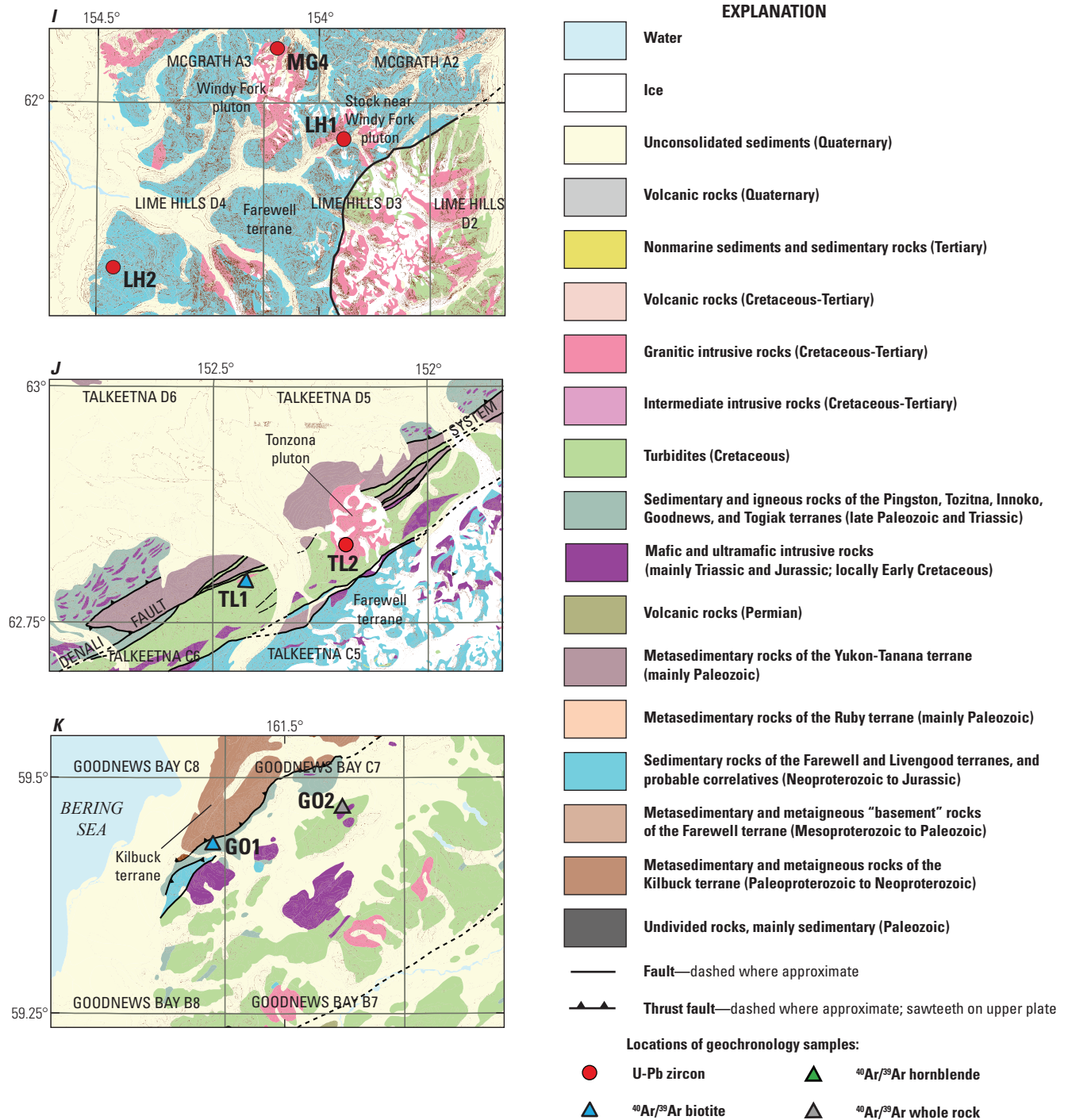


Figure 4. Simplified geologic maps, derived from Wilson and others (2015), showing the context of sample locations in western Alaska. *A*, Granite Mountain area in Candle quadrangle, from Patton and others (2009). *B*, Yukon River corridor in eastern Tanana quadrangle, from Wilson and others (1998). *C*, Sischu Mountain area in the four corners of Kantishna River, Ruby, Medfra, and Mt. McKinley quadrangles, from Wilson and others (1998) after Chapman and others (1975) and Patton and others (1980). *D*, Telida pluton area, Medfra quadrangle, from Wilson and others (1998) after Patton and others (1980). *E*, Yetna volcanic field in Holy Cross and Iditarod quadrangles, from Patton and others (2006) and Miller and Bundtzen (1994). *F*, Part of the Iditarod quadrangle, from Wilson and others (1998) after Miller and Bundtzen (1994). *G*, Lone Mountain area, McGrath quadrangle, from Wilson and others (1998). *H*, Sheep Creek Volcanic Field, McGrath quadrangle, from Wilson and others (1998) after Bundtzen and others (1997). *I*, Part of the western Alaska Range in Lime Hills and McGrath quadrangles, from Wilson and others (1998). *J*, Tonzona pluton in Talkeetna quadrangle, after Wilson and others (1998) after Reed and Nelson (1980). *K*, A part of the Goodnews Bay quadrangle, from Wilson and others (2013) after Hoare and Coonrad (1978). $^{40}\text{Ar}/^{39}\text{Ar}$, argon-40/argon-39; U-Pb, uranium-lead.

Table 1. Summary of new geochronology data for igneous-rock samples from western Alaska.

[Abbreviations: SHRIMP-RG—Sensitive high-resolution ion microprobe, reverse geometry at Stanford University; UBC, TIMS—University of British Columbia, thermal ionization mass spectrometry; UAF—University of Alaska Fairbanks; UBC, argon lab—University of British Columbia argon lab; A to Z LAICPMS—Apatite to Zircon, Inc., laser ablation inductively coupled plasma mass spectrometry; U-Pb, uranium-lead; ⁴⁰Ar/³⁹Ar, argon-40/argon-39; ²⁰⁶Pb/²³⁸U, uranium-206/uranium-238; %, percent; MSDW, mean square of weighted deviates; Mms., Mountains]

Map no.	Sample No.	Location	Latitude	Longitude	Rock unit dated	Rock type	Age (Ma)	Error	Method	Mineral	Lab	Notes
CA1	09ADw2	Candle B5	65.4188	-161.2358	Granite Mountain pluton	Syenite	112.0	0.9	U-Pb	Zircon	SHRIMP RG	Weighted average of 10 ²⁰⁶ Pb/ ²³⁸ U ages.
TN1	03ATI22a	Tanana B1	65.3797	-150.2414	Gabbro in Rampart Group	Gabbro	229.5	0.2	U-Pb	Zircon	UBC, TIMS	Weighted average of 4 overlapping, concordant ²⁰⁶ Pb/ ²³⁸ U ages.
KH1	97ADw126	Kantishna River A6	64.1194	-152.9778	Sischu igneous complex	Granite	65.9	0.5	⁴⁰ Ar/ ³⁹ Ar	Hornblende	UAF	Weighted averages of two plateau ages, Hornblende #1, 9 fractions, 86% ³⁹ Ar released, MSDW=1.7. Hornblende #2 (not illustrated in fig. 7), 9 fractions, 86% ³⁹ Ar released, MSDW=1.5.
MD1	97ADw118	Medfra C1	63.5147	-153.1783	Telida pluton	Granite	72.1	0.4	⁴⁰ Ar/ ³⁹ Ar	Biotite	UAF	Plateau age, 6 fractions, 81% ³⁹ Ar released, MSDW=4.5. Slight hump, perhaps due to recoil effects.
HC1	85AM16a	Holy Cross D1	62.8114	-159.1275	Volcanic rocks of the Yetna River area	Rhyolite	66.8	0.4	U-Pb	Zircon	SHRIMP RG	Weighted average of 10 overlapping, concordant ²⁰⁶ Pb/ ²³⁸ U ages; 3 analyses rejected.
ID1	84AM279b	Iditarod D4	62.8658	-157.6517	Ruby terrane orthogneiss	Orthogneiss	114.9	0.3	U-Pb	Zircon	UBC, TIMS	²⁰⁶ Pb/ ²³⁸ U age of a single concordant zircon.
ID2	85AM87c	Iditarod D3	62.9983	-157.4456	Gabbro in Dishna River mafic-ultramafic complex	Gabbro	116.6	0.1	U-Pb	Zircon	UBC, TIMS	Weighted average of four concordant, overlapping fractions.
MG1	11ADw109a	McGrath B4	62.4836	-154.7537	Satellite of Lone pluton	Granite	61.8	1.1	U-Pb	Zircon	SHRIMP RG	Weighted average of 8 ²⁰⁶ Pb/ ²³⁸ U ages.
MG2	01ADw7a	McGrath B2	62.4037	-153.8294	Tephra in Sheep Creek volcanic field	Felsic tuff	56.0	1.9	U-Pb	Zircon	UBC, TIMS	Age is a lower intercept defined by one concordant and three slightly discordant zircons. MSDW=0.96.
MG2	01ADw7a	McGrath B2	62.4037	-153.8294	Tephra in Sheep Creek volcanic field	Felsic tuff	54.7	0.7	⁴⁰ Ar/ ³⁹ Ar	Hornblende	UBC, Argon lab	Plateau age, 12 fractions, 100% of ³⁹ Ar released, MSDW=0.58.
MG3	01ADw8a	McGrath B2	62.3725	-153.8517	Tephra in Sheep Creek volcanic field	Felsic tuff	42.8	0.5	U-Pb	Zircon	SHRIMP RG	Weighted average of 8 ²⁰⁶ Pb/ ²³⁸ U ages.
MG4	11ADw117a	McGrath A3	62.0574	-154.0945	Windy Fork pluton	Granite	31.8	0.4	U-Pb	Zircon	SHRIMP RG	Weighted average of 7 of 8 ²⁰⁶ Pb/ ²³⁸ U ages.
TL1	03AM10a	Talkeetna D5	62.7497	-152.4281	Intrusion at BM Sheep	Granodiorite	58.7	0.6	⁴⁰ Ar/ ³⁹ Ar	Hornblende	UAF	Plateau age, 4 fractions, 58% ³⁹ Ar released, MSDW=1.2.

Table 1.—Continued

Map no.	Sample No.	Location	Latitude	Longitude	Rock unit dated	Rock type	Age (Ma)	Error	Method	Mineral	Lab	Notes
TL1	03AM10a	Talkeetna D5	62.7497	-152.4281	Intrusion at BMI Sheep	Granodiorite	58.0	0.3	⁴⁰ Ar/ ³⁹ Ar	Biotite	UAF	Plateau age, 8 fractions, 90% ³⁹ Ar released, MSWD=4.3.
TL2	03AM3a	Talkeetna D5	62.8324	-152.1901	Tonzona pluton	Granite	58.0	0.1	U-Pb	Zircon and monazite	UBC, TIMS	Weighted average of three zircon ²⁰⁶ Pb/ ²³⁸ U dates and two monazite ²⁰⁷ Pb/ ²³⁵ U dates.
SM1	97AM130a	Sleetmute D4	61.8672	-157.2369	Intrusion at hill 1195	Granite porphyry	70.9	0.4	⁴⁰ Ar/ ³⁹ Ar	Biotite	UAF	Plateau age, 11 fractions, 97% ³⁹ Ar released, MSWD=0.8.
SM2	97AM49b	Sleetmute C7	61.5314	-158.2622	Aghaluk stock	Granite porphyry	72.1	0.5	⁴⁰ Ar/ ³⁹ Ar	Biotite	UAF	Plateau age, 13 fractions, 99% ³⁹ Ar released, MSWD=1.1.
SM3	97AM161a	Sleetmute C6	61.6392	-158.0797	Intrusion at hill 1662	Quartz diorite	70.5	0.4	⁴⁰ Ar/ ³⁹ Ar	Biotite	UAF	Plateau age, 9 fractions, 90% ³⁹ Ar released, MSWD=1.7.
SM4	98AM62a	Sleetmute C6	61.5531	-158.0511	Intrusion at hill 1908	Granite porphyry	71.8	0.4	⁴⁰ Ar/ ³⁹ Ar	Biotite	UAF	Plateau age, 13 fractions, 98% ³⁹ Ar released, MSWD=0.4.
SM5	98AM192a	Sleetmute C5	61.6028	-157.6400	Intrusion in Oskawalik River drainage	Granite porphyry	71.9	0.4	⁴⁰ Ar/ ³⁹ Ar	Biotite	UAF	Plateau age, 5 fractions, 59% ³⁹ Ar released, MSWD=0.9.
SM6	97AM139a	Sleetmute C5	61.5358	-157.7097	Henderson stock	Monzonite	69.8	0.4	⁴⁰ Ar/ ³⁹ Ar	Biotite	UAF	Plateau age, 6 fractions, 80% ³⁹ Ar released, MSWD=1.0.
SM7	98ADw62e	Sleetmute C4	61.7447	-157.2308	Tephra in Kuskokwim Group	Tuff	88.3	1.0	U-Pb	Zircon	SHRIMP RG	Weighted average of 7 of 10 overlapping ²⁰⁶ Pb/ ²³⁸ U dates.
SM8	98AM274a	Sleetmute C4	61.7217	-157.3758	Barometer pluton	Granite to granodiorite	71.2	0.4	⁴⁰ Ar/ ³⁹ Ar	Biotite	UAF	Plateau age, 11 fractions, 85% ³⁹ Ar released, MSWD=1.2.
SM9	97RJ062	Sleetmute C4	61.7103	-157.3264	Barometer pluton	Granite to granodiorite	70.6	0.4	⁴⁰ Ar/ ³⁹ Ar	Biotite	UAF	Plateau age, 9 fractions, 90% ³⁹ Ar released.
SM10	97AM81a	Sleetmute C4	61.6569	-157.3767	Intrusion in Vreeland Creek drainage	Granite porphyry	74.6	0.5	⁴⁰ Ar/ ³⁹ Ar	Biotite	UAF	Plateau age, 6 fractions, 52% ³⁹ Ar released, MSWD=2.2.
SM11	97ARJ57	Sleetmute C4	61.5886	-157.2644	Red Mountain pluton	Andesite	75.3	0.5	⁴⁰ Ar/ ³⁹ Ar	Biotite	UAF	Plateau age, 4 fractions, 52% ³⁹ Ar released, MSWD=3.1.
SM12	99AM315a	Sleetmute B8	61.4050	-158.6983	Felsite in Victoria Creek headwaters	Felsite	73.7	0.5 (max age)	⁴⁰ Ar/ ³⁹ Ar	Biotite	UAF	Pseudo-plateau age, 5 fractions, 30% ³⁹ Ar released, MSWD=0.7.
SM13	99AM390a	Sleetmute B8	61.2647	-158.6661	Buckstock pluton	Granite	61.2	0.4	⁴⁰ Ar/ ³⁹ Ar	Biotite	UAF	Plateau age, 9 fractions, 93% ³⁹ Ar released, MSWD=0.8.
SM14	93AM46d	Sleetmute B7	61.2725	-158.5858	Buckstock pluton	Granite	59.9	0.4	⁴⁰ Ar/ ³⁹ Ar	Biotite	UAF	Plateau age, 9 fractions, 83% ³⁹ Ar released, MSWD=0.8.
SM15	99AM450a	Sleetmute B7	61.4603	-158.2600	Kaluarawluk igneous complex	Granite porphyry	60.2	0.5	⁴⁰ Ar/ ³⁹ Ar	Biotite	UAF	Plateau age, 11 fractions, 89% ³⁹ Ar released, MSWD=0.4.
SM16	98ARJ102	Sleetmute B6	61.4183	-158.1431	Intrusion near Holukuk Mountain	Felsite	60.5	0.4	⁴⁰ Ar/ ³⁹ Ar	White mica	UAF	Plateau age, 10 fractions, 99% ³⁹ Ar released, MSWD=0.8.
SM17	98ADw42a	Sleetmute B5	61.3355	-157.6780	Chuilinuk pluton	Granite	70.2	1.0	U-Pb	Zircon	SHRIMP RG	Weighted average of 11 overlapping ²⁰⁶ Pb/ ²³⁸ U dates.
SM17	98ADw42a	Sleetmute B5	61.3355	-157.6780	Chuilinuk pluton	Granite	69.8	0.4	⁴⁰ Ar/ ³⁹ Ar	Biotite	UAF	Plateau age, 9 fractions, 86% ³⁹ Ar released, MSWD=1.9.

Table 1.—Continued

Map no.	Sample No.	Location	Latitude	Longitude	Rock unit dated	Rock type	Age (Ma)	Error	Method	Mineral	Lab	Notes
SM18	93AM94a	Sleetmute A8	61.0364	-158.9406	Timber Creek pluton	Granite porphyry	62.9	0.5	⁴⁰ Ar/ ³⁹ Ar	Biotite	UAF	Plateau age, 6 fractions, 71% ³⁹ Ar released, MSWD=0.5.
SM19	99BT187	Sleetmute A8	61.0425	-158.8300	Intrusion in Timber Creek headwaters	Px-hb intrusive	66.0	1.0	⁴⁰ Ar/ ³⁹ Ar	Hornblende	UAF	Pseudo-plateau age, 5 fractions, 79% ³⁹ Ar release MSWD=4.3.
SM20	94AWK353b	Sleetmute A7	61.1906	-158.4181	Intrusion near hill 2639	Px-hb intrusive	80.3	0.9	⁴⁰ Ar/ ³⁹ Ar	Hornblende	UAF	4 fractions 62% ³⁹ Ar release MSWD=2.5.
SM21	94AM309a	Sleetmute B7	61.0139	-156.0314	Intrusion at hill 1764	Granite porphyry	62.8	0.8	⁴⁰ Ar/ ³⁹ Ar	White mica	UAF	10 fractions 65% ³⁹ Ar release MSWD=0.3.
LH1	11ADw115a	Lime Hills D3	61.9618	-153.9439	Stock near Windy Fork pluton	Granite	30.9	0.6	U-Pb	Zircon	SHRIMP RG	Weighted average of 7 of 9 overlapping ²⁰⁶ Pb/ ²³⁸ U dates.
LH2	11AD1a	Lime Hills D4	61.8253	-154.4622	Sill at Gagaryah deposit	Intermediate dike	63.2	2.2	U-Pb	Zircon	A to Z, LAICPMS	Weighted average of 5 overlapping ²⁰⁶ Pb/ ²³⁸ U dates.
BH1	05AM126a	Bethel C1	60.5925	-159.0119	Gemuk Mountain pluton	Quartz monzonite	71.6	0.3	U-Pb	Zircon	UBC, TIMS	Concordia age based on four concordant, overlapping zircon analyses. MSWD (of concordance)=0.47; probability (of concordance)=0.50.
BH2	08AM612a	Bethel A1	60.1874	-159.1193	Unnamed igneous rocks in Tikchik Complex	Intermediate volcanic rock	317.7	0.6	U-Pb	Zircon	UBC, TIMS	Weighted average of four concordant, overlapping ²⁰⁶ Pb/ ²³⁸ U dates.
BH3	08AM615c	Bethel A1	60.0639	-159.1764	Dike at Shadow Bay	Andesite	73.8	1.2	⁴⁰ Ar/ ³⁹ Ar	Hornblende	UAF	Loss spectra; no plateau. Isochron age (preferred) is 73.8 ± 1.2, ⁴⁰ Ar/ ³⁶ Ar=277.3 ± 2.4, N=10, MSWD=1.19.
TA1	05BT148	Taylor Mtns. D8	60.9743	-158.9359	Timber Creek pluton	Granite porphyry	63.2	0.6	U-Pb	Zircon	SHRIMP RG	Weighted average of 9 overlapping ²⁰⁶ Pb/ ²³⁸ U dates.
TA2	05AM247a	Taylor Mtns. D8	60.9268	-158.9533	Timber Creek pluton	Granite porphyry	62.4	0.4	⁴⁰ Ar/ ³⁹ Ar	Biotite	UAF	Plateau age, 9 fractions, 92% ³⁹ Ar released, MSWD=2.7.
TA3	05ADw158a	Taylor Mtns. D8	60.9118	-158.9432	Felsite in Gemuk Group	Felsic tuff	153.0	2.0	U-Pb	Zircon	SHRIMP RG	Weighted average of 9 of 11 overlapping ²⁰⁶ Pb/ ²³⁸ U dates.
TA4	05AM236a	Taylor Mtns. D8	60.8895	-158.8476	Flat Top basalt	Basalt	4.6	0.1	⁴⁰ Ar/ ³⁹ Ar	Whole rock	UAF	Plateau age, 5 fractions, 93% ³⁹ Ar released, MSWD=1.4.
TA5	05ADw29c	Taylor Mtns. D8	60.8619	-158.7453	Dike at hill 2164	Intermediate intrusive	69.6	0.3	⁴⁰ Ar/ ³⁹ Ar isochron	Hornblende	UAF	Isochron age (preferred) is 69.6 ± 0.3, ⁴⁰ Ar/ ³⁶ Ar=281.3 ± 3.7, N=11, MSWD=1.51. Sample does not meet criteria for plateau.
TA6	05AM239a	Taylor Mtns. D8	60.8077	-158.8699	Sill at hill 1768	Intermediate intrusive	74.7	0.4	⁴⁰ Ar/ ³⁹ Ar	Biotite	UAF	Plateau age, 7 fractions, 74% ³⁹ Ar released, MSWD=0.9.

Table 1.—Continued

Map no.	Sample No.	Location	Latitude	Longitude	Rock unit dated	Rock type	Age (Ma)	Error	Method	Mineral	Lab	Notes
TA7	05AM224c	Taylor Mtns. D7	60.9568	-158.5767	Intrusion at hill 2240	Quartz monzonite	87.7	1.7	⁴⁰ Ar/ ³⁹ Ar	Biotite	UAF	Sample does not meet criteria for plateau. Quoted age is based on the weighted mean of the six highest-temperature steps.
TA8	94ADw59b	Taylor Mtns. D7	60.9753	-158.4538	Sill in Kuskokwim Group	Intermediate intrusive	69.3	0.4	⁴⁰ Ar/ ³⁹ Ar	Whole rock	UAF	Plateau age, 4 fractions, 76% ³⁹ Ar released, MSWD=2.3.
TA9	05AM215a	Taylor Mtns. D7	60.9677	-158.4517	Sill in Kuskokwim Group	Intermediate intrusive	74.2	1.1	⁴⁰ Ar/ ³⁹ Ar	Hornblende	UAF	Isochron age, ⁴⁰ Ar/ ³⁶ Ar=285.4 ± 1.5, N=12, MSWD=2.16 (preferred over plateau age).
TA10	04AM45a	Taylor Mtns. D4	60.8723	-157.2393	Little Taylor pluton	Granite porphyry	68.6	0.1	U-Pb	Zircon	UBC, TIMS	Mean of 3 concordant and overlapping ²⁰⁶ Pb/ ²³⁸ U ages.
TA11	05AM144d B1#2	Taylor Mtns. C8	60.5263	-158.7407	Intrusion in Enatalik Creek drainage	Granite	68.7	0.3	⁴⁰ Ar/ ³⁹ Ar	Biotite	UAF	Plateau age, 10 fractions, 98% ³⁹ Ar released, MSWD=0.7. A second biotite split did not yield a plateau age.
TA12	08AM611a	Taylor Mtns. C8	60.5002	-158.7456	Intrusion near BM Tippy	Granite porphyry	69.8	1.6	U-Pb	Zircon	SHRIMP RG	Weighted average of 9 of 10 overlapping ²⁰⁶ Pb/ ²³⁸ U dates.
TA13	05AM115a	Taylor Mtns. C1	60.6839	-156.1376	Sill in Kuskokwim Group	Granite porphyry	68.3	0.3	⁴⁰ Ar/ ³⁹ Ar	White mica	UAF	Plateau age, 12 fractions, 99% ³⁹ Ar released, MSWD=0.2
TA14	05ADw17a	Taylor Mtns. C1	60.6740	-156.1220	Sill in Kuskokwim Group	Granodiorite	68.1	1.9	U-Pb	Zircon	SHRIMP RG	Weighted average of 9 of 10 overlapping ²⁰⁶ Pb/ ²³⁸ U dates.
TA15	05ADw59c	Taylor Mtns. C6	60.5024	-158.0222	Shotgun Hills pluton	Granodiorite	67.2	0.2	⁴⁰ Ar/ ³⁹ Ar	Biotite	UAF	Plateau age, 6 fractions, 85.7% ³⁹ Ar released, MSWD=1.03
TA16	05AM153a	Taylor Mtns. B6	60.4629	-158.0215	Shotgun Hills pluton	Granodiorite	67.9	1.2	U-Pb	Zircon	SHRIMP RG	Weighted average of 9 of 10 overlapping ²⁰⁶ Pb/ ²³⁸ U dates.
TA17	05AM154a	Taylor Mtns. B6	60.3724	-158.0679	Intrusion south of Shotgun airstrip	Granite porphyry	70.1	0.4	⁴⁰ Ar/ ³⁹ Ar	Biotite	UAF	Plateau age, 12 fractions, 98% ³⁹ Ar released, MSWD=1.6.
TA18	08AM630a	Taylor Mtns. B6	60.2675	-158.1642	Intrusion in Winchester claim area	Granite porphyry	69.5	1.0	U-Pb	Zircon	SHRIMP RG	Weighted average of 8 overlapping ²⁰⁶ Pb/ ²³⁸ U dates.
TA19	08SB129b	Taylor Mtns. B6	60.2536	-158.1764	Intrusion in Winchester claim area	Gabbro	77.6	0.7	⁴⁰ Ar/ ³⁹ Ar	Hornblende	UAF	Isochron age, ⁴⁰ Ar/ ³⁶ Ar=293.1 ± 2.7, N=12, MSWD=3.40 (preferred over plateau age).
TA20	08AM654b	Taylor Mtns. B5	60.2562	-157.7768	Intrusion near BM Reach	Granite porphyry	69.9	2.9	U-Pb	Zircon	SHRIMP RG	Weighted average of 12 ²⁰⁶ Pb/ ²³⁸ U dates.
TA21	06ADW557a	Taylor Mtns. B5	60.2816	-157.4571	Intrusion at hill 1311	Granite porphyry	67.3	0.2	⁴⁰ Ar/ ³⁹ Ar plateau	Muscovite	UAF	Plateau age, 6 fractions, 97% ³⁹ Ar released, MSWD=0.21.
TA22	08SK290a	Taylor Mtns. B3	60.3847	-156.8417	Dike at hill 1272	Granite or granodiorite	80.2	1.3	U-Pb	Zircon	SHRIMP RG	Weighted average of 4 of 8 ²⁰⁶ Pb/ ²³⁸ U dates (not reliable)
TA23	08SK316a	Taylor Mtns. B1	60.4189	-156.0143	Dike in Red Bluff area	Granite porphyry	66.7	0.4	U-Pb	Zircon	SHRIMP RG	Weighted average of 7 of 9 overlapping ²⁰⁶ Pb/ ²³⁸ U dates.

Table 1.—Continued

Map no.	Sample No.	Location	Latitude	Longitude	Rock unit dated	Rock type	Age (Ma)	Error	Method	Mineral	Lab	Notes
TA24	06AK42	Taylor Mtns. BI	60.3961	-156.0439	Dike in Red Bluff area	Granite porphyry	67.6	0.2	⁴⁰ Ar/ ³⁹ Ar	Muscovite	UAF	Plateau age, 8 fractions, 96.4% ³⁹ Ar released, MSWD=0.96.
TA25	06AM447a	Taylor Mtns. BI	60.3905	-156.0099	Dike in Red Bluff area	Granite porphyry	66.1	0.3	⁴⁰ Ar/ ³⁹ Ar plateau	White mica	UAF	Plateau age, 9 fractions, 96% ³⁹ Ar released, MSWD=0.1.
TA26	06AM453a	Taylor Mtns. BI	60.2755	-156.0835	Intrusion near Keefer Creek	Gabbro	78.2	0.8	U-Pb	Zircon	SHRIMP RG	Weighted average of 7 of 8 overlapping ²⁰⁶ Pb/ ²³⁸ U dates.
TA27	08AM614a	Taylor Mtns. A7	60.0585	-158.5323	Chaufchivak pluton	Granodiorite	69.2	0.3	⁴⁰ Ar/ ³⁹ Ar	Biotite	UAF	Plateau age, 5 fractions, 81.9% ³⁹ Ar released, MSWD=0.44.
TA28	08SB127c	Taylor Mtns. A6	60.1607	-158.1664	Intrusion at hill 1623	Quartz diorite or tonalite	76.9	0.9	⁴⁰ Ar/ ³⁹ Ar	White mica	UAF	Plateau age, 7 fractions, 99% ³⁹ Ar released.
TA29	08ADw825a	Taylor Mtns. A6	60.1233	-158.1484	Intrusion near hill 1635	Diorite	79.4	0.4	U-Pb	Zircon	SHRIMP RG	Weighted average of 7 of 8 overlapping ²⁰⁶ Pb/ ²³⁸ U dates.
TA29	08ADw825a	Taylor Mtns. A6	60.1233	-158.1484	Intrusion near hill 1635	Granite	79.1	0.3	⁴⁰ Ar/ ³⁹ Ar	Hornblende	UAF	Plateau age, 3 fractions, 96.6% ³⁹ Ar released, MSWD=0.14.
TA30	08ADw822a	Taylor Mtns. A6	60.0336	-158.2426	Tikehik Mountain pluton	Granite	62.2	0.8	U-Pb	Zircon	SHRIMP RG	Weighted average of 8 of 10 overlapping ²⁰⁶ Pb/ ²³⁸ U dates.
TA31	08SB117a	Taylor Mtns. A6	60.0327	-158.2053	Tikehik Mountain pluton	Granite	61.5	0.2	⁴⁰ Ar/ ³⁹ Ar	Biotite	UAF	Plateau age, 9 fractions, 98.3% ³⁹ Ar released, MSWD=1.84.
TA32	08SB147a	Taylor Mtns. A5	60.0999	-157.8410	Arrow pluton	Granite	74.3	1.1	U-Pb	Zircon	SHRIMP RG	Weighted average of 10 overlapping ²⁰⁶ Pb/ ²³⁸ U dates.
TA32	08SB147a	Taylor Mtns. A5	60.0999	-157.8410	Arrow pluton	Granite	74.0	0.2	⁴⁰ Ar/ ³⁹ Ar	Biotite	UAF	Plateau age, 5 fractions, 82.6% ³⁹ Ar released, MSWD=0.21.
TA32	08SB147a	Taylor Mtns. A5	60.0999	-157.8410	Arrow pluton	Granite	73.8	0.3	⁴⁰ Ar/ ³⁹ Ar	Hornblende	UAF	Plateau age, 4 fractions, 96.6.0% ³⁹ Ar released, MSWD=2.9.
TA33	08AM676a	Taylor Mtns. A3	60.0318	-157.0999	Dike near Sleitait Mountain	Granite porphyry	68.7	1.6	U-Pb	Zircon	SHRIMP RG	Weighted average of 9 of 10 overlapping ²⁰⁶ Pb/ ²³⁸ U dates.
TA34	08SB169a	Taylor Mtns. A3	60.0485	-157.0750	Sleitait pluton	Granite	61.4	0.7	U-Pb	Zircon	SHRIMP RG	Weighted average of 6 of 8 overlapping ²⁰⁶ Pb/ ²³⁸ U dates.
TA35	06AK69a	Taylor Mtns. A3	60.1490	-156.8562	Old Man pluton	Granite	66.7	0.3	⁴⁰ Ar/ ³⁹ Ar	Biotite	UAF	Plateau age, 9 fractions, 86% ³⁹ Ar released, MSWD=0.2.
TA36	08ADw896a	Taylor Mtns. A3	60.0545	-156.8036	Intrusion at hill 1004	Quartz monzonite to granite	69.1	0.9	U-Pb	Zircon	SHRIMP RG	Weighted average of 8 overlapping ²⁰⁶ Pb/ ²³⁸ U dates.
TA37	06ADw570e	Taylor Mtns. A2	60.1818	-156.6045	Intrusion at hill 1422	Quartz monzonite	61.0	0.1	U-Pb	Zircon	UBC, TIMS	Concordia age based on five concordant, overlapping zircon analyses. MSWD (of concordance)=0.56; probability (of concordance)=0.46

Table 1.—Continued

Map no.	Sample No.	Location	Latitude	Longitude	Rock unit dated	Rock type	Age (Ma)	Error	Method	Mineral	Lab	Notes
TA38	06ADw62a	Taylor Mtns. A1	60.2076	-156.0311	Rhyolite at hill 1678	Rhyolite	49.1	0.3	U-Pb	Zircon	UBC, TIMS	Concordia age based on two concordant, overlapping zircon analyses. MSWD (of concordance)=0.18; probability (of concordance)=0.67.
TA39	06ADw568a	Taylor Mtns. A1	60.1228	-156.0417	Intrusion at hill 982	Granite	56.3	0.2	U-Pb	Zircon	UBC, TIMS	Concordia age based on five concordant, overlapping zircon analyses. MSWD (of concordance)=0.00039; probability (of concordance)=0.98.
LC1	06ADw558a	Lake Clark B8	60.3650	-155.7922	Overlook pluton	Gabbro	76.5	0.2	U-Pb	Zircon	UBC, TIMS	Concordia age based on five concordant, overlapping zircon analyses. MSWD (of concordance)=1.8; probability (of concordance)=0.17.
GO1	06ADw603b	Goodnews B8	59.4311	-161.6497	Intrusion near Jacksmith Creek	Granite porphyry	70.7	0.3	⁴⁰ Ar/ ³⁹ Ar	biotite	UAF	Plateau age, 6 fractions, 94% ³⁹ Ar released, MSWD=0.9.
GO2	06ADw602c	Goodnews B7	59.4700	-161.3786	Dike at Island Mountain	Basalt	155.0	1.9	⁴⁰ Ar/ ³⁹ Ar	whole rock	UAF	Weighted mean of two plateau ages: 7 fractions, 43% ³⁹ Ar released, MSWD=1.3; and 8 fractions, 77% ³⁹ Ar released, MSWD=1.6.
D11	08ADw826a	Dillingham D7	59.9462	-158.3367	Tikehik Narrows pluton	Granite	60.2	0.2	⁴⁰ Ar/ ³⁹ Ar	biotite	UAF	Plateau age, 3 fractions, 62.0% ³⁹ Ar released, MSWD=1.44.

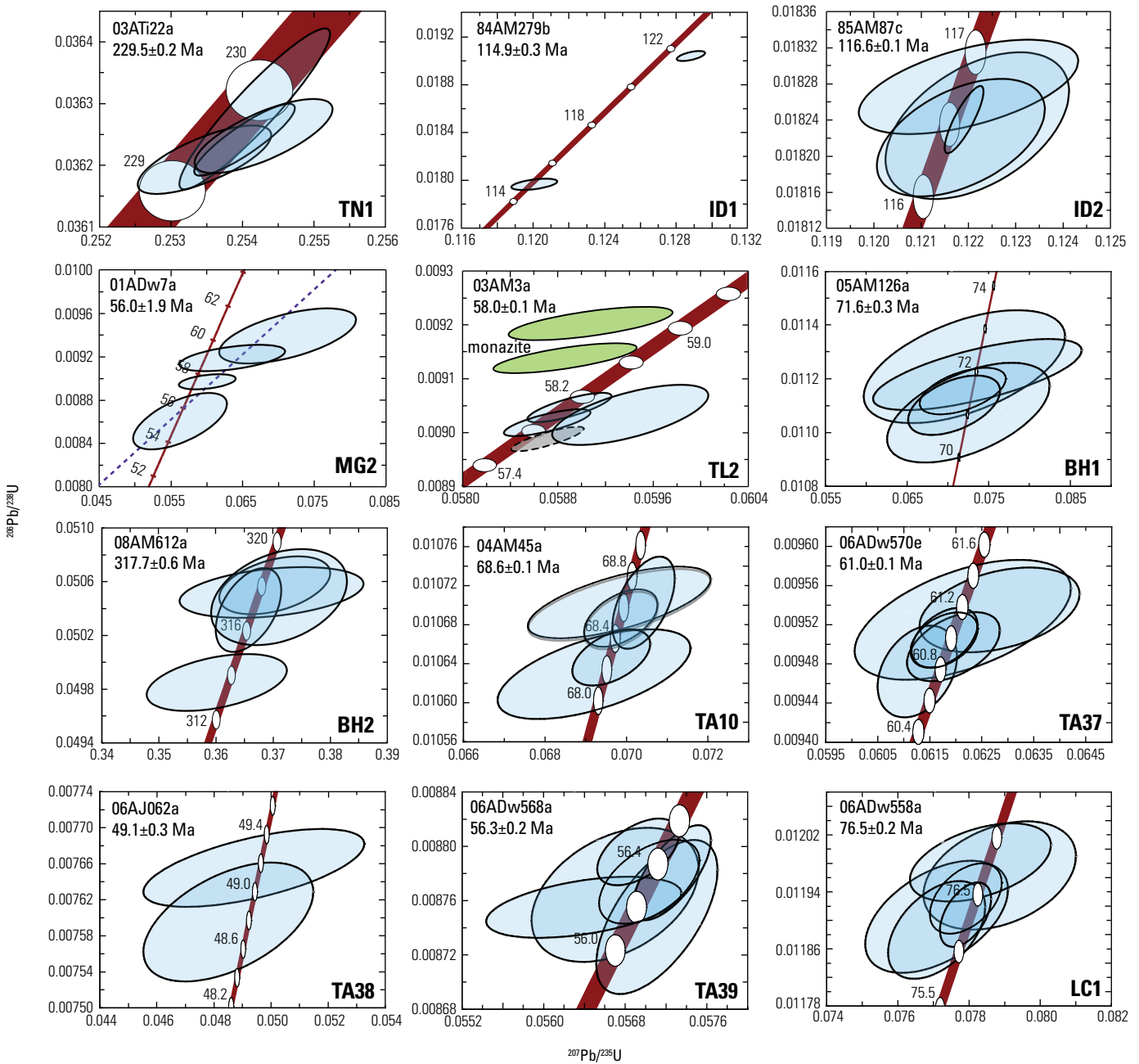


Figure 5. Concordia diagrams for samples of zircon (blue ellipses) and monazite (green ellipses) dated by uranium-lead (U-Pb) thermal ionization mass-spectrometry (TIMS) at the University of British Columbia. Each analysis is represented by an ellipse representing the 2-sigma uncertainty. Concordia curve is the brown line in each plot; these lines are of variable thickness depending on the scale of the plot. For most plots, ages (in millions of years, Ma) along the concordia curve are demarked by white ellipses, which convey the uncertainties in the decay constants of uranium-238 and uranium-235. The dashed line in the plot for sample MG2 meets the concordia curve at the lower intercept age. ²⁰⁶Pb/²³⁸U, lead-206/uranium-238; ²⁰⁷Pb/²³⁵U, lead-207/uranium-235.

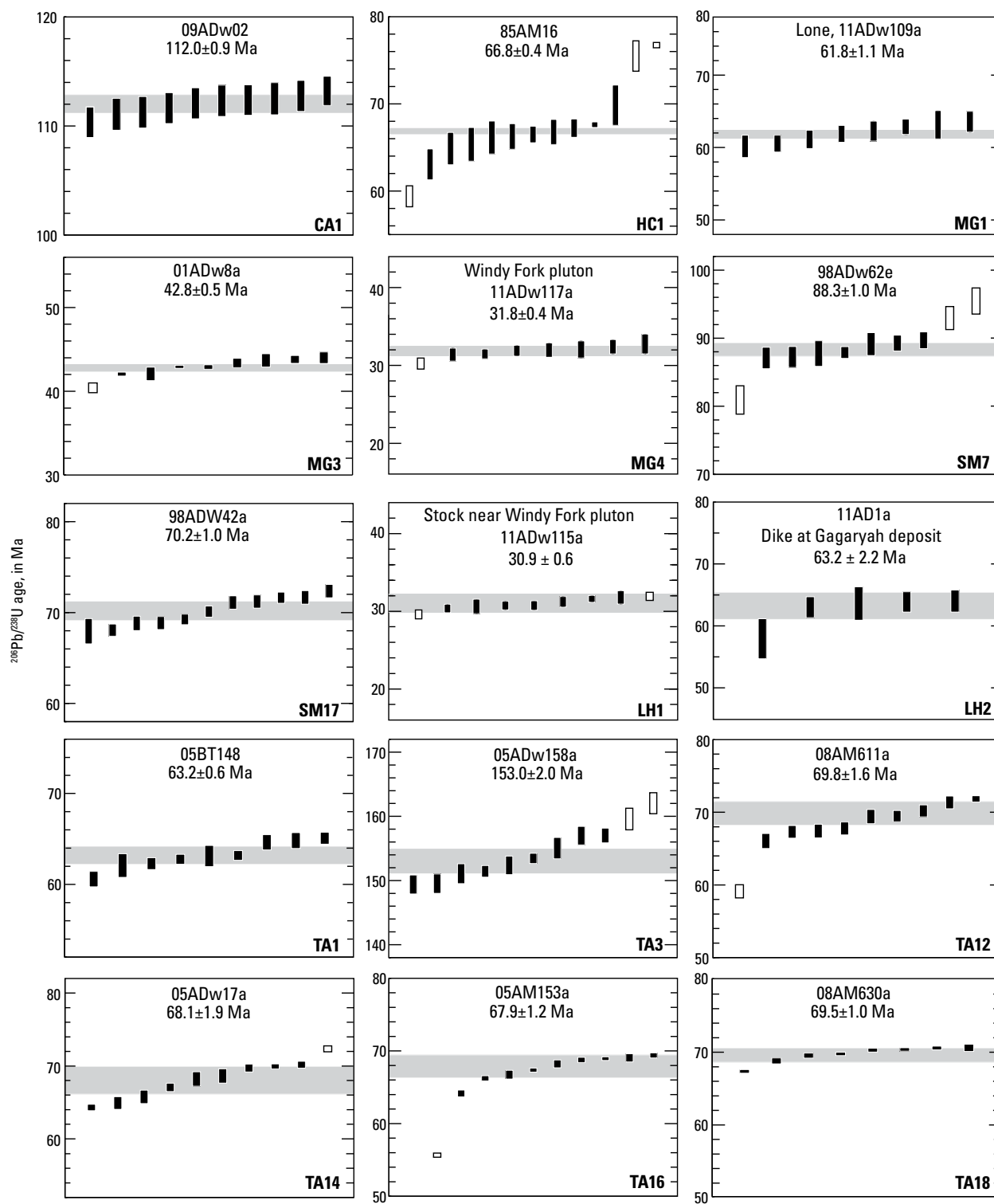


Figure 6. Plots showing weighted average lead-206/uranium-238 ($^{206}\text{Pb}/^{238}\text{U}$) ages of zircon samples (horizontal gray bars) and individual zircon ages (vertical black and white bars, with lengths corresponding to age ± 1 -sigma uncertainties). Analyses represented by black bars were used to calculate each weighted average age. Analytical data are given in appendix 2 (table A1 and table A5, sample LH2 only). Ma, millions of years.

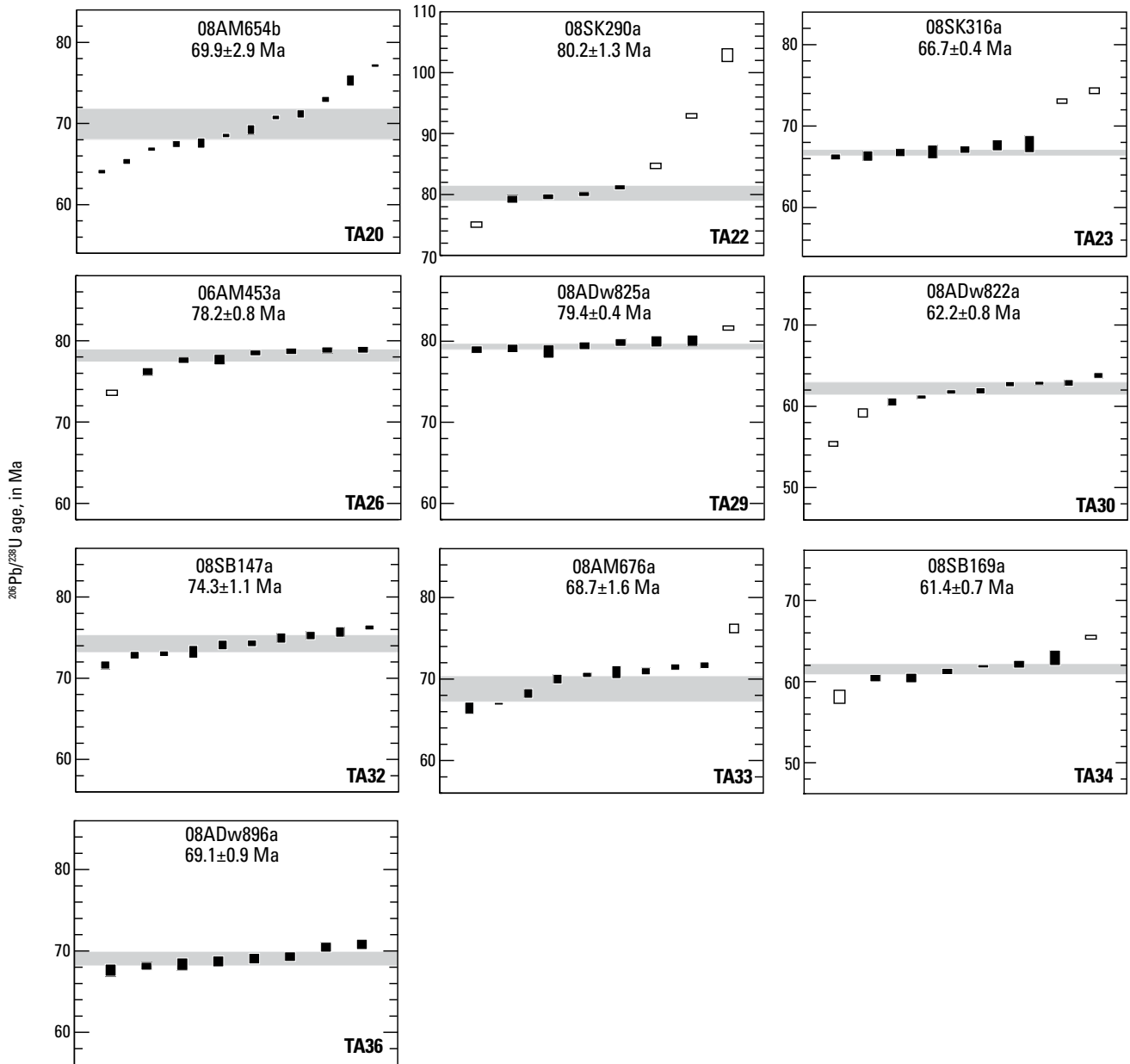


Figure 6.—Continued

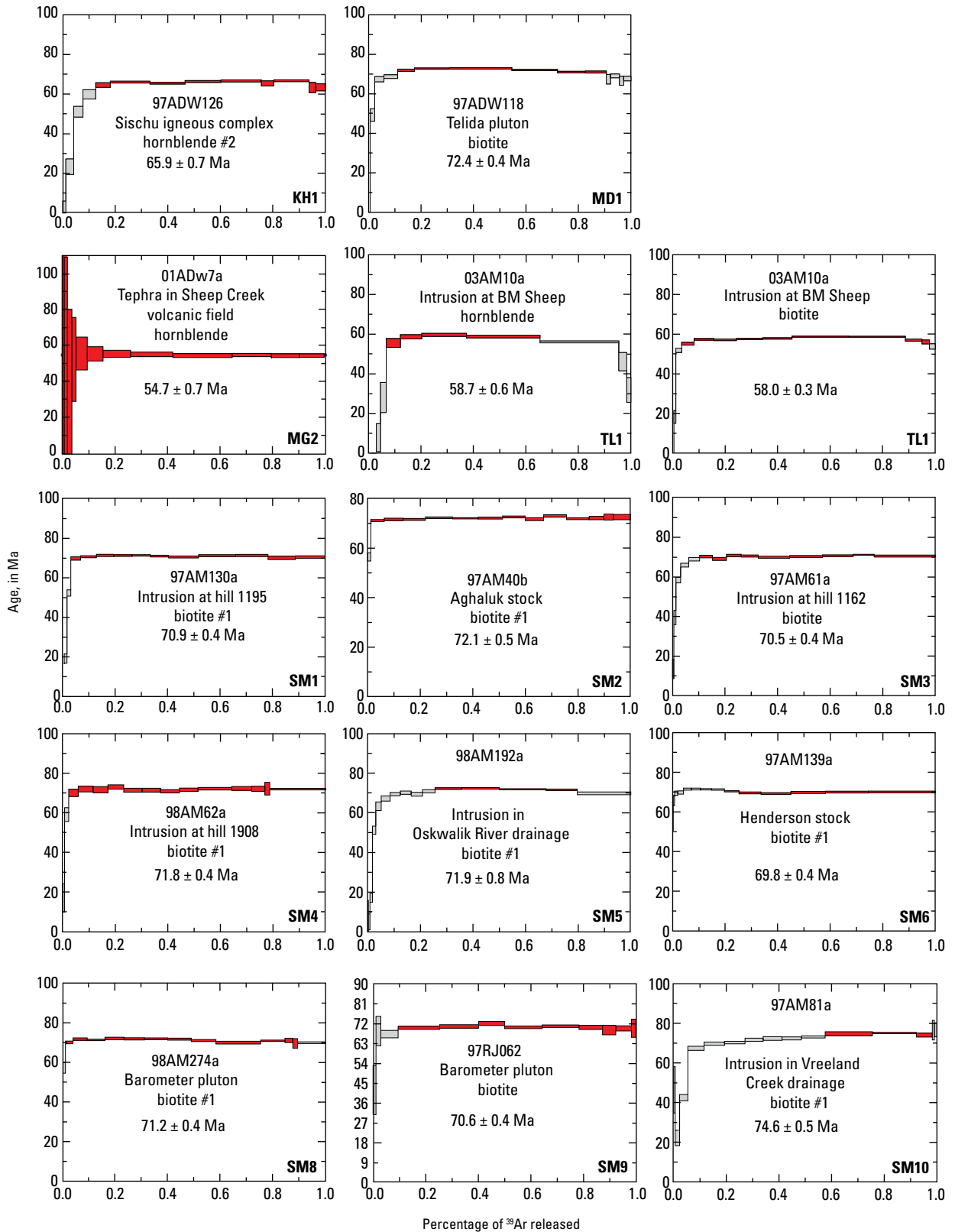


Figure 7. Plots of age spectra showing the results of incremental step heating of argon-40/argon-39 ($^{40}\text{Ar}/^{39}\text{Ar}$) samples. Red rectangles indicated steps used in the weighted mean plateau ages; gray rectangles were rejected. Ma, millions of years.

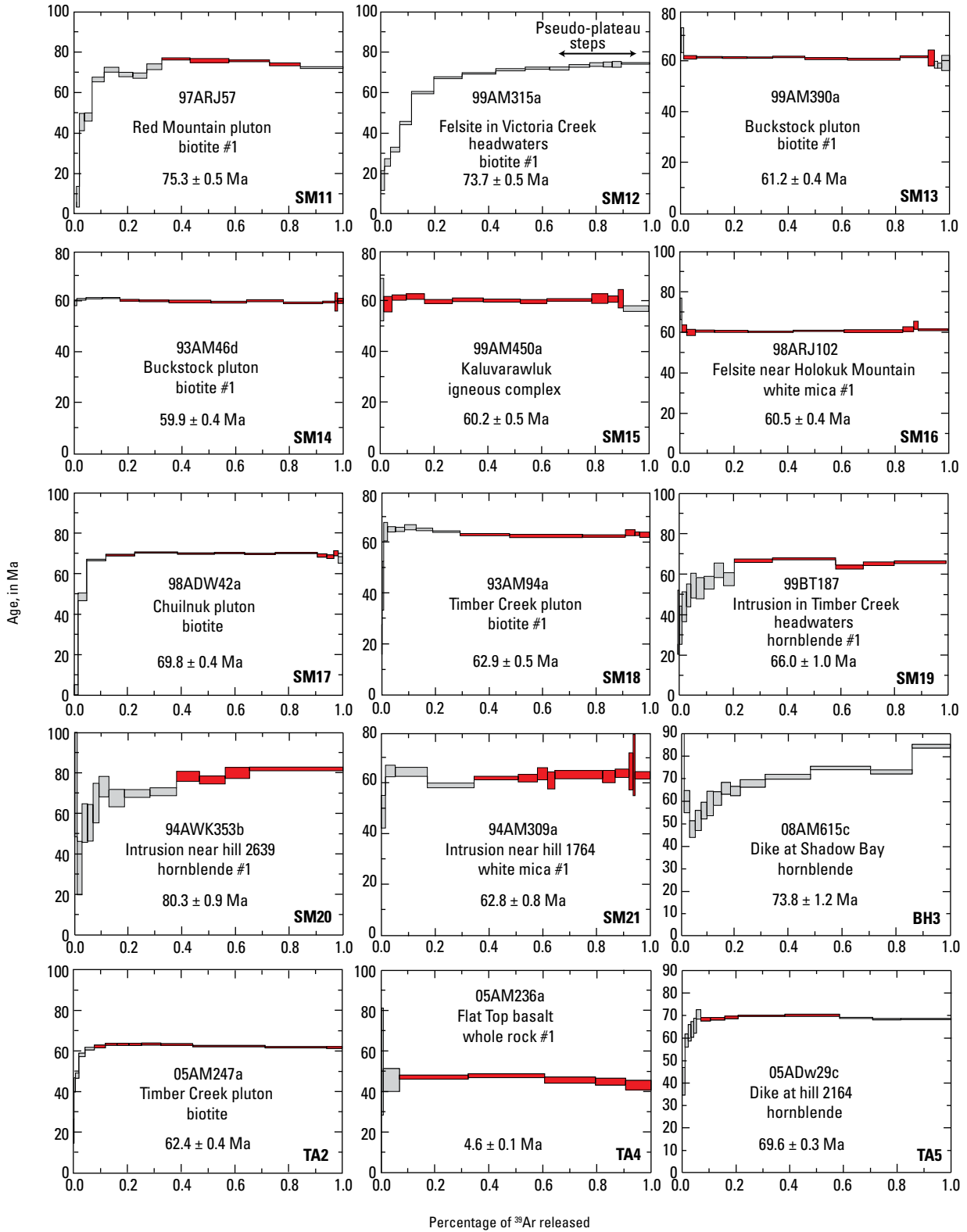


Figure 7.—Continued

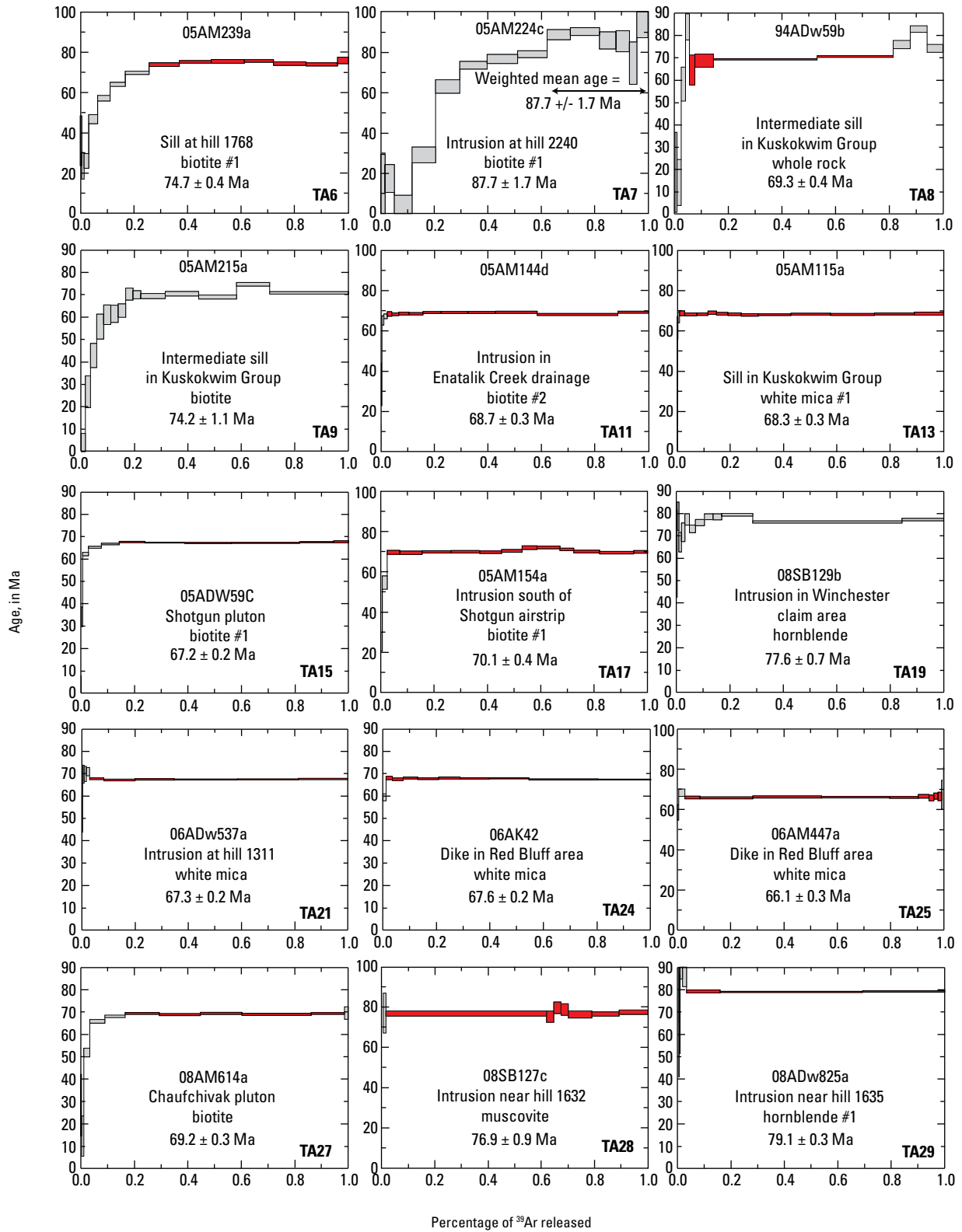


Figure 7.—Continued

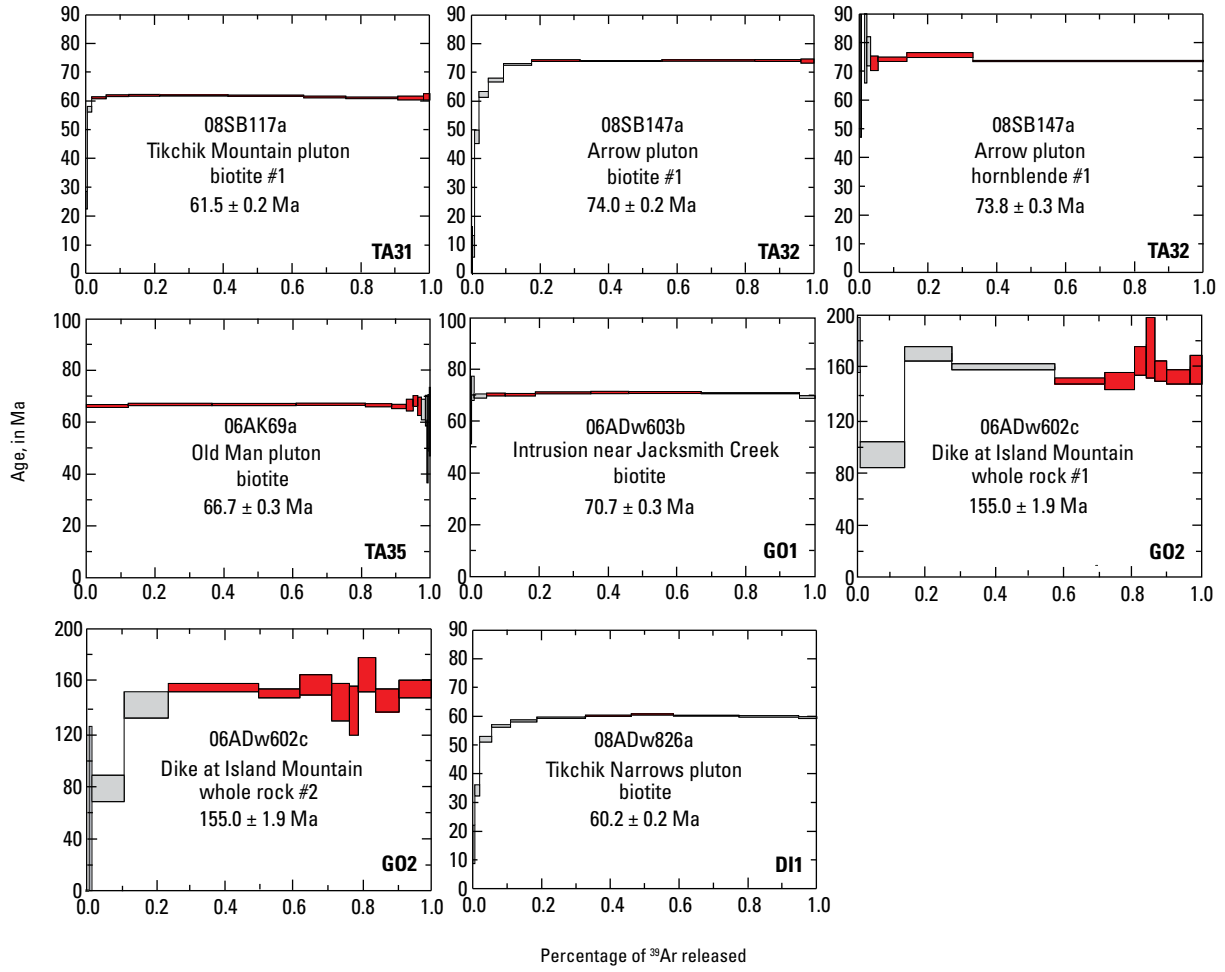


Figure 7.—Continued

Geochronology

Candle Quadrangle

CA1. Granite Mountain Pluton, Candle B5 Quadrangle

The Granite Mountain pluton is a composite body of Early Cretaceous granite, syenite, and nepheline syenite that intrudes Early Cretaceous volcanic rocks of the Koyukuk terrane (Patton and others, 2009) (fig. 4A). The geochronology sample (09ADW2), collected by Tom Donley in 2008, is a coarse-grained syenite containing abundant hornblende crystals that define a comagmatic lineation. Using the USGS-Stanford SHRIMP-RG, we obtained a U-Pb zircon age of 112.0 ± 0.9 million years (Ma). The age is the weighted average of 10 overlapping lead-206/uranium-238 ($^{206}\text{Pb}/^{238}\text{U}$) analyses (fig. 6). This age is consistent with previous U-Pb zircon age determinations of 109 and 112 Ma from elsewhere along this magmatic belt (Patton and others, 2009).

Tanana Quadrangle

TN1. Gabbro in Rampart Group, Tanana B1 Quadrangle

The Rampart Group of Mertie (1937) is an assemblage of mafic sills and flows and interlayered sedimentary rocks along the Yukon River corridor in Tanana quadrangle (fig. 4B). It has been included in the Angayucham-Tozitna terrane (Silberling and others, 1994; Till and others, 2006). The geochronology sample (03ATi22a) is a gabbro from a fault sliver of Rampart Group just north of the Victoria Creek strike-slip fault, in rocks assigned to unit Trmg of Reifenhuth and others (1997). The gabbro is pale orange-weathering, medium to dark green, and medium grained. In thin section, the rock has a subophitic texture and the major minerals are plagioclase and brown amphibole (some cored with relict clinopyroxene); there is minor anhedral quartz. Rims of actinolite on hornblende, fine-grained epidote in plagioclase, and small patches of chlorite indicate partial recrystallization at greenschist-facies conditions. We obtained a precise $^{206}\text{Pb}/^{238}\text{U}$ zircon age of 229.5 ± 0.2 Ma by TIMS. The quoted age is the mean of four overlapping, concordant $^{206}\text{Pb}/^{238}\text{U}$ ages (fig. 5).

Kantishna River Quadrangle

KH1. Sischu Igneous Complex, Kantishna River A6 Quadrangle

The Sischu Mountain igneous complex spans the northeastern corner of Medfra (Patton and others, 1980) and southwestern corner of the Kantishna River (Chapman and

others, 1975) quadrangles (fig. 4C). It intrudes the Farewell terrane. Our sample (97ADw126) is from a coarse-grained, equigranular, nonfoliated biotite-hornblende granite. Two splits of hornblende were analyzed by $^{40}\text{Ar}/^{39}\text{Ar}$ (fig. 7). Both splits yielded essentially identical ages of 65.9 ± 0.5 Ma as detailed in appendix 2 (table A3). Rhyolite samples from a different part of the igneous complex in Medfra quadrangle yielded potassium-argon (K-Ar) whole-rock ages of 71.0 ± 2.8 and 69.9 ± 2.7 Ma and a sanidine age of 66.3 ± 2.0 Ma (Moll and others, 1981).

Medfra Quadrangle

MD1. Telida Pluton, Medfra C1 Quadrangle

The Telida pluton, mapped as unit TKg by Patton and others (1980) in the eastern Medfra quadrangle, intrudes metasedimentary rocks of the Yukon-Tanana terrane (fig. 4D). It is a coarse-grained, A-type biotite granite (Moll and others, 1981). We obtained a $^{40}\text{Ar}/^{39}\text{Ar}$ biotite age of 72.1 ± 0.4 Ma (fig. 7) from a sample (97ADw118) of the granite. The age is based on a six-step plateau representing 81 percent of the ^{39}Ar released; the slight hump may be due to recoil effects. Within 2-sigma uncertainty, this overlaps the K-Ar age of 70.5 ± 2.8 Ma on biotite that was previously reported by Moll and others (1981).

Holy Cross Quadrangle

HC1. Volcanic Rocks of the Yetna River Area, Holy Cross D1 Quadrangle

The volcanic rocks of the Yetna River area crop out in a broad area of low hills in eastern Holy Cross quadrangle (fig. 4E). Miller and Bundtzen (1994) reported lava flows and tuffs of andesite and rhyolite, and minor flows of basalt. They reported eight K/Ar ages (on biotite, whole rock, and sanidine) ranging from 68.7 ± 2.1 to 54.4 ± 1.6 Ma. Our sample (85AM16a) is a welded rhyolite tuff, containing phenocrysts of embayed quartz, sanidine, and minor white mica. We obtained a U-Pb zircon SHRIMP-RG age of 66.8 ± 0.4 Ma (fig. 6). The zircon age is the weighted average $^{206}\text{Pb}/^{238}\text{U}$ age of 10 single-crystal analyses; three zircon analyses were discounted, one for suspected lead loss and two for suspected inheritance. The zircon age is very close to a K-Ar age of 67.0 ± 2.0 Ma on sanidine from the same sample (Miller and Bundtzen, 1994).

Iditarod Quadrangle

ID1. Ruby Terrane Orthogneiss, Unit PzPg, Iditarod D4 Quadrangle

A narrow belt of schist and associated deformed granitoids in Iditarod quadrangle was correlated by Miller and Bundtzen (1994) with the Ruby terrane (fig. 4F). A sample of

granitic orthogneiss (84AM279a) yielded a K-Ar biotite age of 108 ± 3 Ma (Miller and Bundtzen, 1994, p. 11), who interpreted the result as a post-metamorphic cooling age. We obtained a U-Pb zircon TIMS age from an archived sample (84AM279b) from the same outcrop. A single concordant zircon yielded the igneous age that we pick for this rock— 114.9 ± 0.3 Ma (fig. 5). Other zircon fractions, some of which are not shown, showed variable amounts of inheritance. The presence of about 115 Ma granitic rocks is entirely consistent with the interpretation favored by Miller and Bundtzen (1994) that their unit PzPg is part of the Ruby terrane. The main belt of Ruby terrane, north of the Yukon River, is intruded by a number of Early Cretaceous plutons, which have yielded U-Pb zircon ages of 118–113 Ma (Roeske and others, 1998).

ID2. Gabbro in Dishna River Mafic-ultramafic Complex, Iditarod D3 Quadrangle

The Dishna River mafic-ultramafic complex in Iditarod quadrangle (fig. 4F) is a poorly exposed, fault-bounded package of rocks along the Dishna River Fault Zone (Miller, 1990; Miller and Bundtzen, 1994). The following conventional K/Ar ages were reported by Miller and Bundtzen (1994). One gabbro sample yielded hornblende ages of 228 ± 25 and 222 ± 23 Ma; excess argon was suspected in both cases. Another gabbro sample yielded a hornblende age of 92.2 ± 2.8 Ma; partial resetting during the Late Cretaceous was suspected. We obtained a U-Pb zircon TIMS age of 116.6 ± 0.1 Ma from a third, archived sample (85AM87c) of hornblende gabbro (fig. 5). The age is the $^{206}\text{Pb}/^{238}\text{U}$ weighted average of four concordant, overlapping fractions, which establishes an Early Cretaceous intrusive age. Together, the available K-Ar and U-Pb results suggest that the Dishna River mafic-ultramafic complex includes rocks of two ages, Triassic and Early Cretaceous.

McGrath Quadrangle

MG1. Stock South of Lone Mountain, McGrath B4 Quadrangle

This sample is from a small stock that is presumably a satellite to the Lone Mountain pluton about 4 kilometers (km) to the north; it is much smaller than the dot used to locate the sample in figure 4G. Most of the bedrock in the Lone Mountain area is late Neoproterozoic to Paleozoic platformal carbonate deposits assigned to the Farewell terrane. The stock is leucocratic fine-grained granitic rock, or aplite, with sprays of black tourmaline. The sample (11ADw109a) is a medium to fine-grained equigranular granite composed mainly of intergrown equant 1- to 2-millimeter (mm) grains of quartz, plagioclase and microcline with less than 5 percent Fe-oxide stained biotite and 0.5- to 1.0-centimeter (cm) sprays of black tourmaline needles making up much less than 1 percent. Much smaller skeletal grains of brown pleochroic biotite are replaced

in cleavage-parallel strips by green biotite or clear muscovite, and elsewhere by pale green chlorite. Zircon is present in trace amounts. Zircons were dated using the SHRIMP-RG and indicate an age of 61.8 ± 1.1 Ma (fig. 6). The age is the weighted average of 8 overlapping $^{206}\text{Pb}/^{238}\text{U}$ ages. The new age overlaps with error with a biotite K-Ar age of 59.8 ± 1.6 Ma from the nearby Lone Mountain pluton (biotite granite) as reported by Reed and Lanphere (1972) and recalculated by Solie and others (1991).

MG2 and MG3. Tephra in Sheep Creek Volcanic Field, McGrath B2 Quadrangle

The Sheep Creek volcanic field of Bundtzen and others (1997) is a small, Paleogene eruptive center in the western Alaska Range (fig. 4H). We report ages from near the base and from the very top of the section. The lower sample, MG2 (01ADw7a), is a felsic tuff from what Bundtzen and others (1997) mapped as unit Tv_t—“intermediate and felsic air-fall tuff.” The tuff is several meters thick and includes fossil wood. Sample MG2 (01ADw7a) yielded very similar $^{40}\text{Ar}/^{39}\text{Ar}$ and U-Pb ages, both done at University of British Columbia. TIMS analysis of four zircon fractions yielded a discordant-concordant array with a lower intercept age (56.0 ± 1.9 Ma) (fig. 5). This overlaps within error with a $^{40}\text{Ar}/^{39}\text{Ar}$ plateau hornblende age of 54.7 ± 0.7 Ma (fig. 7). The argon age, which is based on 12 steps representing 100 percent of the ^{39}Ar released, is probably more reliable in this case because the zircon population is complex and largely xenocrystic, and the volcanic rocks appear to have lain undisturbed, and certainly not reheated, since they crystallized.

Sample MG3 (01ADw8a) is from the top of the Sheep Creek volcanic field, a reworked felsic tuff 10–20 cm thick interbedded with andesite-cobble conglomerate, possibly a lahar deposit. The sample is from what Bundtzen and others (1997) mapped as unit Tv_s—“volcaniclastic sandstone and lacustrine silt.” The sampled horizon contains abundant, well-preserved fossil leaves. Clear, prismatic zircons were dated using the SHRIMP-RG and indicate an age of 42.8 ± 0.5 Ma (fig. 6). The age is the weighted average of 8 overlapping $^{206}\text{Pb}/^{238}\text{U}$ ages; one outlying analysis was discounted. The new U-Pb zircon age is within error of, but much more precise than, a conventional K-Ar age of 43.5 ± 7.8 Ma on biotite from andesite in the Sheep Creek volcanic field (Solie and others, 1991).

Together, results from our two samples show that the Sheep Creek volcanic succession includes strata of two substantially different ages—(1) near the Paleocene-Eocene boundary and (2) mid-Eocene.

MG4. Windy Fork Pluton, McGrath A3 Quadrangle

The Windy Fork pluton is a peralkaline intrusion that cuts folded deep-water strata of the Paleozoic Dillinger subterrane (Gilbert and others, 1988). It has been targeted for closer scrutiny than most other intrusive complexes in the Alaska Range because

of its rare-earth-element (REE) resource potential (Bundtzen, 1999). The geochronology sample (MG4: 11ADw117a) is from a prominent cirque in the core of the pluton (fig. 4J). The sample is medium-coarse grained granite that has about 5 percent dark green amphibole. The amphibole, which is most likely hornblende, is 0.5–1 mm and lies in a groundmass of feldspar and quartz as large as 6 mm with trace zircon. Prismatic zircons were dated by SHRIMP-RG and indicate an age of 31.8 ± 0.4 Ma (fig. 6). The age is the weighted average of seven overlapping $^{206}\text{Pb}/^{238}\text{U}$ ages; one other analysis was rejected on suspicion of minor lead loss. Our result is similar to two published K-Ar ages from the pluton— 30.9 ± 0.9 on biotite and 29.7 ± 0.9 Ma on hornblende (Reed and Lanphere, 1972, as recalculated by Wilson and others, 1994, using 1976 decay constant).

Talkeetna Quadrangle

TL1. Intrusion at BM Sheep, Talkeetna D5 Quadrangle

This is a narrow, elongate intrusion near the northern front of the Alaska Range near Mystic Pass in Talkeetna quadrangle (fig. 4J) is a fine- to medium-grained biotite granodiorite to diorite. Our geochronology sample (03AM10a) is from near the summit of Peak 5753 (BM Sheep). We obtained a $^{40}\text{Ar}/^{39}\text{Ar}$ hornblende age of 58.7 ± 0.6 Ma. The age is based on a four-step plateau representing 58 percent of the ^{39}Ar released. A very similar but slightly more robust $^{40}\text{Ar}/^{39}\text{Ar}$ biotite age of 58.0 ± 0.3 Ma was also obtained (fig. 7). This age is based on an eight-step plateau representing 90 percent of the ^{39}Ar released. The biotite age, with its better defined plateau, is preferred for this sample.

TL2. Tonzona Pluton, Talkeetna D5 Quadrangle

This is a prominent, spectacularly exposed granite pluton along the northern front of the Alaska Range near Mystic Pass in Talkeetna quadrangle (fig. 4J). It is an unfoliated, medium-grained, biotite granite. Mirolitic cavities suggest relatively shallow-level emplacement. We obtained a U-Pb zircon TIMS age of 58.0 ± 0.1 Ma from sample 03AM3a (fig. 5). The age is a weighted average of three zircon $^{206}\text{Pb}/^{238}\text{U}$ dates and two monazite lead-207/uranium-235 ($^{207}\text{Pb}/^{235}\text{U}$) dates; one zircon date (dashed ellipse in fig. 5, plot TL2) was suspected of minor lead loss and was not included in the age calculation.

Sleetmute Quadrangle

SM1. Intrusion at Hill 1195, Sleetmute D4 Quadrangle

This sample (97AM130a) is from rubble crop of granite porphyry on hill 1195 in the drainage of the South Fork George

River, Sleetmute D4 quadrangle (fig. 2). The surrounding region is underlain by Kuskokwim Group, which the granitic rock presumably intruded; the porphyry body itself is too small to show on the map. The dated sample is a granite porphyry with biotite, quartz, and feldspar phenocrysts. A $^{40}\text{Ar}/^{39}\text{Ar}$ biotite age of 70.9 ± 0.4 Ma is based on a 11-step plateau representing 97 percent of the ^{39}Ar released (fig. 7).

SM2. Aghaluk Stock, Sleetmute C7 Quadrangle

This intrusion, which we refer to as the Aghaluk stock, is a biotite-quartz-feldspar granite porphyry in Sleetmute C6 and C7 quadrangles (fig. 2). We obtained a $^{40}\text{Ar}/^{39}\text{Ar}$ biotite age of 72.1 ± 0.5 Ma from sample 97AM40b (fig. 7). The age is based on a 13-step plateau representing 99 percent of the ^{39}Ar released.

SM3. Intrusion at Hill 1662, Sleetmute C6 Quadrangle

Hill 1662 in Sleetmute C6 quadrangle (fig. 2) is underlain by a north-northwest-striking dike or sill of medium- to fine-grained quartz diorite containing biotite, feldspar, and minor quartz. The dike or sill crosscuts hornfels assigned to the Kuskokwim Group. We obtained a $^{40}\text{Ar}/^{39}\text{Ar}$ biotite age of 70.5 ± 0.4 Ma from sample 97AM61a (fig. 7). The age is based on a nine-step plateau representing 90 percent of the ^{39}Ar released.

SM4. Intrusion at Hill 1908, Sleetmute C6 Quadrangle

Hill 1908 in Sleetmute C6 quadrangle (fig. 2) is underlain by a stock of hypabyssal biotite-quartz granite porphyry. We obtained a $^{40}\text{Ar}/^{39}\text{Ar}$ biotite age of 71.8 ± 0.4 Ma from sample 98AM62a (fig. 7). The age is based on a 13-step plateau representing 98 percent of the ^{39}Ar released.

SM5. Intrusion in Oskawalik River Drainage, Sleetmute C5 Quadrangle

A stock of unknown extent was encountered as a rubble pile along a creek bottom in the Oskawalik River drainage in Sleetmute C5 quadrangle (fig. 2). It is a garnet-biotite-feldspar porphyry of felsic to possibly intermediate composition. We obtained a $^{40}\text{Ar}/^{39}\text{Ar}$ biotite age of 71.9 ± 0.4 Ma from sample 98AM192a (fig. 7). The age is based on a five-step plateau representing 59 percent of the ^{39}Ar released.

SM6. Henderson Stock, Sleetmute C5 Quadrangle

Henderson Mountain, a prominent peak in Sleetmute C5 quadrangle (fig. 2), is underlain by plutonic rocks. The geochronology sample (97AM139a) is a monzonite or quartz

monzonite containing clinopyroxene, biotite, plagioclase, and lesser potassium feldspar and quartz. We obtained a $^{40}\text{Ar}/^{39}\text{Ar}$ biotite age of 69.8 ± 0.4 Ma (fig. 7), based on a six-step plateau representing 80 percent of the ^{39}Ar released.

SM7. Tephra in Kuskokwim Group, Sleetmute C4 Quadrangle

Zircons from a tuff within the Kuskokwim Group were dated using the USGS-Stanford SHRIMP-RG. The tuff (sample 98ADw62e) is a 1- to 2-cm-thick white-weathering, soft, clayey layer interbedded with turbidites of the Kuskokwim Group in cutbanks along the Kuskokwim River in Sleetmute C4 quadrangle (fig. 2). It yielded a U-Pb zircon (SHRIMP) age of 88.3 ± 1.0 Ma. This is the $^{206}\text{Pb}/^{238}\text{U}$ weighted average of seven zircon analyses; three zircon analyses were discounted, two on suspicion of inheritance and one on suspicion of lead loss (fig. 6). The age falls in the Coniacian stage of the Late Cretaceous according to the time scale of Gradstein and others (2012) and is broadly consistent with fossil evidence summarized by Elder and Box (1992).

SM8 and SM9. Barometer Pluton, Sleetmute C4 Quadrangle

Two samples were dated from either end of the prominent pluton that underlies Barometer Mountain near the village of Sleetmute (fig. 2). The pluton intrudes the Kuskokwim Group. From the west end of the summit ridge, sample SM8 (98AM274a) yielded a $^{40}\text{Ar}/^{39}\text{Ar}$ biotite age of 71.2 ± 0.4 Ma (fig. 7); the age is based on a 11-step plateau representing 85 percent of the ^{39}Ar released. From the east end, sample SM9 (97RJ062) is a rhyolite porphyry ($\text{SiO}_2=73$ percent) having a phenocryst assemblage of biotite, hornblende, quartz, and plagioclase. It yielded a $^{40}\text{Ar}/^{39}\text{Ar}$ biotite age of 70.6 ± 0.4 Ma (fig. 7); the age is a nine-step plateau which represents 90 percent of the ^{39}Ar released.

SM10. Intrusion in Vreeland Creek Drainage, Sleetmute C4 Quadrangle (97AM81a)

A granite porphyry body of unknown extent was discovered in the watershed of Vreeland Creek, about 6 km south of Barometer Mountain (fig. 2). The sample is a porphyry with phenocrysts of biotite, quartz, feldspar, and garnet. We obtained a $^{40}\text{Ar}/^{39}\text{Ar}$ biotite age of 74.6 ± 0.5 Ma (fig. 7). The age is based on a six-step plateau representing 52 percent of the ^{39}Ar released.

SM11. Red Mountain Pluton, Sleetmute C4 Quadrangle

The Red Mountain pluton underlies a prominent ridge about 10 km south-southwest of the village of Sleetmute (fig. 2).

The geochronology sample (97ARJ57) is a porphyritic andesite with plagioclase and biotite phenocrysts in a flinty, medium-gray groundmass. Nearby, the intrusion consists of a fine-grained, equigranular diorite. We obtained a $^{40}\text{Ar}/^{39}\text{Ar}$ biotite age of 75.3 ± 0.5 Ma (fig. 7). The age is based on a four-step plateau representing 52 percent of the ^{39}Ar released.

SM12. Felsite in Victoria Creek Headwaters, Sleetmute B8 Quadrangle

This sample is from the headwaters of Victoria Creek in Sleetmute B8 quadrangle (fig. 2). The geochronology sample (99AM315a) is a pyrite-bearing felsite containing phenocrysts of potassium feldspar and biotite. We obtained a poor $^{40}\text{Ar}/^{39}\text{Ar}$ biotite age of 73.7 ± 0.5 Ma (fig. 7). The quoted age is a pseudo-plateau based on the five oldest fractions, which represent only 30 percent of the ^{39}Ar released.

SM13 and SM14. Buckstock Pluton, Sleetmute B8 and B7 Quadrangles

The Buckstock pluton is a 5 by 25 km pluton of granite to granodiorite that broadly parallels the strike of bedding in the host Kuskokwim Group in southwestern Sleetmute quadrangle (fig. 2). Sample SM13 (99AM390a) yielded a single concordant U-Pb zircon with an age of 59.5 ± 0.5 Ma, as reported by Miller and others (2002) (appendix 2, table A5). From the same sample, we here report a $^{40}\text{Ar}/^{39}\text{Ar}$ biotite age of 61.2 ± 0.4 Ma (fig. 7). The argon age is based on a nine-step plateau representing 93 percent of the ^{39}Ar released. The argon geochronology sample is a biotite granite to granodiorite containing feldspar phenocrysts to 1 cm. The discrepancy between the $^{40}\text{Ar}/^{39}\text{Ar}$ biotite and U-Pb zircon ages has no obvious explanation, because typically, U-Pb ages are older not younger than $^{40}\text{Ar}/^{39}\text{Ar}$ ages from the same sample.

Sample SM14 (93AM46d), from about 5 km to the east, is a granite containing quartz, potassium feldspar phenocrysts to several centimeters, plagioclase, and biotite. We obtained a $^{40}\text{Ar}/^{39}\text{Ar}$ biotite age of 59.9 ± 0.4 Ma (fig. 7). The age is based on a nine-step plateau representing 83 percent of the ^{39}Ar released.

SM15. Kaluvarawluk Igneous Complex, Sleetmute B7 Quadrangle

Hypabyssal and volcanic rocks underlie Kaluvarawluk Mountain in northeastern Sleetmute B7 quadrangle (fig. 2). The dated sample (99AM450a), from a prominent northeast-striking dike off the northeastern flank of the mountain, is a granite porphyry containing phenocrysts of feldspar (to 2 cm), biotite, and quartz. We obtained a $^{40}\text{Ar}/^{39}\text{Ar}$ biotite age of 60.2 ± 0.5 Ma (fig. 7), based on an 11-step plateau representing 89 percent of the ^{39}Ar released.

SM16. Intrusion Near Holokuk Mountain, Sleetmute B6 Quadrangle

This sample is from a felsite plug east of, and along strike from, Holokuk Mountain in Sleetmute B6 quadrangle (fig. 2). Small phenocrysts of smoky quartz, feldspar, and white mica are set in a fine-grained pinkish-gray groundmass. We obtained a $^{40}\text{Ar}/^{39}\text{Ar}$ white mica age of 60.5 ± 0.4 Ma from sample 98ARJ102 (fig. 7). The age is based on a 10-step plateau representing 99 percent of the ^{39}Ar released.

SM17. Chuilnuk Pluton, Sleetmute B5 Quadrangle

The Chuilnuk pluton is part of a prominent volcanic-plutonic complex near the Denali Fault in Sleetmute quadrangle (fig. 2). The sample (98ADw42a) is a medium- to coarse-grained biotite granite containing relict garnet, epidote and zircon in trace quantities, and secondary chlorite, white mica, and calcite. The rock was dated by two methods. We obtained a U-Pb zircon age of 70.2 ± 1.0 Ma using the SHRIMP-RG. The age is the weighted average $^{206}\text{Pb}/^{238}\text{U}$ age of 11 single-crystal zircon ages (fig. 6). We also obtained a $^{40}\text{Ar}/^{39}\text{Ar}$ biotite age of 69.8 ± 0.4 Ma (fig. 7), based on a nine-step plateau that accounts for 86 percent of the ^{39}Ar released. Similarly, Decker and others (1995) reported four K-Ar biotite ages from the Chuilnuk pluton that range from 68.7 ± 2 to 67.5 ± 2 Ma. We interpret the U-Pb age as the crystallization age and the $^{40}\text{Ar}/^{39}\text{Ar}$ and K/Ar ages as cooling ages.

SM18, TA1 and TA2. Timber Creek Pluton, Sleetmute A8 and Taylor Mountains D8 Quadrangles

This intrusion, which we refer to as the Timber Creek pluton, straddles the boundary between Sleetmute A8 and Taylor Mountains D8 quadrangles. It was sampled in three locations (fig. 2). Sample SM18 (93AM94a) is from low hills west of Timber Creek in southwestern Sleetmute A8 quadrangle. This sample is a granite porphyry containing phenocrysts of quartz, potassium feldspar, plagioclase, biotite, and rare garnet. We obtained a $^{40}\text{Ar}/^{39}\text{Ar}$ biotite age of 62.9 ± 0.5 Ma (fig. 7). The age is based on a six-step plateau representing 71 percent of the ^{39}Ar released. Sample TA1 (05BT148), from Taylor Mountains D8 quadrangle, is a granite porphyry containing phenocrysts of quartz, biotite, plagioclase, and potassium feldspar. We obtained a U-Pb zircon SHRIMP-RG age of 63.2 ± 0.6 Ma (fig. 6). The age is the mean of nine overlapping $^{206}\text{Pb}/^{238}\text{U}$ ages. Sample TA2 (05AM247a), from Taylor Mountains D8 quadrangle, is a granite porphyry containing phenocrysts of biotite and plagioclase, in a groundmass of quartz, plagioclase, biotite, and potassium feldspar. This sample is from an apophysis or dike just south of the main Timber Creek pluton. Biotite yielded a $^{40}\text{Ar}/^{39}\text{Ar}$ age of 62.4 ± 0.4 Ma, based on a nine-step plateau representing 92 percent of the ^{39}Ar released (fig. 7). All three ages agree within 2-sigma error; we cite the U-Pb age as the preferred age for the Timber Creek pluton.

SM19. Intrusion in Timber Creek Headwaters, Sleetmute A8 Quadrangle

This sample (99BT187) of intermediate intrusive rock from the headwaters of Timber Creek in Sleetmute A8 quadrangle is from an area mainly underlain by the Gemuk Group of Miller and others (2007c) (fig. 2). The dated sample is a porphyritic pyroxene-hornblende intermediate intrusive. Phenocrysts are medium grained in a fine- to medium-grained groundmass of feldspar and quartz. Brown hornblende phenocrysts (as long as 4 mm) are relatively fresh looking. Altered clinopyroxene (?) phenocrysts are broken and rimmed by secondary chlorite. The groundmass shows secondary chlorite, calcite, and local white mica. We obtained a $^{40}\text{Ar}/^{39}\text{Ar}$ hornblende age of 66.0 ± 1.0 Ma (fig. 7), based on a five-step plateau representing 79 percent of the ^{39}Ar released.

SM20. Intrusion Near Hill 2639, Sleetmute A7 Quadrangle

This small stock intrudes the Gemuk Group in Sleetmute A7 quadrangle (fig. 2). The rock is a pyroxene-hornblende intrusive. We obtained a $^{40}\text{Ar}/^{39}\text{Ar}$ hornblende age of 80.3 ± 0.9 Ma from sample 94AWK353b (fig. 7). The age is based on a four-step plateau representing 62 percent of the ^{39}Ar released.

SM21. Intrusion at Hill 1764, Sleetmute B7 Quadrangle

This is a small granite porphyry body at hill 1764 in southwestern Sleetmute quadrangle (fig. 2). It intrudes the Kuskokwim Group. The sample (94AM309a) consists of phenocrysts of muscovite, biotite, quartz, and possible tourmaline in a very fine grained matrix. We obtained a $^{40}\text{Ar}/^{39}\text{Ar}$ white mica age of 62.8 ± 0.8 Ma (fig. 7), based on a 10-step plateau representing 65 percent of the ^{39}Ar released.

Lime Hills Quadrangle

LH1. Stock Near Windy Fork Pluton, Lime Hills D4 Quadrangle

This is a small stock a few kilometers east of the much larger Windy Fork pluton and is presumably a satellite of it (fig. 4I). The stock cuts folded deep-water strata of the Paleozoic Dillinger subterranean (Gamble and others, 2013). The sample is biotite-amphibole(?), medium grained equigranular granite. The biotite is fine-grained and ratty looking. The amphibole phenocrysts are as much as 1 mm in long dimension and appear to have been hornblende but are altered to green biotite(?). The quartz and feldspar in the groundmass are mostly 2–3 mm in size. Trace zircon is noted in thin section. Prismatic zircons from sample

11ADw115a were analyzed using the SHRIMP-RG and indicate an age of 30.9±0.6 Ma (fig. 6). The age is the weighted average of seven overlapping ²⁰⁶Pb/²³⁸U ages; one analysis was rejected on suspicion of minor lead loss, and another was rejected on suspicion of inheritance. The new U-Pb zircon age overlaps within 2-sigma uncertainty with the U-Pb zircon age reported above for the main Windy Fork pluton (31.8±0.4 Ma, sample MG4). Our result is similar to a published K/Ar biotite age of 29.3±0.8 Ma (Reed and Lanphere, 1972; recalculated by Wilson and others, 1991, using the 1976 decay constant).

LH2. Sill at Gagaryah Barite Deposit, Lime Hills D4 Quadrangle

The Gagaryah sedimentary barite deposit is hosted in a shale-dominant Upper Devonian succession in the Mystic subterrane of the Farewell terrane (Bundtzen and Gilbert, 1991). The mineralized section is exposed in a gully in the headwaters of the Gagaryah Creek drainage. We dated a 1-m-thick intermediate sill near the top of the exposed section (fig. 4J). The sample (11AD1a) is a plagioclase porphyry with millimeter-long altered plagioclase and smaller probable pyroxene and scraps of brown pleochroic hornblende mostly replaced by a fine aggregate of chlorite, calcite and epidote with irregular calcite veins. Zircons were dated by laser ablation inductively coupled plasma mass spectrometry (LA-ICP-MS) by Apatite to Zircon, Inc., at Washington State University (fig. 6). The yield was poor; only 13 zircons were recovered, and only 11 of these produced concordant ages. A cluster of five Paleogene zircons yielded a weighted average ²⁰⁶Pb/²³⁸U age of 63.2±2.2 Ma; we interpret this as the crystallization age of the sill. In addition, the sample yielded concordant zircons with ages of 159, 191, 1,243, 1,260, and 1,432 Ma (appendix 2, table A5). These are interpreted as xenocrysts. The Mesoproterozoic zircons were likely derived from Farewell terrane sedimentary rocks into which the sill was emplaced; the two Jurassic zircons presumably were derived from Jurassic igneous rocks at depth.

Bethel Quadrangle

BH1. Gemuk Mountain Pluton, Bethel C1 Quadrangle

The Gemuk Mountain pluton spans the boundary between the Taylor Mountains and Bethel 1:250,000-scale quadrangles (fig. 2). It intrudes dark, hornfelsed metasedimentary rocks that yielded Turonian bivalves (about 90 Ma, Late Cretaceous; Karl and others, 2011). The sample (05AM126a) is a hypidiomorphic-granular, medium-grained quartz monzonite. The mafic phases are biotite and pseudomorphs after pyroxene (now chlorite and calcite). We obtained a U-Pb zircon age of 71.6±0.3 Ma by TIMS (fig. 4). This concordia age is based on four concordant and overlapping single crystal ages.

BH2. Unnamed Igneous Rocks in Tikchik Terrane, Bethel A1 Quadrangle

The oldest rock reported here is an intermediate volcanic rock from Bethel quadrangle. It is part of an accretionary complex termed the Tikchik terrane (Box and others, 1993) (fig. 2). The sample (08AM612a) is a porphyritic volcanic rock containing phenocrysts of feldspar, one or more former mafic phases (now chlorite and calcite), and minor quartz. The groundmass is recrystallized and shows secondary calcite and white mica. We obtained a U-Pb zircon age of 317.7±0.6 Ma by TIMS (fig. 4). The age is the weighted average of four concordant and overlapping single crystal ²⁰⁶Pb/²³⁸U ages. An additional concordant zircon age is somewhat younger, and was not included in the weighted average calculation on suspicion of minor lead loss. Implications of this sample are discussed below.

BH3. Dike Near Shadow Bay, Bethel A1 Quadrangle

A fine-grained, holocrystalline, felsic to intermediate dike cuts greenstone and sandstone of the Tikchik complex north of Shadow Bay on Lake Chauekuktuli in Bethel A1 quadrangle (fig. 2). The sample (08AM615c) is an ophitic, fine-grained hornblende-clinopyroxene-plagioclase andesite. We obtained a ⁴⁰Ar/³⁹Ar isochron age of 73.8±1.2 Ma on hornblende. The age-release spectrum shows evidence of argon loss (fig. 7) and a true plateau cannot be defined.

Taylor Mountains Quadrangle

TA3. Felsite in Gemuk Group, Taylor Mountains D8 Quadrangle

Cutbanks along the Atsakovluk River in Taylor Mountains D8 quadrangle (fig. 2) expose a thick sequence of buff-weathering felsic tuff. The sampled tuff (05ADw158a), at water's edge, is about 20 meters thick; two other tuffs of similar thickness are exposed in inaccessible cliffs above, interbedded with black, green, and iron-stained fine-grained sedimentary rocks. The felsites contain altered glass shards and hence are volcanic rocks, not sills. Clear, prismatic zircons were dated by SHRIMP-RG and suggest an age of 153.0±2.0 Ma (fig. 6). The age is the mean of nine overlapping ²⁰⁶Pb/²³⁸U analyses; two other analyses were discounted on suspicion of inheritance.

We assign the felsic tuff to the restricted Gemuk Group (of Miller and others, 2007c) on the basis of age, lithology, and location. This extends the known age range of explosive volcanism in this unit. In a previous study, Miller and others (2007c) presented a generalized stratigraphic section of the (restricted) Gemuk Group in Taylor Mountains and Sleetmute quadrangles. It consists of Triassic pillow lavas, Triassic to Jurassic cherts and mudstones, and Lower Cretaceous sandstone plus minor tuff. The 153-Ma rhyolite ignimbrite is older than the

previous U-Pb zircon ages of 145.9 ± 1.4 and 136.5 ± 2.2 Ma from Gemuk Group tuffs (Miller and others, 2007c), extending the age of magmatism in this part of the Togiak terrane farther back in the Late Jurassic. The thickness of this tuff section as whole, the thicknesses of individual ignimbrites, and the welded texture together suggest that the eruptive center, and by inference the axis of the Togiak arc, could not have been far away, probably within several tens of kilometers.

TA4. Flat Top Basalt, Taylor Mountains D8 Quadrangle

Flat Top Mountain, in the upper reaches of Atsaksovluk River drainage in Taylor Mountains D8 quadrangle (fig. 2), is underlain by Neogene basalt. The rock is a porphyritic olivine-clinopyroxene-plagioclase basalt with 48 weight percent SiO_2 . Phenocrysts are mostly subhedral and make up about 30 percent of the rock by volume. We obtained a $^{40}\text{Ar}/^{39}\text{Ar}$ whole-rock age of 4.6 ± 0.1 Ma from sample 05AM236a. The age is based on a five-step plateau representing 93 percent of ^{39}Ar released (fig. 7). The new result agrees with previously published K-Ar ages of 4.64 ± 0.14 Ma (plagioclase) and 4.72 ± 0.14 Ma (whole rock) (Reifenstuhl and others, 1985).

TA5. Dike at Hill 2164, Taylor Mountains D8 Quadrangle

This sample is from an intermediate dike cutting the restricted Gemuk Group (of Miller and others, 2007c) at hill 2164 in the easternmost headwaters of Waterboot Creek, Taylor Mountains D8 quadrangle (fig. 2). The sample (05ADw29c) is a hornblende-bearing intermediate rock consisting of a felted lathwork of hornblende and plagioclase with interstitial quartz and much secondary chlorite. We obtained a $^{40}\text{Ar}/^{39}\text{Ar}$ hornblende age of 70.1 ± 0.4 Ma from a five-step plateau representing 52 percent of the ^{39}Ar released (fig. 7). The age spectrum shows evidence of argon loss. The corresponding isochron age (not shown) is 69.6 ± 0.3 Ma and is preferred.

TA6. Sill at Hill 1768, Taylor Mountains D8 Quadrangle

This sample is from hill 1768 on the divide between Waterboot and Cinnabar Creeks in Taylor Mountains D8 quadrangle (fig. 2). It intrudes rocks assigned to the restricted Gemuk Group of Miller and others (2007c), which ranges in age from Triassic to Early Cretaceous and is part of the Togiak terrane. The sample (05AM239a) is a fine-grained, intermediate rock with granular to subophitic texture; plagioclase, minor quartz and secondary biotite are present. Primary clinopyroxene has been altered to chlorite and calcite. We obtained a $^{40}\text{Ar}/^{39}\text{Ar}$ biotite age of 74.7 ± 0.4 Ma, based on a seven-step plateau representing 74 percent of the ^{39}Ar released (fig. 7).

TA7. Intrusion at Hill 2240, Taylor Mountains D7 Quadrangle

A small intermediate intrusive body was discovered at hill 2240 in the northwestern part of the Taylor Mountains D7 quadrangle (fig. 2). It intrudes the Gemuk Group. The sample (05AM224c) is a fine-grained, granular to subhedral, altered quartz monzonite. Mafic phases are early clinopyroxene, later hornblende, and even later biotite. A biotite separate yielded a disturbed $^{40}\text{Ar}/^{39}\text{Ar}$ age spectrum (fig. 7). A plateau age cannot be determined. We suggest an age of 87.7 ± 1.7 Ma based on the weighted mean of the six highest-temperature steps.

TA8 and TA9. Sills in Kuskokwim Group, Taylor Mountains D7 Quadrangle

Sample TA8 (94ADw59b) is from a vesicular, biotite-bearing intermediate sill near the northern edge of Taylor Mountains D7 quadrangle that intrudes the Kuskokwim Group (fig. 2). A baked, concordant basal contact and the lack of pillow structures together suggest that it is more likely a sill than a flow that erupted onto a submarine fan. The geochronology sample is a subophitic textured andesite or basaltic andesite with primary hornblende, minor biotite, and possible minor relict clinopyroxene. Sample 94ADw59B yielded a whole rock sample plateau age of 69.3 ± 0.4 Ma; the age is based a four-step plateau representing 76 percent of ^{39}Ar released (fig. 7).

A lithologically similar igneous rock (sample TA9, 05AM215a) was collected roughly along strike, about 0.5 km to the south. The sample is a fine-grained, subophitic porphyry. Relict clinopyroxene is present; later brown hornblende is commonly rimmed by lesser biotite. We obtained a $^{40}\text{Ar}/^{39}\text{Ar}$ hornblende age of 70.1 ± 0.4 Ma (fig. 7). The age is based on a six-step plateau representing 71 percent of the ^{39}Ar argon released. The age spectrum shows evidence of argon loss. An isochron age is calculated at 74.2 ± 1.1 Ma (not shown). We feel that the isochron age is more representative of the cooling age of this sample, but should be considered a possible minimum age.

TA10. Little Taylor Pluton, Taylor Mountains D4 Quadrangle

The Little Taylor Mountains are underlain by a series of steeply dipping, tabular bodies, which are too small to show on figure 2. These granite porphyry intrusions strike roughly 300° , parallel to regional bedding strike. Minor associated gold mineralization has been reported (Hudson, 2001). The sample (04AM45a) is a granite porphyry containing abundant, blocky phenocrysts of quartz, plagioclase, and potassium feldspar, smaller phenocrysts of white mica, and a fine-grained groundmass of quartz and feldspar. We obtained a U-Pb zircon TIMS age of 68.6 ± 0.1 Ma, based on the mean of three concordant and overlapping single crystal $^{206}\text{Pb}/^{238}\text{U}$ ages (fig. 5).

TA11. Intrusion in Enatalik Creek drainage, Taylor Mountains C8 Quadrangle

A small stock was discovered near the southern edge of the Taylor Mountains C8 quadrangle (fig. 2) in the headwaters of Enatalik Creek, 2–3 km north of BM Tippy (see TA12 below). The sample (05AM144d) is a granite with large crystals of potassium feldspar, quartz (rounded), plagioclase, and less abundant biotite; a finer grained groundmass of the same minerals fills interstices. We obtained a $^{40}\text{Ar}/^{39}\text{Ar}$ biotite age of 68.7 ± 0.3 Ma (fig. 7). The age is based on a 10-step plateau representing 98 percent of the ^{39}Ar released.

TA12. Intrusion Near BM Tippy, Taylor Mountains C8 Quadrangle

Rubble of a medium-grained intrusive rock of intermediate composition was sampled along the southern boundary of the Taylor Mountains C8 quadrangle, about 0.5 km south of BM Tippy (fig. 2). Abundant hornfels in the area of BM Tippy suggests the presence of a sizeable pluton at depth, of which the present sample is the only surface exposure studied. The sample (08AM611a) is a granite porphyry. Phenocrysts are of plagioclase, quartz, and an altered mafic mineral that was probably hornblende. We obtained a U-Pb zircon SHRIMP-RG age of 69.8 ± 1.6 Ma (fig. 6). The age is the mean of nine overlapping $^{206}\text{Pb}/^{238}\text{U}$ analyses; one zircon analysis was suspected of lead loss and was discounted. A nearby detrital zircon sample from contact-metamorphosed Kuskokwim Group yielded zircons as young as 77, 78, and 79 Ma (Miller and others, 2007b). These ages constrain the time between deposition and plutonism in this part of the Kuskokwim Basin to only about 7 million years.

TA13 and TA14. Sills in Kuskokwim Group, Taylor Mountains C1 Quadrangle

Two narrow, apparently sill-like intrusive bodies were mapped along the eastern edge of Taylor Mountains quadrangle (fig. 2). The more northerly of the two (TA13, 05AM115a) is a granite porphyry containing phenocrysts of quartz, feldspar, and white mica, and what appear to be xenocrysts of a chloritized mafic mineral and altered garnet. The fine-grained groundmass consists of quartz, feldspar, and sericite. We obtained a $^{40}\text{Ar}/^{39}\text{Ar}$ white mica age of 68.3 ± 0.3 Ma (fig. 7). This is a 12-step plateau age representing 99 percent of the ^{39}Ar released.

The more southerly intrusion (TA14, 05ADw17a) is a coarse-grained granodiorite. The sample contains large, randomly oriented crystals of plagioclase, quartz, potassium feldspar, and chlorite in a somewhat finer groundmass that includes a population of smaller quartz crystals. We obtained a U-Pb zircon SHRIMP-RG age of 68.1 ± 1.9 Ma (fig. 6). The age is the mean of nine overlapping $^{206}\text{Pb}/^{238}\text{U}$ analyses; one zircon analysis was suspected of minor inheritance and was discounted.

TA15 and TA16. Shotgun Hills Pluton, Taylor Mountains C6 and B6 Quadrangles

The Shotgun Hills pluton is one of the most conspicuous intrusive bodies in Taylor Mountains quadrangle (fig. 2). The more northerly of two geochronology samples (TA15, 05ADw59c) is from near the northern contact where the pluton intrudes and bakes Kuskokwim Group strata that were already tight to isoclinally folded prior to intrusion. The sample is an unfoliated granodiorite containing coarse crystals of plagioclase, quartz, potassium feldspar, and abundant biotite. We obtained a $^{40}\text{Ar}/^{39}\text{Ar}$ biotite age of 67.2 ± 0.2 Ma (fig. 7). The age is based on a six-step plateau representing 86 percent of the ^{39}Ar released. Sample TA16 (05AM153a) is from about 5 km to the south. The sample is an unfoliated granite containing coarse crystals of quartz, potassium feldspar, plagioclase, and biotite. We obtained a U-Pb zircon SHRIMP-RG age of 67.9 ± 1.2 Ma. The age is the mean of nine $^{206}\text{Pb}/^{238}\text{U}$ ages; one zircon analysis was suspected of lead loss and was discounted (fig. 6).

These results are quite similar to a $^{40}\text{Ar}/^{39}\text{Ar}$ biotite plateau age of 68.7 ± 0.2 Ma from the Shotgun Hills pluton reported by Rombach and Newberry (2001; sample location not given). [Rombach and Newberry (2001) also reported $^{40}\text{Ar}/^{39}\text{Ar}$ biotite plateau ages from four samples of a separate body, known, confusingly, as the Shotgun granite porphyry. This irregular, slightly older stock, which hosts quartz-stockwork gold mineralization, is located about 0.5 km southwest of the much larger Shotgun Hills granodiorite pluton. Rombach and Newberry (2001) reported a $^{40}\text{Ar}/^{39}\text{Ar}$ biotite age of 69.7 ± 0.3 Ma from the granite porphyry, the mean age from the four least-altered samples.]

TA17. Intrusion South of Shotgun Airstrip, Taylor Mountains B6 Quadrangle

This intrusion forms a conspicuous, glacially streamlined hill south of the airstrip and mineral exploration camp in the Shotgun Hills (fig. 2). It is a biotite-quartz porphyry. The sample (05AM154a) is characterized by a fine-grained groundmass of quartz, feldspar, and sericite. Large crystals of resorbed quartz, plagioclase, potassium feldspar, and biotite are interpreted as granitic xenocrysts, as the enclosing groundmass is finer grained. We obtained a $^{40}\text{Ar}/^{39}\text{Ar}$ biotite age of 70.1 ± 0.4 Ma (fig. 7). This is a 12-step plateau age representing 99 percent of the ^{39}Ar released.

TA18 and TA19. Intrusions in Winchester Claim Area, Taylor Mountains B6 Quadrangle

We report two new ages from the Winchester claim area, a gold prospect between the King Salmon and Klutuspak Rivers in Taylor Mountains B6 and A6 quadrangles (fig. 2). Sample TA18 (08AM630a), from between hills 1690 and 2036, is a granite porphyry. Phenocrysts are plagioclase (some glomerophytic) to

3 mm, rounded to embayed quartz to 2 mm, and biotite to 1 mm that has been altered to chlorite, sphene, and locally, white mica. The groundmass is fine-grained potassium feldspar, quartz, and plagioclase. We obtained a U-Pb zircon SHRIMP-RG age of 69.5 ± 1.0 Ma, the mean of eight $^{206}\text{Pb}/^{238}\text{U}$ results (fig. 6). Sample TA19 (08SB129b), from near hill 2169, is an altered gabbro with late hornblende. A hornblende age spectrum (fig. 7) shows evidence of argon loss; accordingly, we regard the isochron age (77.6 ± 0.7 Ma) as the best measure of the cooling age of this sample. Field relations between the two intrusive bodies were not determined.

TA20. Intrusion Near BM Reach, Taylor Mountains Quadrangle B5

This sample is from a granite porphyry dike or sill cutting an extensive area of hornfelsed Kuskokwim Group north of BM Reach (fig. 2). The sample (08AM654b) is characterized by a fine-grained groundmass of quartz, feldspar, and sericite. Aggregates of large crystals of quartz, plagioclase, potassium feldspar, and muscovite are interpreted as granitic xenoliths, and individual large crystals of these minerals are considered xenocrysts. The groundmass next to many of these is finer grained. We obtained a poorly constrained U-Pb zircon SHRIMP-RG age of 69.9 ± 2.9 Ma. The age is the mean of 12 $^{206}\text{Pb}/^{238}\text{U}$ results (fig. 6). It is possible that the youngest zircons in this dataset experienced minor lead loss, and the oldest have minor inheritance—but none of the individual analyses are obvious outliers, so all are included in the calculation of the mean.

TA21. Intrusion at Hill 1311, Taylor Mountains B4 Quadrangle

This sample (06ADw537a) is from a granite porphyry dike or sill intruding sedimentary rocks of the Kuskokwim Group in the highlands immediately northwest of the confluence of the Nushagak and King Salmon Rivers (fig. 2). As observed in thin section, the fine-grained groundmass consists of quartz, feldspar, and sericite. What appear at the outcrop scale as phenocrysts are seen in thin section to be aggregates of quartz, plagioclase, potassium feldspar, muscovite, and rare biotite; these aggregates are thus interpreted as xenoliths, and individual large crystals of these minerals are considered xenocrysts. We obtained a $^{40}\text{Ar}/^{39}\text{Ar}$ muscovite age of 67.3 ± 0.2 Ma. The age is based on a six-step plateau representing 97 percent of the ^{39}Ar released (fig. 7).

TA22. Dike at Hill 1272, Taylor Mountains B3 Quadrangle

This sample is from a 6-meter-thick dike that cuts the Kuskokwim Group at hill 1272 in eastern Taylor Mountains B3 quadrangle (fig. 2). The sample (08SK290a) is a highly altered granite or granodiorite containing quartz, plagioclase, and potassium feldspar; one or more relict mafic phases are present,

probably originally biotite and hornblende. We obtained a U-Pb zircon SHRIMP-RG age of 80.2 ± 1.3 Ma. This is the mean of 4 overlapping $^{206}\text{Pb}/^{238}\text{U}$ ages and is rather poorly constrained. We discounted one zircon analysis that was suspected of lead loss, and three suspected of inheritance (fig. 4).

TA23, TA24, and TA25. Dikes in Red Bluff Area, Taylor Mountains B1 Quadrangle

A swarm of east- to northeast-striking felsic dikes cuts a folded turbidite section in the Red Bluff area, just north of the Mulchatna Fault in easternmost Taylor Mountains quadrangle (fig. 2). The three dated samples contain 76–77 weight percent SiO_2 . Sample TA23 (08SK316a), from hill 2086, has a fine grained groundmass of quartz, feldspar, and sericite and abundant, large, anhedral crystals and aggregates of quartz, muscovite, and plagioclase, and potassium feldspar. The aggregates are granitic rock fragments and thus would be termed xenoliths; the solitary crystals are most likely xenocrysts from the same granitic source. We obtained a U-Pb zircon SHRIMP-RG age of 66.7 ± 0.4 Ma. The age is the mean of seven overlapping $^{206}\text{Pb}/^{238}\text{U}$ ages; two zircon analyses were suspected of lead loss and were discounted (fig. 6). Sample TA24 (06AK42), from hill 1841, is lithologically similar to sample TA23. We obtained a $^{40}\text{Ar}/^{39}\text{Ar}$ muscovite age of 67.6 ± 0.2 Ma (fig. 7). The age is based on an eight-step plateau representing 96 percent of the ^{39}Ar released. Sample TA25 (06AM447a) is a granite porphyry that has an extremely fine-grained groundmass of quartz, feldspar, and sericite. Large euhedral crystals of quartz are present and these appear to be phenocrysts; some polymineralic aggregates of quartz, muscovite, and feldspar may be xenoliths. We obtained a $^{40}\text{Ar}/^{39}\text{Ar}$ muscovite age of 66.1 ± 0.3 Ma (fig. 7). The age is based on a nine-step plateau representing 96 percent of the ^{39}Ar released.

TA26. Intrusion Near Keefer Creek, Taylor Mountains B1 Quadrangle

Plutonic rocks underlie Hill 1483, southwest of Keefer Creek in Taylor Mountains B1 quadrangle (fig. 2). The sample (06AM453a) is a coarse-grained gabbro containing plagioclase, hornblende, and altered clinopyroxene. We obtained a U-Pb zircon SHRIMP-RG age of 78.2 ± 0.8 Ma. The age is the mean of seven $^{206}\text{Pb}/^{238}\text{U}$ ages; one zircon analysis was suspected of lead loss and was discounted (fig. 6).

TA27. Chaufchivak Pluton, Taylor Mountains A7 Quadrangle

Mount Chaufchivak is a low but prominent hill of hornfels rising above the eastern end of Lake Chauekuktuli in Taylor Mountains A7 quadrangle; associated plutonic rocks are exposed on a lower knob to the east (fig. 2), where the geochronology sample (08AM614a) was collected. The sample is a granodiorite

containing plagioclase in large crystals, quartz, potassium feldspar, biotite, and lesser hornblende. We obtained a $^{40}\text{Ar}/^{39}\text{Ar}$ biotite age of 69.2 ± 0.3 Ma (fig. 7). The age is based on a five-step plateau representing 82 percent of the ^{39}Ar released.

TA28. Intrusion at Hill 1623, Taylor Mountains A6 Quadrangle

This small intrusion is exposed around the top of hill 1623 in the headwaters of Koneruk Creek in Taylor Mountains A6 quadrangle. It intrudes the Kuskokwim Group. The sample (08SB127c) is a medium-grained hypidiomorphic granular quartz diorite or tonalite. Plagioclase is partly altered to sericite. Quartz is not abundant. Primary muscovite is present. What was probably primary biotite is now represented by clots of chlorite and opaque minerals. Sphene, apatite, and partly hematized opaque minerals are present. Potassium feldspar is absent. We obtained a $^{40}\text{Ar}/^{39}\text{Ar}$ muscovite age of 76.9 ± 0.9 Ma (fig. 7). The age is based on a seven-step plateau representing 99 percent of the ^{39}Ar released. This could either represent an igneous cooling age or cooling from a subsequent hydrothermal system.

TA29. Intrusion Near Hill 1635, Taylor Mountains A6 Quadrangle

This intrusive body was encountered in a single outcrop in Taylor Mountains A6 quadrangle along an unnamed creek between hill 1405 on the west and hill 1635 on the east (fig. 2). The sample (08ADw825a) is an undeformed diorite featuring large plagioclase crystals (some of them rimmed by plagioclase, presumably of a different composition), hornblende, clinopyroxene, and sphene. Zircons yielded a U-Pb SHRIMP-RG age of 79.4 ± 0.4 Ma. The age is the mean of 7 overlapping $^{206}\text{Pb}/^{238}\text{U}$ ages; one zircon analysis was suspected of lead loss and was discounted (fig. 6). We also obtained a $^{40}\text{Ar}/^{39}\text{Ar}$ hornblende age of 79.1 ± 0.3 Ma (fig. 7), based on a three-step plateau representing 97 percent of ^{39}Ar released.

TA30 and TA31. Tikchik Mountain Pluton, Taylor Mountains A6 Quadrangle

The Tikchik Mountain pluton, in Taylor Mountains A6 quadrangle, may or may be part of the same body as what we refer to as the Tikchik Narrows pluton (sample DI1) in Dillingham quadrangle (fig. 2). It was dated by U-Pb zircon at one location and by $^{40}\text{Ar}/^{39}\text{Ar}$ biotite at a second location. Sample TA30 (08ADw822a) is a fine- to medium-grained, hypidiomorphic granular biotite granite containing accessory epidote and allanite. Locally, biotite has been slightly altered to chlorite. Zircons yielded a U-Pb SHRIMP-RG age of 62.2 ± 0.8 Ma (fig. 6). This is the mean of eight overlapping $^{206}\text{Pb}/^{238}\text{U}$ ages; two zircon analyses were suspected of lead loss and were discounted. A sample of biotite granite (TA31,

08SB117a), from about 2 km to the east, was dated by $^{40}\text{Ar}/^{39}\text{Ar}$ (fig. 7). It yielded an age of 61.5 ± 0.2 Ma, based on a nine-step plateau representing 98 percent of the ^{39}Ar released. The two results overlap within uncertainties.

TA32. Arrow Pluton, Taylor Mountains A5 Quadrangle

The Arrow pluton, which takes its informal name from nearby Arrow Creek (fig. 2), was dated by multiple methods. The sample (08SB147a) is a medium-grained, hypidiomorphic hornblende-biotite granite. Tourmaline and sphene are present as accessory phases. We obtained a U-Pb zircon age of 74.3 ± 1.1 Ma using the SHRIMP-RG. The age is the mean of 10 overlapping $^{206}\text{Pb}/^{238}\text{U}$ ages (fig. 6). $^{40}\text{Ar}/^{39}\text{Ar}$ ages were obtained at University of Alaska Fairbanks (fig. 7) from both biotite and hornblende. A biotite age of 74.0 ± 0.2 Ma is based on a five-step plateau representing 83 percent of the ^{39}Ar released. A very similar hornblende age of 73.8 ± 0.3 is based on a four-step plateau representing 97 percent of the ^{39}Ar released. All three ages agree within uncertainty and suggest that the pluton cooled to <400 °C in less than a million years.

TA33. Dike Near Sleitat Mountain, Taylor Mountains A3 Quadrangle

This dike, on Sleitat Mountain, is the most southwesterly of a line of intrusive bodies along the Mulchatna Fault (fig. 2). The country rocks are hornfels that we have assigned, on the basis of detrital zircon ages, to the Kuskokwim Group (Miller and others, 2007b). The sample (08AM676a) is a quartz-biotite-muscovite porphyritic granite containing phenocrysts to 2 mm across in a very fine-grained groundmass. We obtained U-Pb zircon SHRIMP-RG age of 68.7 ± 1.6 Ma. The age is the mean of 9 $^{206}\text{Pb}/^{238}\text{U}$ ages; one zircon analysis was suspected of inheritance and was discounted (fig. 6).

TA34. Sleitat Pluton, Taylor Mountains A3 Quadrangle

The Sleitat pluton is a peraluminous granite along the Mulchatna Fault trend (fig. 2). The sample (08SB169a) is a fine- to medium-grained hypidiomorphic granular biotite granite. Secondary white mica and late (or secondary?) tourmaline fill interstices. We obtained a U-Pb zircon age of 61.4 ± 0.7 Ma using the SHRIMP-RG. The age is the mean of six overlapping $^{206}\text{Pb}/^{238}\text{U}$ ages; we discounted one zircon analysis that was suspected of lead loss, and one suspected of inheritance (fig. 6). Previously, Burleigh (1991) reported a conventional K-Ar age of 56.8 ± 2.8 Ma on muscovite, whereas Layer and Bundtzen (2010) reported $^{40}\text{Ar}/^{39}\text{Ar}$ biotite ages for two intrusive phases, both 59.4 ± 0.2 Ma. Tin-silver-tungsten deposits are associated with the pluton; muscovite from

greisen yielded a $^{40}\text{Ar}/^{39}\text{Ar}$ age of 58.2 ± 0.4 Ma (Layer and Bundtzen, 2010).

TA35. Old Man Pluton, Taylor Mountains A3 Quadrangle

This pluton does not appear to crop out but its presence is inferred from abundant, large boulders strewn across hill 1180 near Old Man Creek in Taylor Mountains A3 quadrangle. It is one of a line of intrusive bodies that lie along or very close to the Mulchatna Fault trend (fig. 2). The sample (06AK69a) is a fine- to medium-grained, hypidiomorphic granular biotite granite. Some but not all of the biotite has been replaced by chlorite. We obtained a $^{40}\text{Ar}/^{39}\text{Ar}$ biotite age of 66.7 ± 0.3 Ma, based on a nine-step plateau representing 86 percent of the ^{39}Ar released (fig. 7).

TA36. Intrusion at Hill 1004, Taylor Mountains A3 Quadrangle

This unnamed intrusive body does not crop out, but its presence is revealed by a field of granite boulders east of Sleitat Mountain (fig. 2). The sample (08ADw896a) is a medium-grained, hypidiomorphic hornblende-biotite quartz monzonite to granite. Clinopyroxene cores are identifiable in some hornblende crystals. We obtained a U-Pb zircon SHRIMP-RG age of 69.1 ± 0.9 Ma; the age is the mean of eight overlapping $^{206}\text{Pb}/^{238}\text{U}$ ages (fig. 6).

TA37. Intrusion at Hill 1422, Taylor Mountains A2 Quadrangle

This small unnamed stock crops out along or near the Mulchatna Fault in southeastern Taylor Mountains quadrangle (fig. 2). The top of hill 1422 is underlain by complexly deformed, contact metamorphosed metasedimentary rocks; quartz monzonite is exposed on the northern flank of the hill. The sample (06ADw570e) is a fine- to medium-grained, hypidiomorphic orthopyroxene-clinopyroxene-biotite quartz monzonite. We obtained a U-Pb TIMS zircon age of 61.0 ± 0.1 Ma, based on five concordant and overlapping single crystal ages (fig. 5).

TA38. Rhyolite at Hill 1678, Taylor Mountains A1 Quadrangle

This small body of rhyolite crops out in low hills in the northeastern corner of the Taylor Mountains A1 quadrangle (fig. 2). The sample (06AJ062a) is a flow-banded, porphyritic rhyolite containing phenocrysts of quartz, plagioclase, and K-feldspar in a very fine-grained groundmass of the same minerals. Angular lithic clasts of country rock are present. The flow banding suggests a pyroclastic origin. We obtained a U-Pb TIMS zircon age of 49.1 ± 0.3 Ma (fig. 5), based on two concordant and overlapping single crystal ages.

TA39. Intrusion at Hill 982, Taylor Mountains A1 Quadrangle

This small unnamed stock crops out on low hills near the eastern edge of the Taylor Mountains A1 quadrangle (fig. 2). The sample (06ADw568a) is a biotite granite. Phenocrysts of K-feldspar (to 5 mm), plagioclase (2–5 mm) and biotite (1 mm) occur throughout a finer groundmass of the same minerals. Biotite is locally altered to chlorite. We obtained a U-Pb TIMS zircon age of 56.3 ± 0.2 Ma (fig. 5), based on five concordant and overlapping single crystal ages.

Lake Clark Quadrangle

LC1. Overlook Pluton, Lake Clark B8 Quadrangle

This pluton crops out at BM Overlook just south of the Mulchatna Fault trace in western Lake Clark quadrangle (fig. 2) and appears to be truncated by the fault. It intrudes Mesozoic turbidites assigned by Nelson and others (1983) to their map unit KJs and by Wallace and others (1989) to their Jurassic-Cretaceous Koksetna River sequence. The sample (06ADw558a) is a coarse-grained gabbro containing large crystals of altered plagioclase, hornblende, clinopyroxene, an opaque phase inferred to be an Fe-Ti oxide, and sphene. We obtained a U-Pb TIMS zircon age of 76.5 ± 0.2 Ma (fig. 5), based on five concordant and overlapping single crystal ages.

Goodnews Bay Quadrangle

G01. Intrusion Near Jacksmith Creek, Goodnews Bay B8 Quadrangle

Separate rubble patches of Cretaceous granite porphyry and Paleoproterozoic granite of the Kilbuck terrane were sampled near hill 820 in the headwaters of Jacksmith Creek (fig. 4K). The older granite, which yielded a U-Pb zircon age of $2,084.9\pm 5.8$ Ma, is the oldest tightly dated rock in Alaska (Bradley and others, 2014). Presumably, the younger granite porphyry (sample 06ADw603b) intruded the older granite. The granite porphyry has medium grained phenocrysts of quartz, plagioclase, biotite, and minor very altered mafics (former hornblende?), in a fine-grained groundmass of quartz, plagioclase, and potassium feldspar. We obtained a $^{40}\text{Ar}/^{39}\text{Ar}$ plateau age of 70.7 ± 0.3 Ma from the granite porphyry (fig. 7). The age is based on a six-step plateau representing 94 percent of the ^{39}Ar released (fig. 7).

G02. Dike at Island Mountain, Goodnews Bay B7 Quadrangle

On the north flank of Island Mountain (fig. 4K), an altered dike (sample 06ADw602c) cuts green, deformed, pebbly sandstone that Hoare and Coonrad (1978) assigned to their

undifferentiated mapping unit, MzPz. The dike is medium grained and consists primarily of plagioclase and clinopyroxene, accessory opaques, and very minor quartz. The plagioclase is altered to fine-grained white mica(?); the edges of the clinopyroxene are altered to chlorite. We obtained a $^{40}\text{Ar}/^{39}\text{Ar}$ whole rock age of 155.0 ± 1.9 Ma based on the weighted mean of two overlapping plateau ages (155.7 ± 3.0 and 154.4 ± 2.6 Ma) (fig. 7).

Dillingham Quadrangle

D11. Tikchik Narrows Pluton, Dillingham D7 Quadrangle

The Tikchik Narrows pluton crops out along the shores and islands of Tikchik Lake in Dillingham D7 quadrangle (fig. 2). The sample (08ADw826a) is a coarse-grained granite containing alkali feldspar (now perthite), quartz, plagioclase, biotite, and conspicuous accessory zircon. We obtained a $^{40}\text{Ar}/^{39}\text{Ar}$ biotite age of 60.2 ± 0.2 Ma. This is a three-step plateau age representing 62 percent of the ^{39}Ar released (fig. 7). The biotite age of this pluton is 1–2 million years younger than the biotite (61.5 ± 0.2 Ma) and zircon (62.2 ± 0.8 Ma) ages of the Tikchik Mountain pluton a few kilometers to the north (samples TA30 and TA31). Owing to lack of exposure, it is not known whether the Tikchik Mountain and Tikchik Narrows plutons are parts of a single igneous body.

Implications for the Magmatic History of Western Alaska

Pennsylvanian

The new U-Pb zircon age of 317.7 ± 0.6 Ma reveals the presence of Pennsylvanian intermediate igneous (probably volcanic) rocks in the Tikchik terrane in the Bethel quadrangle. Igneous rocks of this general age are not well represented in the Alaskan geologic record and the locations of various terranes at the time is conjectural. The new age supports the idea (Box and others, 2015) that the Tikchik terrane represents part of the elusive collider with the Farewell terrane during the Late Pennsylvanian to Early Permian Brown's Fork orogeny (of Bradley and others, 2003b).

Triassic

Our U-Pb zircon age of 229.5 ± 0.2 Ma from gabbro intruding the Rampart Group in the Tanana quadrangle is the most reliable isotopic age yet obtained from anywhere in the Angayucham-Tozitna terrane. It confirms the suspected Triassic age of mafic intrusive rocks that make up a significant part of the terrane (Siwieck and Till, 2006). The new age is somewhat older than a K-Ar hornblende age of 210 ± 6 Ma (recalculated by Wilson and

others, 1994, using 1976 decay constant) from gabbro from the main outcrop belt of Rampart Group (Brosge and others, 1969), roughly 30 km to the north of our sample site.

Jurassic

A mafic dike in Goodnews Bay quadrangle yielded a $^{40}\text{Ar}/^{39}\text{Ar}$ whole rock age of 155.0 ± 1.9 Ma. This establishes a Jurassic or older age for the previously unconstrained Paleozoic to Mesozoic sandstone unit of the Goodnews terrane that it intrudes. A thick felsic tuff in the Gemuk Group in Taylor Mountains quadrangle yielded a U-Pb zircon age of 153.0 ± 2.0 Ma, extending the age of magmatism in this part of the Togiak terrane farther back into the Late Jurassic. It is not known how these nearly coeval magmatic episodes relate to each other.

Early Cretaceous

The three Early Cretaceous plutonic rocks in our sample suite crop out in three different mapped terranes. The about 112-Ma age of the Granite Mountain pluton in the Koyukuk terrane is comparable to U-Pb zircon ages of 112 and 109 Ma that were previously reported from granitoids in this belt (Patton and others, 2009). The about 115-Ma age of the orthogneiss in the Ruby terrane is likewise consistent with the 118–113 Ma age range of plutons that intrude the main outcrop belt of Ruby terrane to the north (Roeske and others, 1998). The about 117-Ma gabbro is part of the Dishna River mafic-ultramafic complex, which has been regarded as part of the Innoko terrane (Miller and Bundtzen, 1994). The gabbro is unexpectedly young and shows that some igneous rocks in the Innoko terrane are coeval with the Early Cretaceous granitoids that intrude the Ruby terrane. Along strike to the southwest, a similar Early Cretaceous age of 117.8 ± 0.7 Ma has been reported from the Nyac pluton ($^{40}\text{Ar}/^{39}\text{Ar}$ hornblende; Wenz, 2005), which intrudes Jurassic arc volcanics of the Nyac terrane in Bethel quadrangle. A 118–112 Ma magmatic belt thus “stitches” the Koyukuk, Ruby, Innoko, and Nyac terranes.

Mid-Cretaceous

The Turonian (about 90 Ma) was an important time in the metallogenic history of south-central Alaska. This is the age of the Pebble deposit, a giant porphyry copper-gold system on the Alaska Peninsula (fig. 1) (Schrader and others, 2001; Goldfarb and others, 2013; Anderson and others, 2013). Approximately 90-Ma plutonic rocks crop out in a discontinuous belt that was previously known to extend from Kemuk Mountain (fig. 1) (Anderson and others, 2013) to the southernmost Talkeetna Mountains (Bleick and others, 2012) (barely east of the eastern edge of figure 1 at latitude 61.5° N). One intrusive rock in our sample suite is about this age—a small intermediate pluton (TA7) with a $^{40}\text{Ar}/^{39}\text{Ar}$ age of 87.7 ± 1.7 Ma that intrudes the Togiak terrane in Taylor Mountains quadrangle. This new result shows that Pebble-age igneous centers are present across a strike-width of 300 km.

At 90 Ma, the Sleetmute and Taylor Mountains quadrangles were the site of submarine fan sedimentation in the Kuskokwim basin. Situated on the inboard side of the Pebble igneous trend, this basin has been interpreted as a collisional foreland basin (Kalbas and others, 2007) or a retroarc foreland basin (Bradley and others, 2009). A tuff interbedded with Kuskokwim Group turbidites yielded a U-Pb zircon age of 88.3 ± 1.0 Ma. This attests to explosive volcanism at this time, presumably from a source somewhere along the Pebble trend.

Late Cretaceous

Most of samples in the present study are Late Cretaceous to Paleocene in age. The regional pattern of magmatism is shown in a series of 2-m.y. time slices in figure 8A–N. The maps show a combination of ages obtained by various methods (for example, U-Pb zircon ages that essentially date magmatism versus K-Ar muscovite ages that date cooling through about 350 °C). This mix likely blurs some details.

Only a smattering of magmatic activity is shown in the scenes covering 78 to 72 Ma (fig. 8A–C). A flare-up followed, which was most intense from about 72 to 68 Ma. Magmatism continued across the region from about 68 to 56 Ma, and then waned, particularly in the south. In general, changes from one scene to the next are gradual, but four exemplary time slices, shown with bold outlines, are sufficiently spaced to highlight the most significant changes in patterns of magmatism over a 24-m.y. interval: 78–76, 72–70, 64–62, and 56–54 Ma (figs. 8A, D, H, and L).

The distribution of Late Cretaceous paleogeographic elements is an important constraint in deciphering the cause of the 72–68 Ma flare-up (fig. 9). This interval overlaps with the age range of a thick package of trench turbidites that comprise the Valdez Group and correlatives in the Chugach accretionary complex (V in fig. 9). Coeval turbidites of the Matanuska Formation record the existence and location of a subsiding forearc basin (Trop and Ridgway, 2007; M in fig. 9). In the central Alaska Range, the lower Cantwell Formation was deposited and deformed in a thrust-top, retroarc foreland basin setting (Trop and Ridgway, 2007; C in fig. 9). Ash beds in the lower Cantwell have yielded U-Pb zircon ages of 71.5 ± 0.9 and 71.0 ± 1.1 Ma (Tomsich and others, 2014). The inferred boundaries between accretionary wedge, forearc basin, orogenic belt, and retroarc foreland basin can be reconstructed on these grounds (fig. 9). Gold and mercury mineralization across much of southwestern Alaska dates from this same interval (Bundtzen and Miller, 1997; Gray and others, 1997). Most of the magmatic activity during this time appears to have been in the retroarc region.

The cause of this wide, 72–68 Ma belt of magmatism along a continental-margin arc setting is not well understood. One possibility is low-angle subduction (Miller and others, 2007a). The inboard-to-outboard shift in the area of greatest magmatic activity between 72 and 68 Ma (see figs. 8D, E, and F) could perhaps have been produced by rollback of a subducted oceanic plate, as has been postulated for the Apennine orogen of Italy and its Ligurian Sea hinterland (Malinverno and Ryan, 1986).

Melting, in this scenario, would be induced by decompression of asthenosphere that would have welled up into the resulting gap. Another possible mechanism for magma genesis at about 72 to 68 Ma is that southwestern Alaska was extended as it escaped westward toward a free face in the Bering Sea (Redfield and others, 2007). An analog would be the Neogene of Turkey, where westward escape of Anatolia along strike-slip faults produced a broad magmatic province not related to subduction (Pearce and others 1990). The shortcoming of this model is the lack of any structural evidence for extension; 70 Ma, instead, was a time of dextral strike-slip faulting and associated transpressional folding (Miller and others, 2002). Another conceivable way to generate both a magmatic flareup and regional mercury mineralization is a slab window resulting from ridge subduction. Northern California's mercury belt originated above a slab window (Smith and others, 2008). Ridge subduction has been well documented on Alaska's Pacific margin—but at 61 and 50 Ma (Bradley and others, 2000 and 2003a; see next section) it is too young. In any event, Neogene ridge subduction in the southern Andes has produced a magmatic lull along the arc (Forsythe and Prior, 1992; Gorrington and others, 1997), not a flare-up.

Two dated rock units from the 72–68 Ma interval provide improved age constraints on deformation events. The Chuilnuk pluton was emplaced just north of the Denali Fault in Sleetmute quadrangle (fig. 2). It truncates dextral en echelon folds in the Kuskokwim Group, which Miller and others (2002) attributed to pre-Chuilnuk dextral displacement along the Denali Fault. Previously, this event was bracketed between a conventional K-Ar biotite age on the Chuilnuk pluton of 68 Ma and about 85 Ma, which corresponds to the youngest nearby fossil ages from the Kuskokwim Group (Miller and others, 2002). This episode of dextral motion can be more narrowly constrained as older than the 70.2 ± 1.0 Ma zircon age from the Chuilnuk, as reported herein, but younger than deposition of the youngest Kuskokwim Group strata at about 76 Ma, based on detrital zircons (Miller and others, 2007b).

Paleocene and Early Eocene

The case for ridge subduction along the Gulf of Alaska margin is based largely on a tightly dated belt of near-trench plutons in the Chugach accretionary complex (Bradley and others, 2000, 2003a; Haeussler and others, 2003). These 61 to 50 Ma plutons intruded into trench deposits, including some that had been accreted to the upper plate only a few million years before. Each pluton is interpreted to mark the place where an oceanic spreading center was subducted; the triple junction migrated west to east between 61 and 50 Ma. In the area of figure 8, the position of the triple junction is shown for four time slices. Tellingly, magmatism in western Alaska diminished or shut off entirely about when the triple junction was at the now-adjacent part of the accretionary complex. Analogous behavior is seen in Chile where the Nazca-Antarctic spreading center is being subducted beneath South America. There, the present position of a slab window (which has as its center the downdip projection of the subducted ridge) corresponds to a magmatic gap along the arc (Forsythe and Prior,

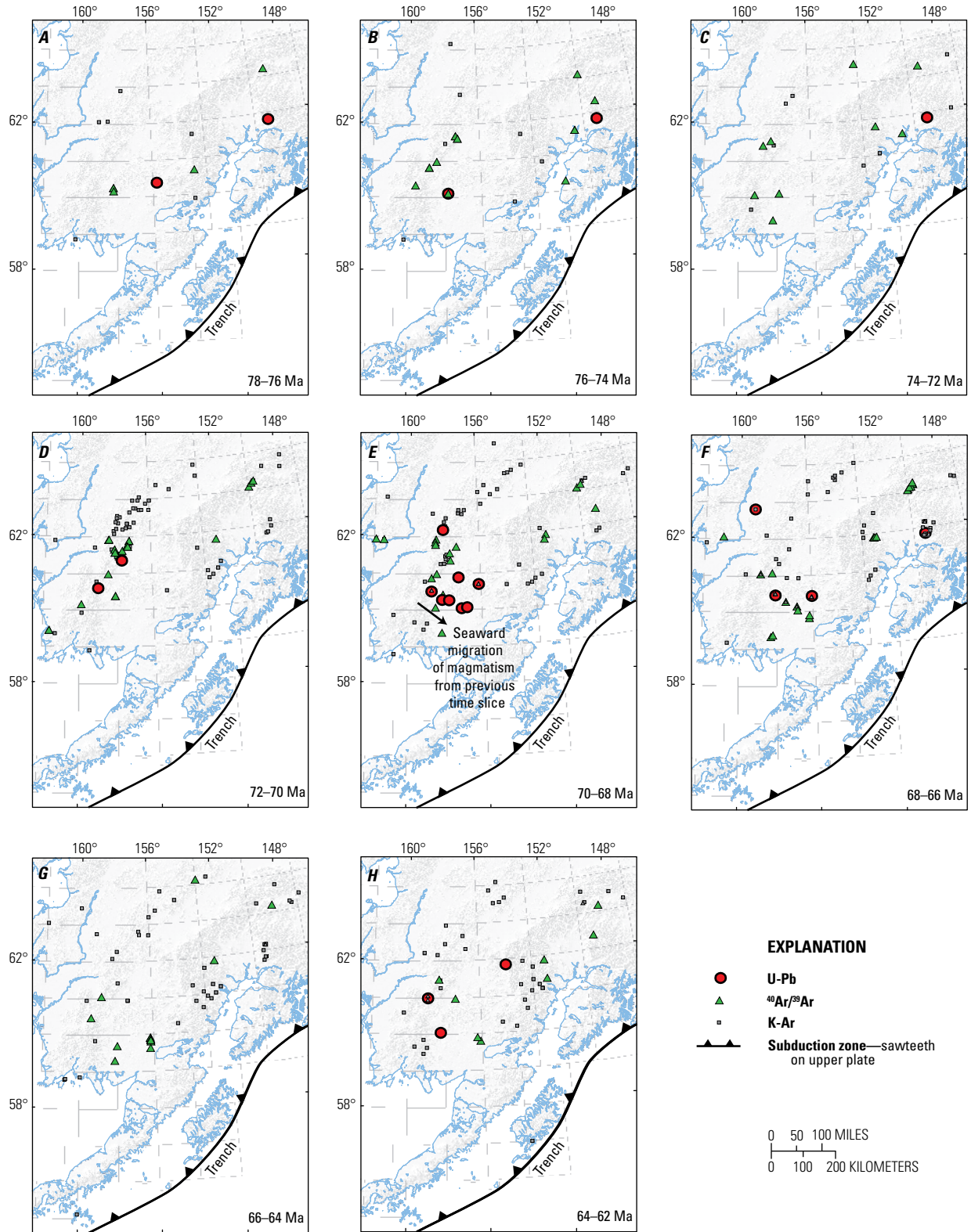


Figure 8. Maps (A to M) showing the distribution of isotopic ages from igneous rocks in western Alaska in 2-million-year increments from 78 to 50 million years ago (Ma). The shaded relief was generated from the U.S. Geological Survey National Elevation Dataset (NED) 2-arc-second Digital Elevation Model (DEM). Conventional K-Ar ages are from the Alaska radiometric age database, accessible at <https://mrddata.usgs.gov/akages/>. Additional ages are plotted from Bradley and others (2000), Farris and others (2006), Goldfarb and others (2004), and Miller and others (2002). O, Index to 1:250,000-scale quadrangle maps; see caption to figure 1 for key to abbreviations. Orientation of the hypothesized Kula-Resurrection ridge is schematic.

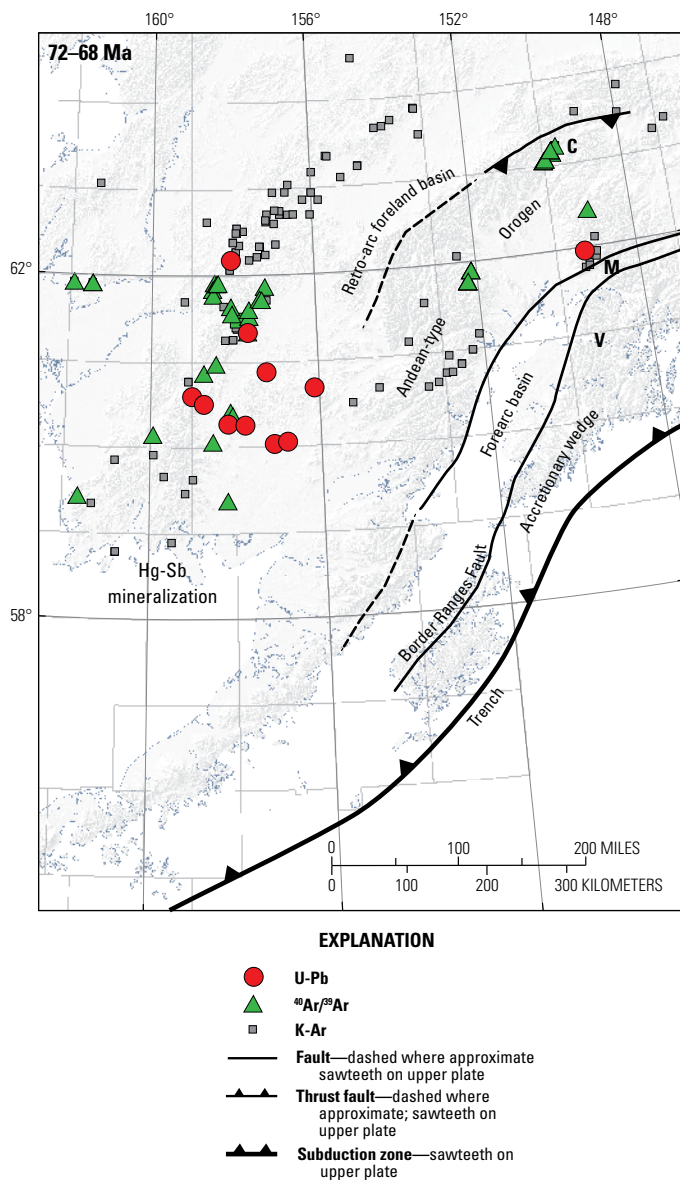


Figure 9. Map showing Late Cretaceous paleogeographic elements and igneous rock samples with ages of 72–68 million years (Ma) in western Alaska. The shaded relief was generated from the U.S. Geological Survey National Elevation Dataset (NED) 2-arc-second Digital Elevation Model (DEM).

1992). We interpret the 55–43 Ma magmatic lull in southwestern Alaska as a time when a slab window lay at depth.

An important related issue is the amount of coast-parallel strike-slip displacement between the Chugach terrane, which hosts the 61–50 Ma near-trench plutons, and its immediate backstop, the Peninsular terrane. The boundary between these two terranes is the Border Ranges Fault (fig. 9). If displacement is in the range of thousands of kilometers, as Cowan (2003) has suggested, our interpretation would be invalid. Provenance data and field relations, however, indicate that the Paleogene fill of the Matanuska forearc basin was derived from both outboard (Little,

1988) and inboard (Kortyna and others, 2013) flanks. For this sector of the margin, at least, this precludes large (terrane-scale) displacements since about 54 Ma between the Chugach terrane and its backstop. We therefore take the apparent paleogeographic relations at face value and in so doing find a ready explanation for what otherwise would be a problematic magmatic shutdown (Bradley and others, 2006).

The slab window concept also bears on magma genesis immediately before the magmatic lull that began at about 55 Ma. The time leading up to the lull was one of widespread magmatism. For example, in the western Alaska Range (Tyonek quadrangle, fig. 1), Todd and others (2015) reported a magmatic flare-up from 63 to 56 Ma. In an overall setting of ridge subduction, subducting oceanic crust immediately adjacent to a slab window is only a few million years old, and its corresponding lithosphere is young, hot, and thin (Thorkelson, 1996). Where plate geometry is such that the slab window migrates, hot and thin oceanic lithosphere is subducted beneath a given location just before arrival of the slab window. If the slab window interpretation is valid in the present instance, these conditions would have existed in the western Alaska Range during the interval of a few million years leading up to about 55 Ma (Bradley and others, 2006), with subduction of young, hot, thin lithosphere along the edge of the slab window being responsible for widespread plutonism during this interval (figs. 8J–L).

Mid-Eocene to Pliocene

The present study has yielded only a few new dates that bear on younger events (Jones and others, 2014). During the entire mid-Eocene to Pliocene interval, the modern subduction geometry has been in place, with the Pacific Plate subducting to the northwest beneath the western Gulf of Alaska margin. Two newly dated Eocene rocks are likely related to this phase of subduction. One is the rhyolite dated at 49.1 ± 0.3 Ma in Taylor Mountains quadrangle; the other is the ashfall tuff dated at 42.8 ± 0.5 Ma in McGrath quadrangle.

Two Oligocene plutons in the western Alaska Range, at 31.8 ± 0.4 and 30.9 ± 0.6 Ma, belong to a distinctly younger intrusive suite that ranges from gabbro to peralkaline granite. These plutons are located far inboard of the modern volcanic arc and the cause of magmatism is not clear.

Finally, the 4.6 ± 0.1 -Ma basalt from a flow in Taylor Mountains quadrangle belongs to the Neogene basaltic province of western Alaska. These rocks were erupted in a distal retroarc setting; the cause of magmatism also remains elusive (Moll-Stalcup, 1994). The Flat Top flows were erupted onto a topographic surface that was already about as rugged and mountainous as today. The flows bury a straight valley along the Atsakovluk strand of the Denali strike-slip fault. The volcanics themselves may be slightly disturbed by the fault (satellite images are equivocal on this point), but in any case the Atsakovluk lineament clearly is older than the Pliocene volcanism.

Acknowledgments

Heather Bleick, our coauthor and friend, contributed greatly to this report but passed away while it was in review. Jim Riehle, Jay Kalbas, Ed Klimasauskas, and the late Bill Keith participated in sampling during mapping of the Sleetmute and Taylor Mountains quadrangles. Tom Donley collected the Granite Mountain sample in connection with a remediation effort by the U.S. Air Force. We thank Janet Gabites for help with the argon data from University of British Columbia. Reviews by Erin Todd and Chris Holm-Denoma substantially improved the paper.

References Cited

- Anderson, E.D., Hitzman, M.W., Monecke, T., Bedrosian, P.A., Shah, A.K., and Kelley, K.D., 2013, Geological analysis of aeromagnetic data from southwestern Alaska—Implications for exploration in the area of the Pebble porphyry Cu-Au-Mo deposit: *Economic Geology*, v. 108, p. 421–436.
- Bickford, M.E., Cullers, R.L., Shuster, R.D., Premo, W.R., and Van Schmus, W.R., 1989, U-Pb zircon geochronology of Proterozoic and Cambrian plutons in the Wet Mountains and southern Front Range, Colorado: *Geological Society of America Special Paper* 235, p. 49–64.
- Black, L.P., Kamo, S., Allen, C., Davis, D., Aleinikoff, J.A., Valley, J., Mundil, R., Campbell, I.H., Korsch, R., Williams, I.S. and Foudoulis, C., 2004, Improved $^{206}\text{Pb}/^{238}\text{U}$ microprobe geochronology by the monitoring of a trace-element related matrix effect; SHRIMP, ID-TIMS, ELA-ICP-MS and oxygen isotope documentation for a series of zircon standards: *Chemical Geology*, v. 205, p. 115–140.
- Box, S.E., Moll-Stalcup, E.J., Frost, T.P., and Murphy, J.M., 1993, Preliminary geologic map of the Bethel and southern Russian Mission quadrangles, southwestern Alaska: U.S. Geological Survey Miscellaneous Field Studies Map MF-2226-A, 20 p., scale 1:250,000.
- Box, S.E., Karl, S.M., Bradley, D.C., Miller, M.L., Ayuso, R.A., and Friedman, R.M., 2015, Tikchik terrane (SW Alaska) records Pennsylvanian–Early Permian collision of oceanic arc with continental Farewell terrane: *Geological Society of America Abstracts with Programs*, v. 47, no. 4, p. 8.
- Bradley, D.C., Parrish, R., Clendenen, W., Lux, D., Layer, P., Heizler, M., and Donley, D.T., 2000, New geochronological evidence for the timing of early Tertiary ridge subduction in southern Alaska: U.S. Geological Survey Professional Paper 1615, p. 5–21.
- Bradley, D., Kusky, T., Haeussler, P., Goldfarb, R., Miller, M., Dumoulin, J., Nelson, S., and Karl, S., 2003a, Geologic signature of early Tertiary ridge subduction in Alaska, *in* Sisson, V.B., Roeske, S.M., and Pavlis, T.L., eds., *Geology of a transpressional orogen developed during ridge-trench interaction along the north Pacific margin*: Geological Society of America Special Paper 371, p. 19–49.
- Bradley, D.C., Dumoulin, J., Layer, P., Sunderlin, D., Roeske, S., McClelland, W., Harris, A.G., Abbott, G., Bundtzen, T.K., and Kusky, T., 2003b, Late Paleozoic orogeny in Alaska's Farewell terrane: *Tectonophysics*, v. 372, p. 23–40.
- Bradley, D.C., Friedman, R.M., Layer, P.W., Haeussler, P.J., Till, A.B., Roeske, S.M., and Miller, M.L., 2006, Far-field effects of early Tertiary ridge subduction in Alaska: Backbone of the Americas, Patagonia to Alaska, GSA Specialty Meetings Abstracts with Programs, v. 2, p. 91.
- Bradley, D.C., Haeussler, P.J., O'Sullivan, P.B., Friedman, R.M., Till, A.B., Bradley, D.B., and Trop, J.M., 2009, Detrital zircon geochronology of Cretaceous and Paleogene strata across the south-central Alaskan convergent margin, *in* Haeussler, P.J., and Galloway, J.P., *Studies by the U.S. Geological Survey in Alaska, 2007*: U.S. Geological Survey Professional Paper 1760-F, 36 p.
- Bradley, D.C., McClelland, W.C., Friedman, R.M., O'Sullivan, P., Layer, P.W., Miller, M.L., Dumoulin, J.A., Till, A.B., Wooden, J.L., and Abbott, J.G., 2014, Proterozoic geochronological links between the Farewell, Kilbuck and Arctic Alaska Terranes: *The Journal of Geology*, v. 122, p. 237–258, doi:10.1086/675663.
- Brosge, W.P., Lanphere, M.A., Reiser, H.N., and Chapman, R.M., 1969, Probable Permian age of the Rampart Group, central Alaska: U.S. Geological Survey Bulletin 1294-B, p. B1–B18.
- Bundtzen, T.K., Harris, E.E., and Gilbert, W.G., 1997, Geologic map of the eastern half of the McGrath quadrangle, Alaska: Alaska Division of Geological and Geophysical Surveys Report of Investigation 97-14a, 38 p., scale, 1:125,000.
- Bundtzen, T.K., and Miller, M.L., 1997, Precious metals associated with Late Cretaceous–early Tertiary igneous rocks of southwestern Alaska, *in* Goldfarb, R. J., and Miller, L. D., editors. *Mineral deposits of Alaska: Economic Geology Monograph* 9, p. 242–286.
- Bundtzen, T.K., 1999, Alaska Resource Data File, McGrath quadrangle: U.S. Geological Survey Open-File Report 99-357, 195 p.
- Bundtzen, T.K., and Gilbert, W.G., 1991, Geology and geochemistry of the Gagaryah barite deposit, western Alaska Range, Alaska: Alaska Division of Geological and Geophysical Surveys Professional Report 111, p. 9–20.

- Burleigh, R.E., 1991, Geology and geochemistry of the Sleitat Mountain tin deposit, southwestern Alaska: Alaska Division of Geological and Geophysical Surveys Professional Report 111, p. 29–39.
- Chapman, R.M., Yeend, W.E., and Patton, W.W., Jr., 1975, Preliminary reconnaissance geologic map of the western half of Kantishna River quadrangle, Alaska: U.S. Geological Survey Open-File Report 75–351, scale 1:250,000.
- Chang, Z., Vervoort, J.D., McClelland, W.C., and Knaack, C., 2006, U-Pb dating of zircon by LA-ICP-MS: Geochemistry, Geophysics, Geosystems, v. 7, no. 5, p. 1–14.
- Clement, S.W.J., and Compston, W., 1994, Ion probe parameters for very high resolution without loss of sensitivity: U.S. Geological Survey Circular 1107, 62 p.
- Cowan, D.S., 2003, Revisiting the Baranof–Leech River hypothesis for early Tertiary coastwise transport of the Chugach–Prince William terrane: Earth and Planetary Science Letters, v. 213, p. 463–475.
- Decker, J.E., Reifstuhel, R.R., Robinson, M.S., Waythomas, C.F., and Clough, J.G., 1995, Geology of the Sleetmute A-5, A-6, B-5, and B-6 quadrangles, southwestern Alaska: Alaska Division of Geological and Geophysical Surveys Professional Report 99, 16 p., 2 sheets, scale 1:63,360.
- Elder, W. P., and Box, S.E., 1992, Late Cretaceous inoceramid bivalves of the Kuskokwim Basin, southwestern Alaska, and their implications for basin evolution: The Paleontological Society Memoir 26, 37 p.
- Farris, D.W., Haeussler, P., Friedman, R., Paterson, S.R., Saltus, R.W., and Ayuso, R., 2006, Emplacement of the Kodiak batholith and slab-window migration: Geological Society of America Bulletin, v. 118, p. 1360–1376.
- Forsythe, R., and Prior, D., 1992, Cenozoic continental geology of South America and its relations to the evolution of the Chile Triple Junction: College Station, Texas, Ocean Drilling Program, Proceedings of the Ocean Drilling Program, Initial reports, v. 141 p. 23–31.
- Gamble, B.M., Reed, B.L., Richeter, D.H., and Lanphere, M.A., 2013, Geologic map of the east half of the Lime Hills 1:250,000-scale quadrangle, Alaska: U.S. Geological Survey Open-File Report 2013–1090, 1 sheet, scale 1:250,000, <https://pubs.usgs.gov/of/2013/1090/>.
- Gehrels, G.E., Valencia, V.A., and Ruiz, J., 2008, Enhanced precision, accuracy, efficiency, and spatial resolution of U-Pb ages by laser ablation-multicollector inductively coupled plasma-mass spectrometry: Geochemistry Geophysics Geosystems, v. 9, 13 p.
- Gilbert, W.G., Solie, D.N., and Kline, J.T., 1988, Geologic map of McGrath A-3 quadrangle, Alaska: Alaska Division of Geological and Geophysical Surveys Professional Report 92, 2 sheets, scale 1:63,360.
- Goldfarb, R.J., Ayuso, R., Miller, M.L., Ebert, S., Marsh, E.E., Petsel, S.A., Miller, L.D., Bradley, Dwight C., Johnson, C., and McClelland, W., 2004, The Late Cretaceous Donlin Creek gold deposit, southwestern Alaska—Geological and geochemical controls on epizonal ore formation: Economic Geology, v. 99, p. 643–672.
- Goldfarb, R.J., Anderson, E.D., and Hart, C.J.R., 2013, Tectonic setting of the Pebble and other copper-gold molybdenum porphyry deposits within the evolving middle Cretaceous continental margin of northwestern North America: Economic Geology, v. 108, p. 405–419.
- Gorring, M.L., Kay, S.M., Zeitler, P. K., Ramos, V. A., Rubiolo, D., Fernandez, M.I., and Panza, J.L., 1997, Neogene Patagonian plateau lavas: continental magmas associated with ridge collision at the Chile Triple Junction: Tectonics, v. 16, p. 1–17.
- Gradstein, F.M., Ogg, J.G., Schmitz, M.D., and Gabi, M., 2012, The geologic time scale 2012: Elsevier, 2 volumes, 1174 p.
- Gray, J.E., Gent, C.A., Snee, L.W., and Wilson, F.H., 1997, Epithermal mercury-antimony and gold-bearing vein lodes of southwestern Alaska: Economic Geology Monograph 9, p. 287–305.
- Haeussler, P.J., Bradley, D.C., Wells, R.E., and Miller, M.L., 2003, Life and death of the Resurrection Plate; evidence for an additional plate in the northeastern Pacific in Paleocene-Eocene time: Geological Society of America Bulletin, v. 115, p. 867–880.
- Hoare, J.M., and Coonrad, W.L., 1978, Geologic map of the Goodnews and Hagemester Island quadrangles region, southwestern Alaska: U.S. Geological Survey Open-File Report 78–9–B, scale 1:250,000, 2 sheets.
- Hudson, T., 2001, Alaska Resource Data File, Taylor Mountains quadrangle: U.S. Geological Survey Open-File Report 01–200, 51 p.
- Ireland, T.R., and Williams, I.S., 2003, Considerations in zircon geochronology by SIMS: Reviews in Mineralogy and Geochemistry, v. 53, p. 215–241.
- Jones, J.V., III, Todd, E., Box, S.E., Haeussler, P.J., Holm-Denoma, C., Ayuso, R.A., and Bradley, D.C., 2014, Late Cretaceous through Oligocene magmatic and tectonic evolution of the western Alaska Range: Geological Society of America Abstracts with Programs, v. 46, no. 6, p. 781.

- Kalbas, J.L., Ridgway, K.D., Miller, M.L., and Bradley, D.C., 2007, Multi-stage Cretaceous basin development in southwestern Alaska: Marine depositional responses during syn- to early post-collision(?) margin evolution: Geological Society of America, Annual Meeting, Abstracts with Programs, v. 39, no. 6, p. 489.
- Karl, S.M., Blodgett, R.B., Labay, K.A., Box, S.E., Bradley, D.C., Miller, M.L., Wallace, W.K., and Baichtal, J.F., 2011, Fossil locations and data for the Taylor Mountains, and parts of the Bethel, Goodnews, and Dillingham quadrangles, southwestern Alaska: U.S. Geological Survey Open-File Report 2011–1065, 2 p., <https://pubs.usgs.gov/of/2011/1065/>.
- Kortyna, C., Donaghy, E., Trop, J.M., and Idleman, B., 2013, Integrated provenance record of a forearc basin modified by slab-window magmatism: detrital-zircon geochronology and sandstone compositions of the Paleogene Arkose Ridge Formation, south-central Alaska: Basin Research, v. 26, p. 436–460.
- Krogh, T.E., 1982, Improved accuracy of U-Pb zircon ages by the creation of more concordant systems using an air abrasion technique: *Geochimica et Cosmochimica Acta*, 46, p. 637–649.
- Lanphere, M.A., and Dalrymple, G.B., 2000, First-principles calibration of ^{38}Ar tracers: Implications for the ages of $^{40}\text{Ar}/^{39}\text{Ar}$ fluence monitors, U.S. Geological Survey Professional Paper 1621, 10 p., <https://pubs.er.usgs.gov/publication/pp1621>.
- Layer, P.W., 2000, Argon-40/argon-39 age of the El'gygytyn impact event, Chukotka, Russia: *Meteoritics and Planetary Science*, v. 35, p. 591–599.
- Layer, P.W., and Bundtzen, T.K., 2010, Petrology and $^{40}\text{Ar}/^{39}\text{Ar}$ geochronology of granitic rocks and greisens at Sleitat Mountain tin-silver-tungsten deposit, southwest Alaska: Geological Society of America Abstracts with Programs, v. 42, no. 5, p. 676.
- Layer, P.W., Hall, C.M., and York, D., 1987, The derivation of $^{40}\text{Ar}/^{39}\text{Ar}$ age spectra of single grains of hornblende and biotite by laser step heating: *Geophysical Research Letters*, v. 14, p. 757–760.
- Little, T.A., 1988, Tertiary tectonics of the Border Ranges fault system, northcentral Chugach Mountains, Alaska: Sedimentation, deformation, and uplift along the inboard edge of a subduction complex: Stanford, California, Stanford University, Ph.D. dissertation, 343 p.
- Ludwig, K.R., 1980, Calculation of uncertainties of U–Pb isotopic data: *Earth and Planetary Science Letters*, 46, p. 212–220.
- Ludwig, K.R., 2001, Squid 1.00—A user's manual: Berkeley, California, Berkeley Geochronology Center Special Publication No. 2, 17 p.
- Ludwig, K.R., 2003, Isoplot 3.00, a geochronological toolkit for Microsoft Excel: Berkeley, California, Berkeley Geochronology Center, Special Publication No. 4a, 71 p.
- Malinverno, A., and Ryan, W.B., 1986, Extension in the Tyrrhenian Sea and shortening in the Apennines as result of arc migration driven by sinking of the lithosphere: *Tectonics*, v. 5, p. 227–245.
- McDougall, I., and Harrison, T.M., 1999, Geochronology and thermochronology by the $^{40}\text{Ar}/^{39}\text{Ar}$ method—2nd ed.: Oxford University Press, New York, 269 p.
- Mertie, J.B., Jr., 1937, The Yukon-Tanana Region, Alaska: U.S. Geological Survey Bulletin 872, 276 p.
- Miller, M.L., 1990, Mafic and ultramafic rocks of the Dishna River area, north-central Iditarod quadrangle, west-central Alaska: U.S. Geological Survey Bulletin 1946, p. 44–50.
- Miller, M.L., Bradley, D.C., Bundtzen, T.K., and McClelland, W., 2002, Late Cretaceous through Cenozoic strike-slip tectonics of southwestern Alaska: *Journal of Geology*, v. 110, p. 247–270.
- Miller, M.L., Bradley, D.C., Goldfarb, R.J., and Bundtzen, T.K., 2007a, Tectonic setting of Late Cretaceous gold and mercury metallogenesis, Kuskokwim Mineral Belt, southwestern Alaska, in Andrew, C.J., and others, editors, Digging Deeper: Irish Association for Economic Geology, Proceedings of the Ninth Biennial Meeting of the Society for Geology Applied to Mineral Deposits, Dublin, Ireland, August 20–23, 2007, v. 1, p. 683–686.
- Miller, M.L., Bradley, D.C., Kalbas, J.L., Friedman, R., and O'Sullivan, P.B., 2007b, Detrital zircon geochronology of the Upper Cretaceous Kuskokwim Group, southwestern Alaska: Geological Society of America Abstracts with Programs, v. 39, no. 6, p. 489.
- Miller, M.L., Bradley, D.C., Bundtzen, T.K., Pessagno, E.A., Jr., Blodgett, R.B., Tucker, R., and Wooden, J., 2007c, The restricted Gemuk Group—A Triassic to Early Cretaceous succession in southwest Alaska, in Ridgway, K.D., Trop, J.M., Glen, J.M.G., and O'Neill, J.M., eds., Tectonic growth of a collisional continental margin, crustal evolution of southern Alaska: Geological Society of America Special Paper 431, p. 273–305.
- Miller, M.L., and Bundtzen, T.K., 1994, Generalized geologic map of the Iditarod quadrangle, Alaska, showing potassium-argon, major oxide, trace element, fossil, paleocurrent, and archaeological sample localities. U.S. Geological Survey Miscellaneous Field Studies Map MF–2219–A, 48 p., scale, 1: 250,000.
- Moll, E.J., Silberman, M.L., and Patton, W.W., Jr., 1981, Chemistry, mineralogy, and K-Ar ages of igneous and metamorphic rocks of the Medfra Quadrangle, Alaska: U.S. Geological Survey Open-File Report 80–811–C, 19 p., 2 sheets, scale 1:250,000.

- Moll-Stallcup, E.J., 1994, Latest Cretaceous and Cenozoic magmatism in mainland Alaska, *in* Plafker, G., and Berg, H.C., eds., *The geology of Alaska: Geological Society of America, Decade of North American Geology (DNAG) Series, v. G-1*, p. 589–619.
- Nelson, W.H., Carlson, C., and Case, J.E., 1983, Geologic map of the Lake Clark quadrangle, Alaska: U.S. Geological Survey Map MF-1114-A, scale 1:250,000.
- Paces, J.B., and Miller, J.D., 1993, U-Pb ages of the Duluth Complex and related mafic intrusions, northeastern Minnesota; geochronologic insights into physical, paleomagnetic and tectonomagmatic processes associated with the 1.1 Ga mid-continent rift system: *Journal of Geophysical Research*, v. 98, p. 13997–14013.
- Parrish, R., Roddick, J.C., Loveridge, W.D., and Sullivan, R.W., 1987, Uranium-lead analytical techniques at the geochronology laboratory, Geological Survey of Canada, *in* Radiogenic age and isotopic studies, report 1: Geological Survey of Canada, Paper 87-2, p. 3–7.
- Paton, C., Woodhead, J.D., Hellstrom, J.C., Hergt, J.M., Greig, A., and Maas, R., 2010, Improved laser ablation U-Pb zircon geochronology through robust downhole fractionation correction: *Geochemistry, Geophysics, Geosystems*, v. 11, Q0AA06, doi:10.1029/2009GC002618.
- Patton, W.W., Jr., Moll, E.J., Dutro, J.T., Jr., Silberman, M.L., and Chapman, R.M., 1980, Preliminary geologic map of the Medfra quadrangle, Alaska. U.S. Geological Survey Open-File Report 80-811-A, scale 1:250,000.
- Patton, W.W., Jr., Wilson, F.H., and Labay, K.A., 2006, Preliminary integrated geologic map databases for the United States—Digital data for the reconnaissance geologic map of the lower Yukon River region, Alaska: U.S. Geological Survey Open-File Report 2006-1292, <https://pubs.usgs.gov/of/2006/1292/>.
- Patton, W.W., Jr., Wilson, F.H., Labay, K.A., and Shew, N., 2009, Geologic Map of the Yukon-Koyuk Basin, Alaska: U.S. Geological Survey Scientific Investigations Map 2909, scale 1:500,000, 2 sheets and 26 p. pamphlet, <https://pubs.usgs.gov/sim/2909/>.
- Pearce, J.A., Bender, J.F., De Long, S.E., Kidd, W.S.F., Low, P.J., Güner, Y., Saroglu, F., Yilmaz, Y., Moorbath, S., and Mitchell, J.G., 1990, Genesis of collision volcanism in eastern Anatolia, Turkey: *Journal of Volcanology and Geothermal Research*, v. 44, p. 189–229.
- Redfield, T.F., Scholl, D.W., Fitzgerald, P.G., and Beck, M.E., 2007, Escape tectonics and the extrusion of Alaska—Past, present, and future: *Geology*, v. 35, p. 1039–1042.
- Reed, B.L., and Lanphere, M.A., 1972, Generalized geologic map of the Alaska-Aleutian Range batholith showing potassium-argon ages of the plutonic rocks: U.S. Geological Survey Miscellaneous Field Studies Map MF-372, 2 sheets.
- Reed, B.L., and Nelson, S.W., 1980, Geologic map of the Talkeetna quadrangle, Alaska: U.S. Geological Survey Miscellaneous Investigations Series Map I-1174, 15 p., 1 plate, scale 1:250,000.
- Reifenstuhl, R.R., Dover, J.H., Pinney, D.S., Newberry, R.J., Clautice, K.H., Liss, S.A., Blodgett, R.B., Bundtzen, T.K., and Weber, F.R., 1997, Geologic map of the Tanana B-1 Quadrangle, central Alaska: Alaska Division of Geological and Geophysical Surveys Report of Investigation 97-15A, scale 1:63,360.
- Reifenstuhl, R.R., Decker, J.E., and Coonrad, W.L., 1985, Compilation of geologic data from the Taylor Mountains D-8 Quadrangle, southwestern Alaska: Alaska Division of Geological and Geophysical Surveys Report of Investigation 85-4, 1 sheet, scale 1:63,360, doi:10.14509/2394.
- Renne, P.R., Swisher, C.C., III, Deino, A.L., Karner, D.B., Owens, T. and DePaolo, D.J., 1998, Intercalibration of standards, absolute ages and uncertainties in $^{40}\text{Ar}/^{39}\text{Ar}$ dating: *Chemical Geology*, v. 145, no. 1–2, p. 117–152.
- Roddick, J.C., 1987, Generalized numerical error analysis with application to geochronology and thermodynamics: *Geochimica et Cosmochimica Acta*, v. 51, p. 2129–2135.
- Roeske, S.M., McClelland, W.C., and Koepele, P.C., 1998, Late Early Cretaceous transtension in the western Ruby Terrane, West-Central Alaska: *Geological Society of America Abstracts with Programs*, v. 30, no. 7, p. 176.
- Rombach, C.S., and Newberry, R.J., 2001, Shotgun deposit: granite-porphyry hosted gold-arsenic mineralization southwest Alaska: *Mineralium Deposita*, v. 36, p. 607–621.
- Samson, S.D., and Alexander E. C., 1987, Calibration of the interlaboratory $^{40}\text{Ar}/^{39}\text{Ar}$ dating standard, MMhb1: *Chemical Geology*, v. 66, p. 27–34.
- Schrader, C.M., Crowe, D., Turner, K., and Stein, H.J., 2001, $^{40}\text{Ar}/^{39}\text{Ar}$ and Re-Os geochronology of the Pebble Copper Cu-Au-Mo porphyry deposit, southwest Alaska: *Geological Society of America Abstracts with Programs*, v. 33, no. 6, p. 418.
- Silberling, N.J., Jones, D. L., Monger, J.W.H., Coney, P.J., Berg, H.C., and Plafker, G., 1994, Lithotectonic terrane map of Alaska and adjacent parts of Canada, *in* Plafker, G., and Berg, H.C., eds., *The Geology of Alaska: Boulder, Colorado, Geological Society of America, DNAG Series G-1*, plate 3, scale 1:2,500,000.

- Siwieck, B.R., and Till, A.B., 2006, Synthesis of geochronologic, geochemical, metamorphic, and paleontological data on rocks of oceanic origin in northern Alaska: Geological Society of America Abstracts with Programs, v. 38, no. 5, p. 83.
- Solie, D.N., Bundtzen, T.K., and Gilbert, W.G., 1991, K-Ar ages of igneous rocks in the McGrath quadrangle, Alaska: Alaska Division of Geological and Geophysical Surveys Public Data File Report 160, 17 pages, one sheet, 1:250,000 scale.
- Smith, C.N., Kesler, S.E., Blum, J.D., and Rytuba, J.J., 2008, Isotope geochemistry of mercury in source rocks, mineral deposits and spring deposits of the California Coast Ranges, USA: Earth and Planetary Science Letters, v. 269, p. 399–407.
- Stacey, J.S., and Kramers, J.D., 1975, Approximation of terrestrial lead isotope evolution by a two-stage model: Earth and Planetary Science Letters, v. 26, p. 207–221.
- Steiger, R.H., and Jaeger, E., 1977, Subcommittee on geochronology—Convention on the use of decay constants in geo and cosmochronology: Earth and Planet Science Letters, v. 36, p. 359–362.
- Thirlwall, M.F., 2000, Inter-laboratory and other errors in Pb isotope analyses investigated using a ^{207}Pb – ^{204}Pb double spike: Chemical Geology, v. 163, p. 299–322.
- Thorkelson, D.J., 1996, Subduction of diverging plates and the principles of slab window formation: Tectonophysics, v. 255, p. 47–63.
- Till, A.B., Dumoulin, J.A., Phillips, J.D., Stanley, R.G., and Crews, Jesse, 2006, Generalized bedrock geologic map, Yukon Flats region, east-central Alaska: U.S. Geological Survey Open-File Report 2006–1304, scale 1:500,000, https://pubs.usgs.gov/of/2006/1304/YF_text.pdf.
- Todd, E., Jones, J.V., III, Box, S.E., Saltus, R., Karl, S.M., and Haeussler, P.J., 2015, Western Alaska Range magmatic response to progressive accretion of the Wrangellia composite terrane and evolution of the southern Alaska margin: Geological Society of America Abstracts with Programs, v. 47, no. 4, p. 53.
- Tomsich, C.S., McCarthy, P.J., Fiorillo, A.R., Stone, D.B., Benowitz, J.A., and O’Sullivan, P.B., 2014, New zircon U-Pb ages for the lower Cantwell Formation—Implications for the Late Cretaceous paleoecology and paleoenvironment of the lower Cantwell Formation near Sable Mountain, Denali National Park and Preserve, central Alaska Range, USA, in Stone, D.B., Grikurov, G.E., Clough, J.G., Oakey, G.N., and Thurston, D.S., eds., Proceedings of the International Conference on Arctic Margins VI, Fairbanks, Alaska, May 2011: St. Petersburg, Russia, A.P. Karpinsky Russian Geological Research Institute (VSEGEI), p. 19–60. [Also available at http://www.vsegei.ru/public/icam/icam-all_vvs.pdf.]
- Trop, J.M., and Ridgway, K.D., 2007, Mesozoic and Cenozoic tectonic growth of southern Alaska—A sedimentary basin perspective, in Ridgway, K.D., Trop, J.M., Glen, J.M.G., and O’Neill, J.M., eds., Tectonic growth of a collisional continental margin, crustal evolution of southern Alaska: Geological Society of America Special Paper 431, p. 55–94, doi:10.1130/2007.2431(04).
- Wallace, W.K., Hanks, C.L., and Rogers, J.F., 1989, The southern Kahiltna terrane; implications for the tectonic evolution of southwestern Alaska: Geological Society of America Bulletin, v. 101, p. 1389–1407.
- Wenz, Z.J., 2005, An investigation of the geology and gold mineralization of the Nycac district, southwest Alaska: U.S. Bureau of Land Management, Alaska State Office, Open-File Report 103, 156 p.
- Williams, I.S., 1998, U-Th-Pb geochronology by ion microprobe: Reviews in Economic Geology, v. 7, p. 1–35.
- Wilson, F.H., Dover, J.H., Bradley, D.C., Weber, F.R., Bundtzen, T.K., and Haeussler, P.J., 1998, Geologic map of central (interior) Alaska: U.S. Geological Survey Open-File Report 98–133, 64 p., 3 plates, scale 1:500,000.
- Wilson, F.H., Hults, C.P., Mohadjer, S., and Coonrad, W.L., compilers, 2013, Reconnaissance geologic map of the Kuskokwim Bay region, southwest Alaska, including the Bethel, Goodnews Bay, Nushagak Bay, Hagemester Island, Baird Inlet, Cape Mendenhall, Kuskokwim Bay, Nunivak Island, Saint Matthew, and Pribilof Islands 1:250,000-scale quadrangles: U.S. Geological Survey Scientific Investigations Map 3100, pamphlet 46 p., 1 sheet, scales 1:500,000, 1:300,000, 1:250,000, <https://pubs.usgs.gov/sim/3100/>.
- Wilson, F.H., Hults, C.P., Mull, C.G., and Karl, S.M., compilers, 2015, Geologic map of Alaska: U.S. Geological Survey Scientific Investigations Map 3340, pamphlet 196 p., 2 sheets, scale 1:1,584,000, <https://doi.org/10.3133/sim3340>.
- Wilson, F.H., Shew, N., and DuBois, G.D., 1994, Map and tables showing isotopic age data, in The geology of North America: Geological Society of America DNAG Series, v. G-1, scale 1:2,500,000.
- York, D., Hall, C.M., Yanase, Y., Hanes, J.A., and Kenyon, W.J., 1981, $^{40}\text{Ar}/^{39}\text{Ar}$ dating of terrestrial minerals with a continuous laser: Geophysical Research Letters, v. 8, 1136–1138.
- Zhang, M., Ewing, R.C., Boatner, L.A., Salje, E.K.H., Weber, W.J., Daniel, P., Zhang, Y., and Farnan, I., 2009, Pb* irradiation of synthetic zircon (ZrSiO_4)—Infrared spectroscopic study—Reply: American Mineralogist, v. 94, p. 856–858.

Appendixes

Appendix 1.—Analytical Methods

U-Pb Zircon TIMS Analytical Methods, University of British Columbia

Sample preparation, geochemical separations and thermal ionization mass-spectrometry (TIMS) were done at the Pacific Centre for Isotopic and Geochemical Research in the Department of Earth and Ocean Sciences, University of British Columbia. Zircon and other accessory phases were separated from samples using conventional crushing, grinding, and Wilfley table techniques, followed by final concentration using heavy liquids and magnetic separations. Mineral fractions for analysis were selected based on grain quality, size, magnetic susceptibility, and morphology. All zircon fractions were air abraded before dissolution to minimize the effects of post-crystallization Pb-loss, using the technique of Krogh (1982). Samples were dissolved in concentrated hydrofluoric (HF) and nitric (HNO₃) acids in the presence of a mixed ²³³⁻²³⁵U-²⁰⁵Pb tracer for 40 hours at 240 °C in polytetrafluoroethylene (PTFE) or poly(furfuryl alcohol) (PFA) microcapsules contained in high pressure vessels (Parr™ bombs). Sample solutions were then dried to salts at ~125 degrees Celsius (°C), rebombed and redissolved in 3.1 normal (N) hydrochloric acid (HCl) for 12 hours at 210 °C. Separation and purification of Pb and U employed ion exchange column techniques modified slightly from those described by Parrish and others (1987). Pb and U were sequentially eluted into a single beaker and loaded together on a single zone refined Re filament using a phosphoric acid-silica gel (SiCl₄) emitter. Isotopic ratios were measured using a modified single collector VG-54R thermal ionization mass spectrometer equipped with an analogue Daly photomultiplier. Measurements were done in peak-switching mode on the Daly detector. U and Pb analytical blanks were in the range of 1 and 1–5 picograms (pg), respectively, during the course of this study. U fractionation was determined directly on individual runs using a ²³³⁻²³⁵U tracer, and Pb isotopic ratios were corrected for fractionation of 0.37 percent/atomic mass unit, based on replicate analyses of the NBS-981 Pb standard and the values recommended by Thirlwall (2000). All analytical errors were numerically propagated through the entire age calculation using the technique of Roddick (1987). Weighted average ²⁰⁶Pb/²³⁸U ages and concordia ages were calculated using Isoplot (Ludwig, 2003). Concordia intercept ages and associated errors were calculated using a modified version the York-II regression model (wherein the York-II errors are multiplied by the MSWD) and the algorithm of Ludwig (1980). Unless otherwise noted, all errors are quoted at the 2-sigma level.

U-Pb Zircon SHRIMP-RG Analytical Methods, USGS-Stanford University

Zircon separations were done at the U.S. Geological Survey (USGS) in Anchorage using standard density and magnetic separation techniques. At the jointly operated USGS-Stanford University sensitive high-resolution ion

microprobe-reverse geometry (SHRIMP-RG) lab at Stanford University, zircons were hand-picked for final purity, mounted on double-stick tape on glass slides in 1×6-millimeter (mm) rows, cast in epoxy, ground and polished to a 1-micron (μm) finish on a disc 25 mm in diameter by 4 mm thick. All grains were imaged with transmitted light and reflected light (and incident light if needed) on a petrographic microscope, and with cathodoluminescence and back scattered electrons as needed on a JEOL 5600 scanning electron microscope to identify internal structure, inclusions, and physical defects. The mounted grains were washed with 1N HCl or ethylenediaminetetraacetic acid solution (if acid soluble) and distilled water, dried in a vacuum oven (to fully degas the sample), and coated with Au. Mounts typically sit in a loading chamber at high pressure (10⁻⁷ torr) for several hours before being moved into the source chamber of the SHRIMP-RG. Secondary ions are generated from the target spot with an O₂⁻ primary ion beam varying from 4 to 6 nano-ampere (nA). The primary ion beam typically produces a spot with a diameter of 20–40 μm and a depth of 1–2 μm for an analysis time of 9–12 minutes. Nine peaks are measured sequentially for zircons (the SHRIMP-RG is limited to a single collector, usually an EDP electron multiplier): ⁹⁰Zr¹⁶O, ²⁰⁴Pb, Bgd (background, 0.050 mass units above ²⁰⁴Pb), ²⁰⁶Pb, ²⁰⁷Pb, ²⁰⁸Pb, ²³⁸U, ²⁴⁸Th¹⁶O, and ²⁵⁴U¹⁶O. Autocentering on selected peaks and guide peaks for low or variable abundance peaks (that is, ⁹⁶Zr²¹⁶O, 0.165 mass unit below ²⁰⁴Pb) are used to improve the reliability of locating peak centers. The number of scans through the mass sequence and counting times on each peak are varied according to sample age and U and Th concentrations to improve counting statistics and age precision. Measurements are made at mass resolutions of 6,000–8,000 (10 percent peak height), which eliminates all interfering atomic species. The SHRIMP-RG was designed to provide higher mass resolution than the standard forward geometry of the SHRIMP-RG I and II (Clement and Compston, 1994). This design also provides very clean backgrounds and, combined with the high mass resolution, the acid washing of the mount, and rastering the primary beam for 90–120 seconds over the area to be analyzed before data are collected, assures that any counts found at mass of ²⁰⁴Pb are actually Pb from the zircon and not surface contamination. In practice, greater than 95 percent of the spots analyzed have no common Pb. Concentration data for zircons are standardized against zircon standard SL-13 (238 parts per million, ppm, U) or CZ3 (550 ppm U) and age data against AS3 and AS57 zircons (1098 Ma, millions of years,) from the Duluth Gabbro (Paces and Miller, 1993), RG-6 (1440 Ma, granite of Oak Creek stock; Bickford and others, 1989), or R33 (419 Ma, quartz diorite of Braintree complex, Vermont; Black and others, 2004), which are analyzed repeatedly throughout the duration of the analytical session. Data reduction follows the methods described by Williams (1998) and Ireland and Williams (2003) and use the Squid and

Isoplot programs of Ludwig (2001, 2003). For this study, the quoted U-Pb zircon ages are $^{206}\text{Pb}/^{238}\text{U}$ weighted-average ages calculated using Isoplot (Ludwig, 2003).

$^{40}\text{Ar}/^{39}\text{Ar}$ Analytical Methods, University of Alaska, Fairbanks

For $^{40}\text{Ar}/^{39}\text{Ar}$ analysis, samples were submitted to the Geochronology laboratory at the University of Alaska Fairbanks, where they were crushed, sieved, washed and hand-picked for mineral phases or small phenocryst free whole-rock chips. The monitor mineral MMhb-1 (Samson and Alexander, 1987) with an age of 513.9 Ma (Lanphere and Dalrymple, 2000) was used to monitor neutron flux (and calculate the irradiation parameter, J). The samples and standards were wrapped in aluminum foil and loaded into aluminum cans of 2.5 centimeter (cm) diameter and 6 cm height. The samples were irradiated in position 5c of the uranium enriched research reactor of McMaster University in Hamilton, Ontario, Canada for 20 megawatt-hours (MWh).

On their return from the reactor, the samples and monitors were loaded into 2 mm diameter holes in a copper tray that was then loaded in an ultra-high vacuum extraction line. The monitors were fused, and samples heated, using a 6-watt argon-ion laser following the technique described in York and others (1981), Layer and others (1987) and Layer (2000). Argon purification was achieved using a liquid nitrogen cold trap and a SAES Zr-Al getter at 400 °C. The samples were analyzed in a VG-3600 mass spectrometer at the Geophysical Institute, University of Alaska Fairbanks. The argon isotopes measured were corrected for system blank and mass discrimination, as well as calcium, potassium and chlorine interference reactions following procedures outlined in McDougall and Harrison (1999). System blanks generally were 2×10^{-16} mole (mol) ^{40}Ar and 2×10^{-18} mol ^{36}Ar , which are 10 to 50 times smaller than fraction volumes. Mass discrimination was monitored by running both calibrated air shots and a zero-age glass sample. These measurements were made on a weekly to monthly basis to check for changes in mass discrimination.

A summary of all the $^{40}\text{Ar}/^{39}\text{Ar}$ results is given in table 1, with all ages quoted to the +/- 1-sigma level and calculated using the constants of Steiger and Jaeger (1977). The integrated age is the age given by the total gas measured and is equivalent to a potassium-argon (K-Ar) age. The spectrum provides a plateau age if three or more consecutive gas fractions represent at least 50 percent of the total gas release and are within two standard deviations of each other (Mean Square Weighted Deviation less than ~2.7). All samples were run three times to check on sample consistency.

$^{40}\text{Ar}/^{39}\text{Ar}$ Analytical Methods, University of British Columbia

These methods apply to a single sample, 01ADw07a, which was processed first for zircon, which also yielded a hornblende

fraction. The hand-picked hornblende separate was washed in acetone, dried, wrapped in aluminum foil and stacked in an irradiation capsule with similar-aged samples and neutron flux monitors (Fish Canyon Tuff sanidine, 28.02 Ma; Renne and others, 1998).

The sample was irradiated on February 15 through 17, 2006 at the McMaster Nuclear Reactor in Hamilton, Ontario, for 90 MWh, with a neutron flux of approximately $3 \times 1,016$ neutrons/cm². Analyses ($n=57$) of 19 neutron flux monitor positions produced errors of <0.5 percent in the J value.

The samples were analyzed on April 11 and 12, 2006, at the Noble Gas Laboratory, Pacific Centre for Isotopic and Geochemical Research, University of British Columbia, Vancouver, British Columbia, Canada. The mineral separates were step-heated at incrementally higher powers in the defocused beam of a 10 watt (W) CO₂ laser (New Wave Research MIR10) until fused. The gas evolved from each step was analyzed by a VG5400 mass spectrometer equipped with an ion-counting electron multiplier. All measurements were corrected for total system blank, mass-spectrometer sensitivity, mass discrimination, radioactive decay during and subsequent to irradiation, as well as interfering Ar from atmospheric contamination and the irradiation of Ca, Cl, and K (isotope production ratios: $(^{40}\text{Ar}/^{39}\text{Ar})_{\text{K}}=0.0302 \pm 0.00006$, $(^{37}\text{Ar}/^{39}\text{Ar})_{\text{Ca}}=1416.4 \pm 0.5$, $(^{36}\text{Ar}/^{39}\text{Ar})_{\text{Ca}}=0.3952 \pm 0.0004$, Ca/K = $1.83 \pm 0.01(^{37}\text{Ar}_{\text{Ca}}/^{39}\text{Ar}_{\text{K}})$).

Details of the analyses, including plateau (spectrum) and inverse correlation plots, are presented in Excel spreadsheets. The plateau and correlation ages were calculated using Isoplot ver. 3.09 (Ludwig, 2003). Errors are quoted at the 2-sigma (95-percent confidence) level and are propagated from all sources except mass-spectrometer sensitivity and age of the flux monitor. The best statistically justified plateau and plateau age were picked based on the following criteria:

- Three or more contiguous steps comprising more than 50 percent of the ^{39}Ar ;
- Probability of fit of the weighted mean age greater than 5 percent;
- Slope of the error-weighted line through the plateau ages equals zero at 5 percent confidence;
- Ages of the two outermost steps on a plateau are not significantly different from the weighted-mean plateau age (at 1.8 sigma, six or more steps only);
- Outermost two steps on either side of a plateau must not have nonzero slopes with the same sign (at 1.8 sigma, nine or more steps only)

U-Pb Zircon LA-ICP-MS Analytical Methods, Apatite to Zircon, Inc.

Data were collected for the following isotopic masses: ^{202}Hg , $^{204}\text{Hg}+^{204}\text{Pb}$, ^{206}Pb , ^{207}Pb , ^{208}Pb , ^{232}Th , ^{235}U , and ^{238}U

(250 data scans over 30 seconds) followed by ^{28}Si and ^{91}Zr (5 data scans over 4 seconds). The instruments used were a New Wave YAG 213 nm laser ablation (LA) system in line with a Finnigan Element2 magnetic sector, inductively coupled plasma, mass spectrometer (ICP-MS) at the Washington State University Geoanalytical Laboratory in Pullman, Washington (for example, Chang and others, 2006). All analyses were performed using a 20- μm spot. Following approximately 6 seconds of background data collection, laser ablation commenced and data were collected for the ablated material. Ablated material was transported to the plasma line using He; Ar was the plasma gas.

Zircon standards for which independently accepted ages are published were designated as primary, secondary, and tertiary for purposes of U-Pb age calibration (appendix 2, table A4). Two primary and two secondary standard spots were analyzed before and following each group of ~25–30 tertiary standards and (or) unknown sample spots. Five spots of each tertiary standard were analyzed near the beginning and again near the end of the session.

Data Modeling

Previous LA-ICP-MS studies of U-Pb zircon dating deployed the so-called intercept method, which assumes that isotopic ratio varies linearly with scan number due solely to linearly varying isotopic fractionation (Chang and others, 2006; Gerhels and others, 2008). For the intercept method, a line is fitted to background-corrected isotopic ratio (for example, $^{206}\text{Pb}/^{238}\text{U}$) versus data scan number and the intercept of the fitted line (corresponding to data scan number=0) is used as the isotopic ratio for age calculation and the error on the intercept is used for age error calculation. In this study, individual isotopes were modeled by fitting a sum of 10 Gaussian equations to the raw signal data (not background corrected) using chi-squared minimization. Two fitting passes were performed: after the first pass, all raw signal values greater than two standard deviations away from the sum of fitted Gaussians were designated outliers; the second pass fit the sum of Gaussians to the data excluding the outliers. The advantage of the present approach is that it avoids the assumption of linearly varying isotopic ratio with scan number, an assumption easily violated for zircons that may contain useful information (for example, a zircon for which the ablation pit variably penetrates two zones having different U-Pb ages).

Measured background values for each isotope at each LA-ICP-MS spot were calculated as follows: (1) the final background scan was assigned as the scan closest to the global minima ^{232}Th and ^{238}U values; if no such global minima were found, the analysis was deemed a failure, (2) a line was fitted to the background values, outliers identified, and a line again fitted to the data excluding the outliers, (3) for a fitted line exhibiting a negative slope (indicative of a decaying background), the value of the line at the last background

scan was assigned as the background value; for a fitted line exhibiting a zero or positive slope, the mean value of the data excluding the outliers was assigned as the background value, and (4) the error of the background value was set equal to the standard deviation of the all background values (excluding outliers) about their fitted line (negative slope) or mean (zero or positive slope).

Session-wide fitted background values for each isotope were determined using all zircon standards and applied to all spots in the session. These steps were taken for each isotope—(1) measured background value versus spot number in the session was fitted to a 3rd-order polynomial, outliers identified, and the fitting repeated excluding the outliers, and (2) fitted background at each session spot was calculated using the 3rd-order polynomial. Session-wide fitted background error was set equal to the standard deviation of the measured background values (excluding outliers) about their respective fitted 3rd-order polynomial. For any spot (standard or unknown) where the measured background value exceeded the session-wide fitted value by more than 2 sigma, the background error was set equal to 1 sigma plus one half of the amount by which the measured background value exceeded the session-wide fitted value by 2 sigma.

The sum of fitted Gaussians was used here primarily to identify outlier data and characterize signal noise. After the second fitting pass, the standard deviation of the nonoutlier data about their respective sum of fitted Gaussians was taken as the absolute signal error for each data scan. When N data scans contribute to a single isotopic signal value used for age calculation (only concordant scans when the number of concordant data scans is greater than zero; all data scans for common Pb-correction based on isotopic sums), the error of the single isotopic signal value was set equal to the product of (1) $N^{1/2}$ and (2) the absolute signal error for each data scan.

Pb/U Fractionation Factor

Fractionation factors were determined for each data scan of each primary standard spot. For a particular isotopic ratio (for example, $^{206}\text{Pb}/^{238}\text{U}$), the fractionation factor as used here equals the accepted isotopic ratio divided by the measured ratio. A two-dimensional grid (spot number, scan number) of fractionation factors for each isotopic ratio was constructed for the session as a whole by fitting a series of 4th-order polynomials (excluding outliers). Under the operating conditions of the LA-ICP-MS sessions in this study, fractionation factors were found to vary strongly with scan number, decreasing with increasing scan number (presumably due to increasing ablation pit depth and the effect this had on fractionation; for example, Paton and others, 2010).

Fractionation factors were calculated using isotopic values based on the sum of fitted Gaussians. Ages, including when the standards were treated as unknowns, were calculated using raw isotopic signal values (excluding outliers) to avoid any bias due to artifacts of the fitting of the sum of Gaussians.

Fractionation Factor Adjustment for Integrated alpha-damage

Zircon is widely known to accumulate α -radiation damage (for example, Zhang and others, 2009 and references therein). It is assumed here that increased α -damage in a zircon leads to a decrease in the hardness of the zircon; this in turn leads to a faster rate of laser penetration into the zircon during ablation leading to shift in isotopic fractionation. Ages calculated for the primary, secondary, and tertiary zircon standards, when those standards were treated as unknowns, were used to construct a fractionation factor correction curve (exponential form). Much previous work has attempted to understand the chemical basis for why some standards work better with some zircons. The notion of matrix-matched standard and unknown zircons has been proposed largely on the basis of trace element chemistry (for example, Black and others, 2004). Here, time and crystallographic damage, parameters invisible to instruments used to characterize trace element chemistry, were introduced and applied in conjunction with U and Th chemistry.

Common Pb Correction

Common Pb was subtracted out using the Stacey and Kramers (1975) common Pb model for Earth. Ages and common Pb ratio were determined iteratively using a preset, session-wide minimum common Pb age value (default for each session was the age of the oldest age standard, which for both apatite and zircon was 1099 Ma FC-1 and (or) FC-5z).

Preferred Age

Uranium decay constants and the $^{238}\text{U}/^{235}\text{U}$ isotopic ratio reported in Steiger and Yäger (1977) were used in this study. $^{207}\text{Pb}/^{235}\text{U}_c$ ($^{235}\text{U}_c = 137.88^{238}\text{U}$), $^{206}\text{Pb}/^{238}\text{U}$, and $^{207}\text{Pb}/^{206}\text{Pb}$ ages were calculated for each data scan and checked for concordance; concordance here was defined as overlap of all three ages at the 1-sigma level (the use of 2-sigma level was found to skew the results to include scans with significant common Pb). The background-corrected isotopic sums of each isotope were calculated for all concordant scans. The precision of each isotopic ratio was calculated by using the background and signal errors for both isotopes. The fractionation factor for each data scan, corrected for the effect of accumulated α -damage, was weighted according to the ^{238}U or ^{232}Th signal value for that data scan; an overall weighted-mean fractionation factor for all concordant data scans was used for final age calculation.

If the number of concordant data scans for a spot was greater than zero, then either the $^{206}\text{Pb}/^{238}\text{U}$ or $^{207}\text{Pb}/^{206}\text{Pb}$ age was chosen as the preferred age, whichever exhibited the lower relative error. If zero concordant data scans were observed, then the common Pb-corrected age based on isotopic sums of all acceptable scans was chosen as the preferred age. Common Pb was subtracted out using the Stacey and Kramers (1975) common Pb model for Earth. Ages and common Pb ratio were determined iteratively using a preset, sessionwide minimum common Pb age value (default for each session was the age of the oldest age standard which for both apatite and zircon was 1099 Ma FC-1 and (or) FC-5z).

Appendix 2.—New Geochronology Data for Igneous-Rock Samples from Western Alaska

This appendix of new geochronology data for igneous-rock samples from western Alaska is available online only as comma separated value (.csv) files and an Excel (.xlsx) file at <https://doi.org/10.3133/pp1814D>. The files contain the following tables:

Table A1. Uranium-lead (U-Pb) thermal ionization mass-spectrometry (TIMS) data for zircon and monazite samples from western Alaska analyzed at the University of British Columbia.

Table A2. Uranium-lead (U-Pb) secondary ion mass-spectrometry (SIMS) data for igneous-rock samples from western Alaska analyzed at the U.S. Geological Survey-Stanford sensitive high-resolution ion microprobe-reverse geometry (SHRIMP-RG) facility at Stanford University, California.

Table A3. Argon-40/argon-39 ($^{40}\text{Ar}/^{39}\text{Ar}$) data for igneous-rock samples from western Alaska analyzed at the University of Alaska Fairbanks.

Table A4. Argon-40/argon-39 ($^{40}\text{Ar}/^{39}\text{Ar}$) data for igneous-rock samples from western Alaska analyzed at the University of British Columbia.

Table A5. Laser ablation inductively coupled plasma mass spectrometry (LA-ICP-MS) data for zircon in igneous-rock samples from western Alaska analyzed by Apatite to Zircon, Inc., at Washington State University.

Menlo Park Publishing Service Center, California
Manuscript approval date December 7, 2016
Edited by James W. Hendley II
Design and layout by Cory Hurd

